INCREASED STEAM TEMPERATURE IN GRATE FIRED BOILERS - STEAMBOOST

KME-709

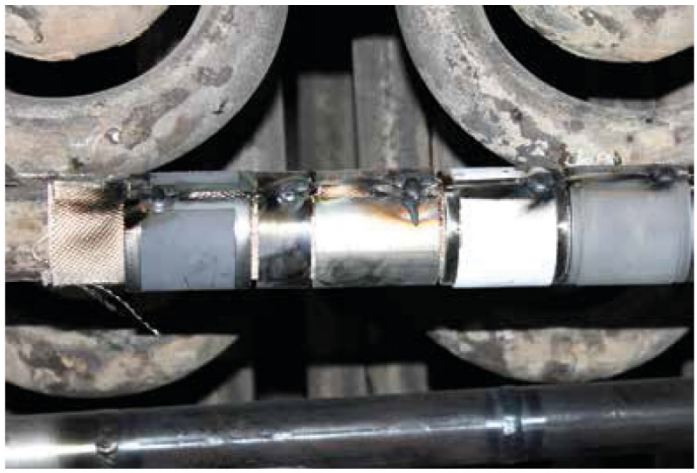

CONSORTIUM MATERIALS TECHNOLOGY
for thermal energy processes

KME
CONSORTIUM MATERIALS TECHNOLOGY
for thermal energy processes

Increased steam temperature in grate fired boilers - Steamboost

L.MIKKELSEN, T. JONSSON, L.PAZ, J. EKLUND, J. LISKE, B. JONSSON, N. ISRAELSSON, S. SELIN, J HERNBLOM J. HÖGBERG, J. NOCKERT OLOVSJÖ

ISBN 978-91-7673-090-4 | © 2018 ENERGIFORSK

Energiforsk AB | Phone: 08-677 25 30 | E-mail: kontakt@energiforsk.se | www.energiforsk.se

Preface

The project has been performed within the framework of the materials technology research programme KME, Consortium materials technology for thermal energy processes, period 2014-2018. The consortium is at the forefront of developing material technology to create maximum efficiency for energy conversion of renewable fuels and waste. KME has its sights firmly set on continuing to raise the efficiency of long-term sustainable energy as well as ensuring international industrial competitiveness.

KME was established 1997 and is a multi-cliental group of companies over the entire value chain, including stakeholders from the material producers, manufacturers of systems and components for energy conversion and energy industry (utilities), that are interested in materials technology research. In the current programme stage, eight industrial companies and 14 energy companies participate in the consortium. The consortium is managed by Energiforsk.

The programme shall contribute to increasing knowledge within materials technology and process technology development to forward the development of thermal energy processes for efficient utilisation of renewable fuels and waste in power and heat production. The KME goals are to bring about cost-effective materials solutions for improved fuel flexibility, improved operating flexibility, increased availability and power production with low environmental impact.

KME's activities are characterised by long term industry and demand driven research and constitutes an important part of the effort to promote the development of new energy technology with the aim to create value and an economic, environmentally friendly and long term sustainable energy society.

The industry has participated in the project through own investment (60 %) and the Swedish Energy Agency has financed the academic partners (40 %).

Bertil Wahlund, Energiforsk

Abstract

The aim of this project is to investigate two strategies to reduce the high temperature corrosion/increase the electrical efficiency in bio/waste fired boilers.

- A new position for superheaters in the furnace of the boiler.
- A new material class (FeCrAl) as superheater material.

The results from the project show that both the new superheater position and the, in this application, new material class (FeCrAl) are promising pathways to reduce the high temperature corrosion/increase the electrical efficiency in bio/waste fired boilers. The investigation of the new superheater position showed deposit composition similar as in a normal superheater position and that it is possible to influence all aspects of the deposit formation. The investigation of pre-oxidized FeCrAl alloys showed that the alumina scale has a very large potential to protect the material in these environments if it is intact. The laboratory and field study of the FeCrAl model alloys without pre-oxidation in addition showed two different trends to increase the corrosion resistance, i.e. increasing the Cr content in the alloy and/or adding a small amount of Si to the alloy. This new knowledge may contribute to higher steam parameters and thereby higher electrical efficiency from waste fired boilers.

Sammanfattning

Det övergripande målet med projektet är att förbättra potentialen vid förbränning av biomassa/avfall. Idag är högtemperaturkorrosion av överhettare vid avfallsförbränning den begränsande faktorn för att utnyttja den fulla potentialen i dessa bränslen. Speciellt utifrån en energieffektivitetssynpunkt är högt ångtryck/hög överhettemperaturen av största vikt. Detta projekt undersöker två möjliga strategier för att minska korrosionen av överhettare och därmed möjliggöra högre temperaturer/ångdata i dessa processer. De två strategierna som undersöks är:

- Placering av överhettare på ett nytt ställe i pannan, dvs i ugnen. Denna strategi bygger på möjligheten att identifiera nya positioner med högt värmevärde och mindre korrosiv rökgas.
- Använda en ny materialklass som överhettarmaterial. För närvarande används kromiabildande material i dessa pannor. En möjlig strategi för att undvika korrosionproblemen skulle kunna vara att använda aluminiumoxidbildande legeringar, t.ex. FeCrAl legeringar.

Arbetet har genomförts av Babcock & Wilcox Vølund, Sandvik Materials Technology AB, Kanthal AB inom ramen för KME, finansierat av deltagande industri ochg Energimyndigheten. Chalmers/HTC (Torbjörn Jonsson) har varit projektledare. Resultaten från projektet visar att både den nya överhettarpositionen och den i sammanhanget nya materialklassen är lovande strategier för att minska korrosionen och därmed möjliggöra högre temperaturer/ångdata.

För att undersöka den nya positionen för placering av överhettare har ett stort antal olika överhettarmaterial material exponerats på den nya tänkta positionen i ugnen i en kommersiell avfallseldad panna (AffaldPlus).

- Både beläggningsbildning, initial- och långtidskorrosion har undersökts genom korrosionssonder och fast installerat material.
- Resultatet av beläggningsanalysen visade att det var möjligt att uppnå Cl-nivåer i samma storleksordning som vid en normal överhettarposition. Vidare visar undersökningen att det är möjligt att påverka alla aspekter av beläggningsbildningen vid den potentiella överhettarpositionen, dvs det finns en potential att ytterligare optimera beläggningsbildningen och därmed minska korrosiviteten.
- Korrosionsundersökningen av rostfria stål visade ingen klar trend mellan materialförlust och sammansättning av legeringarna. Den detaljerade undersökningen visade att alla undersökta rostfria stål har förlorat sin skyddande kromrika oxid vilket är väntat i närvaro av alkalimetaller såsom kalium som har rapporterats reagera med den skyddande Cr-rika oxiden.

FeCrAl legeringar har i projektet undersökts båda i laboratoriemiljö samt i AffaldPlus. Denna materialklass bildar aluminiumoxid vid höga temperaturer och egenskaperna hos denna oxid har undersökts både genom modellegeringar samt genom föroxidering

av kommersiella material.

- Laboratorieresultaten visar att om materialet genom föroxidering som bildar ett α-aluminiumoxidskikt utgör det en effektiv barriär mot korrosion i alkaliska/klorhaltiga miljöer. Detta visar potentialen hos aluminiumoxidbildare i denna miljö.

- Exponeringen av ett föroxiderat kommersiellt FeCrAl material som exponerats i pannan under 4500 timmar vid ca 900 ° C stärker denna slutsatsen från laboratoriet eftersom det fortfarande fanns ett skyddande α-aluminiumoxid intakt på delar av materialet och därmed försumbar korrosion på dessa delar. Detta resultat ligger i linje med laboratorieresultatet trots att exponeringstemperaturen var högre och miljön mer komplex.
- Laboratorie- och fältstudien av FeCrAl-modellegeringarna utan föroxidering uppvisade två olika trender, dvs en ökad korrosionsresistens vid ökning av Cr-halten i legeringen samt en ökad korrosionsresistens vid tillsats av en små mängd Si till legeringen.

- Resultaten indikerar att korrosionsresistensen för de bästa modellegeringarna ligger linje med en påläggssvetsad legering 625. Denna slutsats kräver dock mer undersökningar för att bekräfta eftersom direkta materialförlustmätningar av legering 625 inte genomförts inom ramen för detta projekt. Det bör noteras att en ökad mängd Cr gav en ökad sprödhet i materialet.

Måluppfyllelse

Det övergripande målet med projektet är att förbättra potentialen vid förbränning av biomassa/avfall.
Nedan presenteras de olika målen och graden av måluppfyllelse. En mer genomgripande måluppfyllelse presenteras senare i rapporten.

Projektet har genererat kunskap om den nya superheaterpositionen (Steamboost). Detta inkluderar kunskap om beläggning/korrosionsattack. Kunskapen har redan under projektet används för att utesluta behovet av en keramisk sköld som separerar mer korrosiva rökgaser i ugnen. Stora mängder korrosions- och beläggningsdata har i projektet genererats vilket kan fungera som underlag då ett framtida överhettarmaterial skall väljas. Denna kunskap tillsammans med kunskapen hur beläggningen kan påverkas kommer att användas i nästa steg för att skapa en överhettare på den nya Steamboost-positionen.

Projektet har genererat kunskap om korrosionsmekanismerna för FeCrAl-legeringar. Denna kunskap kommer att användas för att identifiera var dessa material kan användas (temperatur och miljö) och hur de kan modifieras för att bli mer korrosionsbeständiga i en avfalls/biomasseldad pannmiljö.

Nyckelord: Korrosion i pannor eldade med avfall, Överhettare, Högtemperaturekorrosion, FeCrAl legering, Steamboost

Summary

The overall aim of this project is to improve the potential of bio/waste fired boiler. High temperature corrosion of superheater materials in waste fired boilers is a major challenge in utilization of the energy in domestic and industrial waste. From an energy recovery efficiency point of view high steam pressure and superheater temperature are of paramount importance. This project investigates two pathways to reduce the corrosion of superheaters in order to utilize higher steam data from these processes.

- A new technology proposed by Babcock & Wilcox Vølund aiming to increase the steam temperature. The idea is to identify positions for superheaters where the flue gas from the grate have a high heat flux and a less corrosive flue gas/deposit.
- Increase the energy output by utilizing new materials that can cope with these aggressive environments. Currently, stainless steels are the material of choice for use in these boilers. A possible strategy to avoid component failure in a power boiler would be to use an alumina-forming alloy such as the well-known FeCrAl alloys.

This report is based on a project that have been performed by Babcock & Wilcox Vølund, Sandvik Materials Technology AB, Kanthal AB, Göteborg Energi AB, within the KME program, financed by participating industry and the Swedish Energy Agency. Chalmers/HTC (Torbjörn Jonsson) has been acting as project manager. The results show that both the use of the new positions over the grate and to utilize new materials that can cope with these aggressive environments are promising.

In order to investigate the new superheater position (Steamboost) a large range of possible superheater materials has been investigated.

- Deposit, short and long-term corrosion investigations has also been performed at the AffaldPlus boiler.
- The results of the deposit formation investigation at the boiler showed Cl levels in the same range as in a normal superheater position. The deposit investigation in addition shows that it is possible to influence all aspects of the deposit formation at the Steamboost position, i.e. there is a potential to further optimize the deposit formation and reduce the corrosiveness.
- The corrosion investigation of the stainless steels showed no clear trend between material loss and composition of the alloys. The microstructural investigation shows that the stainless steels are in breakaway mode as is expected in the presence of alkali metals, such as potassium, that have been reported to react with the protective Cr rich scale normally formed on stainless steels.

The corrosion resistance of FeCrAl alloys has in the project been investigated both in the laboratory and in a commercial waste fired boiler.

- The laboratory results from pre-oxidized FeCrAl alloys indicate that if the α-alumina scale is intact it constitutes an effective barrier towards corrosion also in alkali/chlorine containing environments showing the potential of the alumina formers in this corrosive environment.

- The pre-oxidized FeCrAl tube exposed in the boiler for 4500h at about 900 °C strengthen this conclusion since the exposed tube still had a protective α-alumina intact on parts of the investigated tube material. These areas did not suffer from any corrosion. This result is in line with the laboratory results even though the exposure temperature was higher and the environment very complex and shows the potential of the alumina scale in these environments.
- The laboratory and field study of the FeCrAl model alloys without pre-oxidation showed two different trends, an increased corrosion resistance when increasing the Cr content in the alloy as well as an increased corrosion resistance when adding a small amount of Si to the alloy.
- The performance of the best model alloys is in the same range as over weld alloy 625. However, more work is needed to confirm this as direct material loss measurements were not possible to perform within the scope of this project. It should also be noted that an increased amount of Cr also showed an embrittlement of the samples.

Goal fulfilment

The overall goal of this study was to improve plant economy by enabling an increased green electricity production and optimum material selection. Below the different goals and it fulfilment is presented. A more thorough goal fulfilment is presented in the report.

The project has generated knowledge about the new superheater position (Steamboost). This includes knowledge about deposit/corrosion formation which has already been used to rule out the need for a ceramic shield separating more corrosive gases. Large amounts of corrosion/deposit data have in addition been generated to be used in order to select superheatermaterial in the future. This knowledge will be used in the next step towards a superheater in the new Steamboost position.

The project has generated knowledge regarding the corrosion mechanisms of the FeCrAl alloys. This knowledge will be used to identify where these materials can be used (temperature and environment) or how they could be modified in order to become more corrosion resistant in a waste/biomass fired boiler environment.

Key words: Waste fired boiler, Superheater, FeCrAl, Steamboost, High temperature corrosion

List of content

1 Introduction

1.1 BACKGROUND

Renewable energy sources such as biomass and waste are important for the Swedish energy supply. However, these fuels are challenging to combust because of their heterogeneous nature and the relatively high levels of alkali and chlorine, see e.g. [1-3]. The fuel composition results in a flue gas environment, which is more corrosive compared to fossil fuels.

High temperature corrosion of the pressure part materials in waste-fired boilers and heat recovery boilers is a major challenge in utilisation of the energy in domestic and industrial waste. From an energy recovery efficiency point of view high steam pressure and superheater temperature are of paramount importance. In order to achieve a thermal efficiency close to other types of boiler fuels e.g. fossil fuels and clean biomass fuels the superheater temperature must be increased from now being in the area of 400 °C. This is with the present boiler and material technology not possible due to excessive high temperature corrosion.

High temperature corrosion in waste-fired boilers is caused by chemical reactions between the boiler tube metals and the aggressive components in the combustion gases. Combustion gases from waste-fired boilers are compared with fossil fuel gases known to contain particularly reactive and aggressive to most steel metals and alloys. Among the most critical chemical elements are Chlorine, Sulphur, Alkali Metals, Lead and Zinc. These have for the last years been the basic problem of improving the efficiency and performance of waste fired boilers using steals and stainless steels.

1.2 DESCRIPTION OF THE RESEARCH FIELD

The combustion processes taking place in waste-fired boilers are complex. The processes in a burning fuel bed include several different processes over the grate [4, 5]. Babcock & Wilcox Vølund has proposed a new technology aiming to increase the steam temperature called Steamboost. The idea behind Steamboost is that the corrosive species are released over the first part of the grate such that the flue gas is less corrosive over the last part of the grate, see Figure 1. Full-scale experiments have been performed on a plant in Denmark to verify the concentration of corrosive species in the flue gas over the grate. These measurements confirmed a low concentration of corrosive species near the end of the grate. A material test was also performed with a 300cm superheater installation. The inlet temperature of the steam was 340 °C and the outlet temperature was 380 °C. Post-test analyses were very promising and showed that the steels tested exhibited reasonable low corrosion losses of less than 1,5 mm/year.

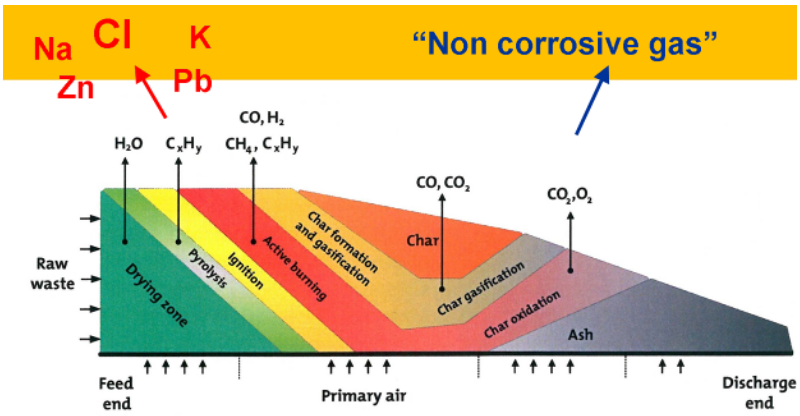

Figure 1: A schematic drawing of the idea behind Steamboost. The corrosive species are released (of the grate such that the flue gas is less corrosive over the last part of the grate [4].

The scientific idea behind Steamboost is to utilize the CFD modelling in order to identify fractions (positions) where the flue gas from the grate have a high heat flux and a low chlorine concentration. Superheaters may then be positioned in a part of the furnace within the less corrosive flue gas and subsequently increase the steam temperature up towards 500 °C. This novel approach will then increase the possibility to generate higher steam data contributing more electricity being produced and thereby to the KME objectives.

However, the CFD calculations needs to be verified by deposit probes linking the theoretical approach to the actual deposit formed in the furnace. Little is, in addition, known about the corrosion of superheaters within the furnace. This project will therefore investigate the link between the CFD calculations and the actual deposits formed in the boiler. The corrosion properties of several possible superheater materials will additionally be investigated in order to get a fundamental knowledge of the corrosion behaviour of alloys within the furnace. The project will also investigate possibilities of optimizing the flue gas chemistry in the furnace more to decrease the corrosion rate even further.

Another way to increase the energy output is to utilize new materials that can cope with these aggressive environments. Presently, stainless steels are the material used in these boilers. The ability of these alloys to withstand high temperatures relies on the formation of a protective, Cr-rich oxide $(Cr,Fe)_2O_3$. Previous studies have shown that chemical reactions with alkali and water vapour consume the protective chromia scale and leave a poorly protective iron oxide behind [6, 7]. This may result in a sudden increase in corrosion rate (breakaway corrosion). A possible strategy to avoid component failure in these boilers with high levels of alkali and water vapour would be to use a different type of material. One option would be to use an alumina-forming alloy such as the well-known FeCrAl. While FeCrAl alloys are known to form protective α-alumina scales when exposed to air and other oxygen-containing environments at 900 °C and higher[8, 9], much less study has been devoted to the oxidation behaviour of FeCrAl alloys at lower temperatures. The project will investigate possibilities of using FeCrAl alloys to decrease the corrosion rate even further.

1.3 RESEARCH TASK

Research has generally been directed towards fireside corrosion and fouling in these plants in order to decrease maintenance costs and enable increased power efficiency. However, this novel approach using less corrosive positions in the furnace has never been used before and if successful it will increase the possibility to increase the heat change in the boiler and generate higher electrical efficiency. The aim with the project is to generate knowledge about the steamboost position and the deposit/corrosion formation. This has been done through several steps:

• Link CFD calculations and actual deposit compositions at the steambost position.

• Investigate the corrosion behaviour of the different materials at the different temperatures (both time resolved probe tests and Steamboost solutions).

• Investigate the corrosion properties of FeCrAl material, both by a tube consisting of FeCrAl inside the furnace near the Steamboost superheater and by corrosion probe tests.

• Investigate the need for a ceramic shield.

• Generate knowledge regarding the corrosion mechanisms in order to identify where FeCrAl materials can be used (temperature and environment) or how they could be modified in order to become more corrosion resistant.

The aim of this project is in addition to test conventional superheater materials as well as state of the art stainless steels in the steamboost position. These materials will be compared with FeCrAl alloys, which also will be studied in the laboratory in order to identify and understand the usefulness and limitations of aluminum oxide forming materials as components for biomass- and waste-fired boilers.

Careful characterization of the deposit chemistry at different positions gives a unique possibility to generate knowledge about the corrosion resistance of different material classes. Exposures of commercial and model FeCrAl alloys will also be conducted in the waste fired boiler. The purpose is to expose aluminum oxide forming materials in different environments and temperatures.

1.4 GOAL

The overall goal of the project is to improve plant economy by enabling an increased electricity production. This will be achieved by generating new knowledge to facilitate the implementation of CFD modelling, deposit test and corrosion tests. The aim of this project is also to find suitable materials in terms of corrosion for a Steamboost superheater positioned within the furnace. Conventional superheater materials as well as state of the art stainless steels will therefore be investigated. These materials will be compared with FeCrAl alloys, which will be studied in the laboratory in order to identify and understand the usefulness and limitations of aluminum oxide forming materials as components for biomass- and waste-fired boilers. Exposures of manufactured FeCrAl model alloys will also be conducted in the waste fired boiler. These investigations contribute to the following KME goals:

- Higher steam parameters and thereby higher electrical efficiency.
- Development of novel solutions where steam is superheated in the furnace.

- Develop improved material solutions – including alumina forming alloys.

1.5 PROJECT ORGANIZATION

The project is jointly performed by Babcock & Wilcox Vølund, Sandvik Materials Technology AB, Kanthal AB, Göteborg Energi AB and HTC at Chalmers University of Technology. The distribution of work was:

Part	**Participants role in the project**	**Total financial contribution**
Babcock & Wilcox Vølund	Responsible for boiler operation, gas analysis and fuel analysis. Participating in the project group.	3 000 kSEK
Sandvik Materials Technology AB	Providing test material to the boiler exposures. Participating in the project group.	400 kSEK
Kanthal AB	Developing new model alloys for boiler applications. Providing test material to the boiler exposures. Participating in the project group.	3 000 kSEK
Göteborg Energi AB	Contributed financially to the project.	23 kSEK
Chalmers/HTC	Project management. Responsible for corrosion evaluation of exposed samples. Responsible for short term probe exposures.	

Table 1. Participating partners in the KME-709 project

Within the project the following researchers has been active: L.Paz (Post doc), J. Eklund (Ph. D. Student), T. Jonsson (Docent), J. Phother (Ph. D. Student), N Israelsson (PhD student/Postdoc) and J .Liske (Assoc. Prof).

The members of the reference group were, besides members of the project;

Annika Stålenheim	Vattenfall Research & Development
Pamela Henderson	Vattenfall Research & Development
Rikard Norling	Swerea-KIMAB
Christoph Gruber	Andritz
Edgardo Coda	Foster Wheeler
Bengt-Åke Andersson	E.ON

The project was financed by the Swedish Energy Agency together with cash and in-kind contributions from the company members of the project. The total project budget was 10 612 kSEK and the project time was 2014-2017.

2 Description of the combined heat and power plant AffaldPlus

The boiler is a grate-waste fired boiler with a thermal capacity of 27 MW. It produces steam used for electricity production and district heating. The line 4 of the Combined Heat and Power (CHP) plant is placed at the AffaldPlus plant in Næstved and it has a nominal capacity of 8t/h.

The combustion system is based on the latest state-of-the art technology from Babcock & Wilcox Vølund; a combination of the technologies from the Vølund systems and the latest results from a number of research and development projects within control, CFD calcultations and combustion technologies.

The air-cooled grate (DynaGrate®) is ideal for the incineration of both domestic and industrial waste because of the high efficiency combustion, utilization of energy and good bottom ash quality. DynaGrate® is capable of handling all sorts of unsorted solid waste and can be used for co-combustion with biomass. In order to control the thickness of the fuel bed, the grate is made up of a number of individual controlled sections. Each grate section has a complete drive mechanism consisting of double action hydraulic cylinders and control valves.

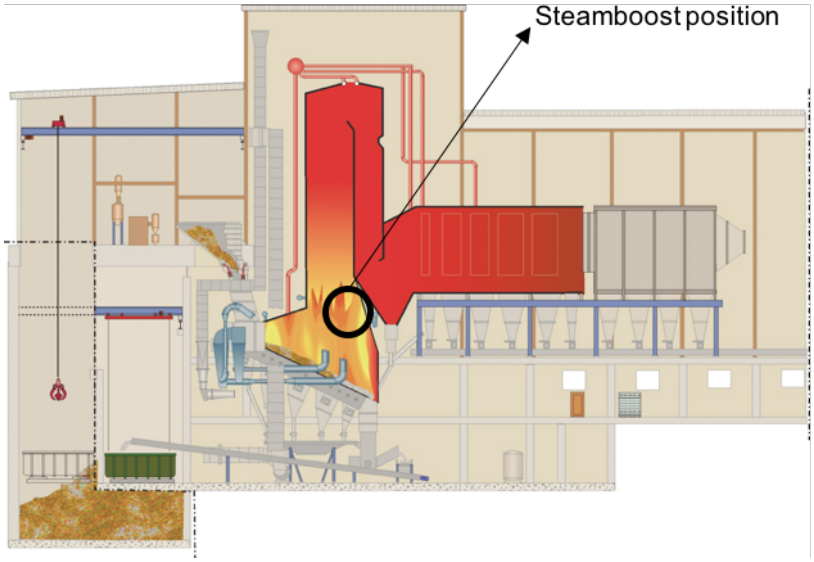

Figure 2: Schematic drawing of the combined Heat and Power plant AffaldPlus (Denmark)[10]

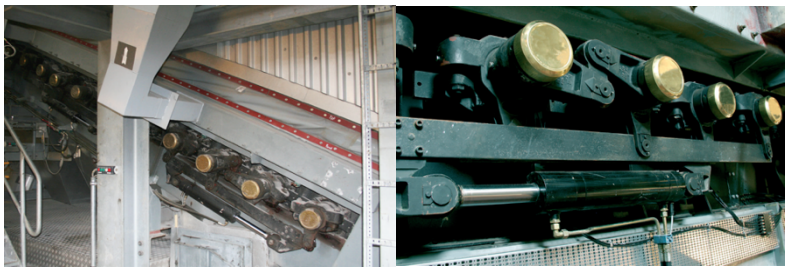

Figure 3: Photos showing details of the air-cooled grate [10]

A VoluMix® system is installed at the inlet of the 1st pass, consisting of a nozzle arrangement that pushes the flue gas to make it move in two, spiral resembling lines. The purpose of the VoluMix® is to ensure good, turbulent mixing of the flue gases and consequently a better combustion process and burnout as well as proper filling of the 1st pass with flue gas. This results in better heat absorption in the boiler. Furthermore, VoluMix® may also prevent recycling zones in the 1st pass.

The whole plant has been designed on the basis of the results of detailed CFD calculations and analyses (Figure 4).

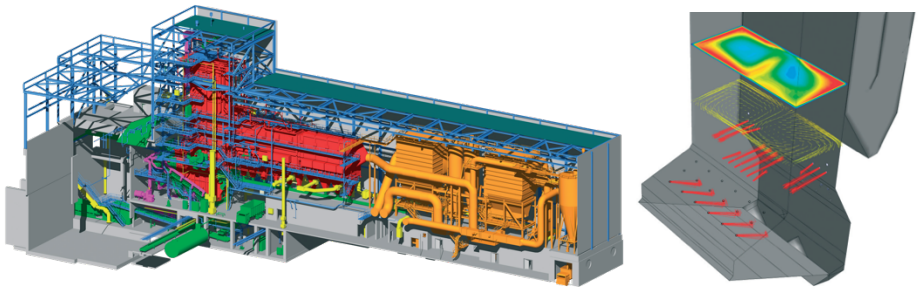

Figure 4: Examples of CFD calculations used to design the plant [10]

The impact of the VoluMix® is visible on the low content of CO and TOC in the flue gas (Table 1), as these substances are indicators of the completeness of the combustion process.

The principle of the plant design is a midstream furnace followed by a boiler with 2 ½ empty radiation passes and a horizontal convection part and economizer. The boiler radiation passes are protected against corrosion with refractory lining and Inconel®.

Plant design data		
Process parameters	**Values**	**Units**
Waste capacity	8	t/h
Heat value, lower	12	MJ/kg
Steam output	30 1/2	t/h
Steam temperature	405	˚C
Steam pressure	54	bar
Energy input	26.6	MW
Heat efficiency	85.7	%
TOC, bottom ash	1/4	%
Flue gas temp. before SH	620	˚C
Exit temp. boiler	180	˚C
Flue gas values: Out of boiler	**Values**	**Units**
NOx	137	mg/Nm³
CO	~ 0	mg/Nm³
TOC, gas	~ 0	mg/Nm³

The plant limit values comply with the EU directive on waste-fired boilers

Table 1: AlfaldPlus plant design data.

3 Production of model FeCrAl alloys

The model alloys from Kanthal have been produced by induction heating and cast in a copper mold under an argon protective atmosphere. The induction furnace is shown in Figure 5 and Figure 6.

Figure 5: Induction furnace used in the production of the lab-melts at Kanthal.

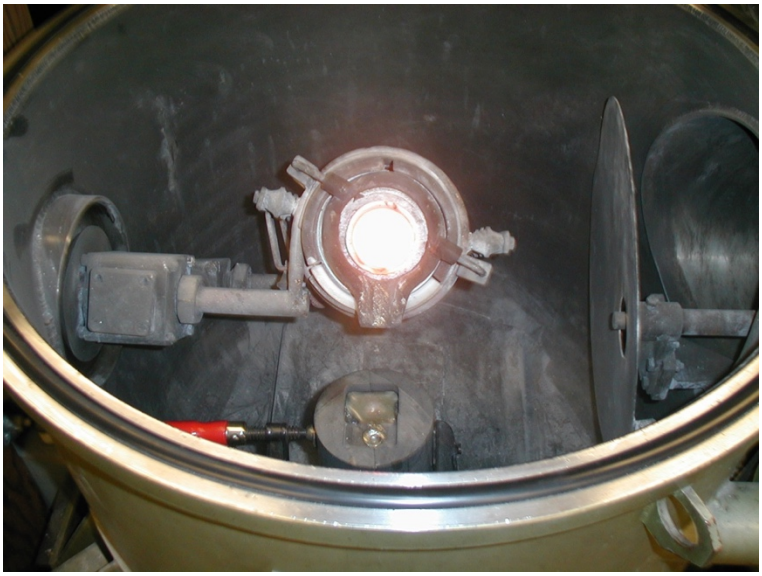

Figure 6: Interior of the induction furnace showing the crucible in the center and the mold below.

The cylindrical ingots were machined prior to hot rolling to remove surface defects and form a cylinder with diameter 24 mm which goes into the hot rolling process. The ingots were heated to 1150 °C prior to hot rolling down to a strip sample with the approximate cross section 13x3 mm. During the hot rolling the material was reheated approximately 4 times.

After hot rolling the strip samples were heat treated to achieve a suitable grain size. The ferritic model alloys were heat treated at 950 °C for 1 hour. This was done for materials 1-7 and 9, which correspond to the samples investigated in the laboratory. After heat treatments, the strip samples were machined to a 12x2 mm cross section and thereafter delivered to CTH.

Rings for field exposures with similar compositions as the lab samples were produced as well. The ingots were produced in the same way as the ones for the lab samples. Afterwards they were forged at 900 °C and pressed into the form of a puck. The pucks were then made into rings by lathe machining.

4 Experimental Conditions

4.1 LABORATORY INVESTIGATION OF FECRAL ALLOYS

The materials used were the commercial FeCrAl alloys (Kanthal APMT and Kanthal AF) as well as model alloys. The as-received 2 mm plate was cut into coupons with the dimensions of 15x15 mm. A hole of about 1.5 mm in diameter was drilled to simplify sample handling during spraying and weighing. The samples were ground down to P320 grit on SiC paper, and polished with 9, 3 and 1 µm diamond suspension to achieve a mirror polished grade surface. After polishing, the samples were cleaned and degreased with acetone and ethanol in an ultrasonic agitation bath.

4.1.1 The influence of KCl on commercial/model FeCrAl alloys

Amounts of salt of 0,1 mg/cm^2 and 1mg/cm^2 were applied to the polished samples by spraying with a saturated solution of the salt in water/ethanol. The samples were subsequently dried with warm air and stored in a desiccator prior to exposure.

A horizontal furnace with a 45-mm diameter SiO_2 tube was used to carry out the exposure (Figure 7). The gas flow conditions were set to 5 % O_2 and 20 % H_2O and N_2 in balance. The temperature was held under isothermal conditions at 600 ± 3 °C. The dry gases were led through water circulated Perma Pure membrane in order to obtain the humid environment with 20 % H_2O. The sample coupons were placed in the centre of the furnace and left for approximately 1 – 2 minutes in dry exposure before starting the wet exposure in order to avoid condensation.

After the exposure, the water was switched off and the samples were left to cool down in N_2 atmosphere for 20 minutes. The exposed pieces where weighed and the mass gain was calculated.

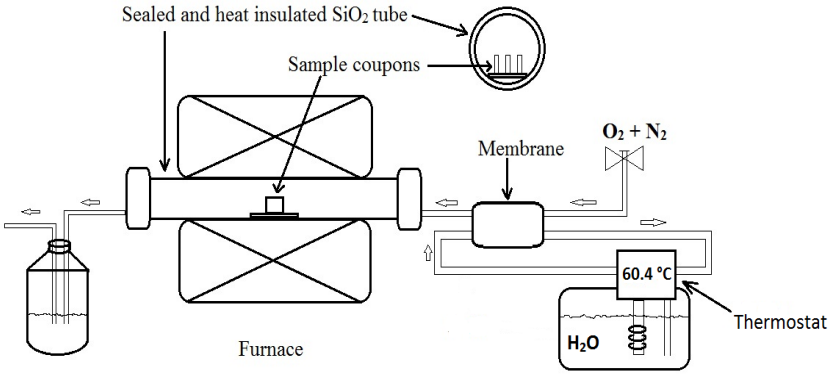

Figure 7: Schematic drawing of the experimental setup designed for the lab exposures

4.1.2 Pre-oxidation of commercial FeCrAl alloys – influence of KCl

The corrosion properties and the effect of pre-oxidation of the commercial FeCrAl alloy Kanthal APMT was studied by Nicklas Israelsson as a part of his PhD thesis[11]. The same setup was used as described in Figure 7. Pre-oxidation was performed at 700 °C in 20% O_2 + 80% N_2 for 24 h. After pre-oxidation 0.1 mg/cm^2 KCl was deposited onto the samples by spraying before additionally exposing the samples for 1h, 24h and 168h in 5% O_2 + 40% H_2O (N_2 in balance) at 600 °C. Exposures of samples that had not been pre-oxidized were also sprayed with the same amount of KCl and exposed in the same environment and for the same amount of time except that these were also exposed at 72h.

4.2 LABORATORY INVESTIGATION OF MODEL FECRAL ALLOYS

In order to optimise the corrosion properties of FeCrAl alloys a number of model alloys have been produced by Kanthal. The aim to study the effect of key elements and compositions in a KCl rich environment. However, a microstructure investigation and heat treatments of the as received material and reference exposures where first performed. Two different matrices of model alloys were used in which the content of chromium and silicon was varied, see Table 2 and Table 3 (internal names are presented in Table 13 in Appendix). All alloys in these tables were exposed in the reference environment and with KCl present (described in section 4.2.1 and 4.2.2).

Table 2: Chemical composition of FeCrAl model alloys in which Cr content is varied

Alloy	Cr	Al	Si	Re
Fe**5Cr**Al2Si	5	3	2	x
Fe**10Cr**Al2Si	10	3	2	x
Fe**15Cr**Al2Si	15	3	2	x
Fe**20Cr**Al2Si	20	3	2	x

Table 3: Chemical composition of FeCrAl model alloys in which Si content is varied

Alloy	Cr	Al	Si	Re
FeCrAl**0Si**	10	4	0	x
FeCrAl**1Si**	10	4	1	x
FeCrAl**2Si**	10	4	2	x

4.2.1 Reference Exposures in O2 + H2O at 600 °C for 168 hours

Samples were first polished down to 1µm and degreased in an ultrasonic bath before they were weighed and put in an alumina sample holder. The sample holder with the samples were put into a horizontal silica tube furnace and left there for 168 hours. The composition of

the gas flow through the tube furnace consisted of 5% O_2 + 20% H_2O + 75% N_2. After taking out the samples they were left in a desiccator to cool for about an hour before weighing.

4.2.2 Exposures in O2 + H2O at 600 °C with KCl present for 168 hours

The samples were prepared with the same procedure as described for the reference samples. However, before exposure, KCl was deposited on the samples by spraying. The samples were weighed before spraying KCl and weighed again afterwards until the desired amount of KCl (1.0 mg/cm^2) had been deposited. A tube furnace of the same set up as in the reference exposures (with a flow with the same gas composition as for the reference exposures) was used and after 168 hours of exposure the samples were put in a desiccator to cool down for about an hour before weighing.

4.3 EXPOSURES IN THE COMBINED HEAT AND POWER PLANT AFFALDPLUS

A general description of the AffaldPlus plant is given in section 2. In the boiler, a series of deposit/corrosion test were performed. The corrosiveness of the steamboost position was investigated through fixed installed tubes, deposit probe exposures, corrosion probe exposures and an un-cooled FeCrAl tube exposure all at the Steamboost position, see Figure 8.

The fixed installed Steamboost tubes were removed after 8000h. New tubes were installed and and exposed for 6500h. The uncooled FeCrAl tube was installed and removed after 12000h and the tip was cut for analysis. A deposit test was performed in order to study the environment of the Steamboost region and to choose the optimal boiler conditions to run the corrosion test. Table 4 shows an overview of all the different exposures preformed at the Steamboost position during the project.

Table 4: Different tests run at the Steamboost region

	Steamboost	FeCrAl tube	Deposit test	Corrosion test
Material Temperature	390°C-525°C	900°C	525°C/700°C	525°C/700°C
Exposure Time	8000h	12000h	2h	24 and 1000h

4.3.1 Fixed installation of superheater tubes at the Steamboost position

The Steamboost test with fixed installed material was conducted at AffaldPlus in Næstved, Denmark, see section 2. In the test, superheater tubes are connected to the main steam of the plant. The inlet temperature of the steam is 340 °C and the outlet temperature is 470 °C giving a metal temperature of approximately 520 °C at the outlet tube. The tubes were composed of different materials welded together (Figure 8) and was run for approximately 8000h. Overlay welding as tube protection was tested as well as solid materials.

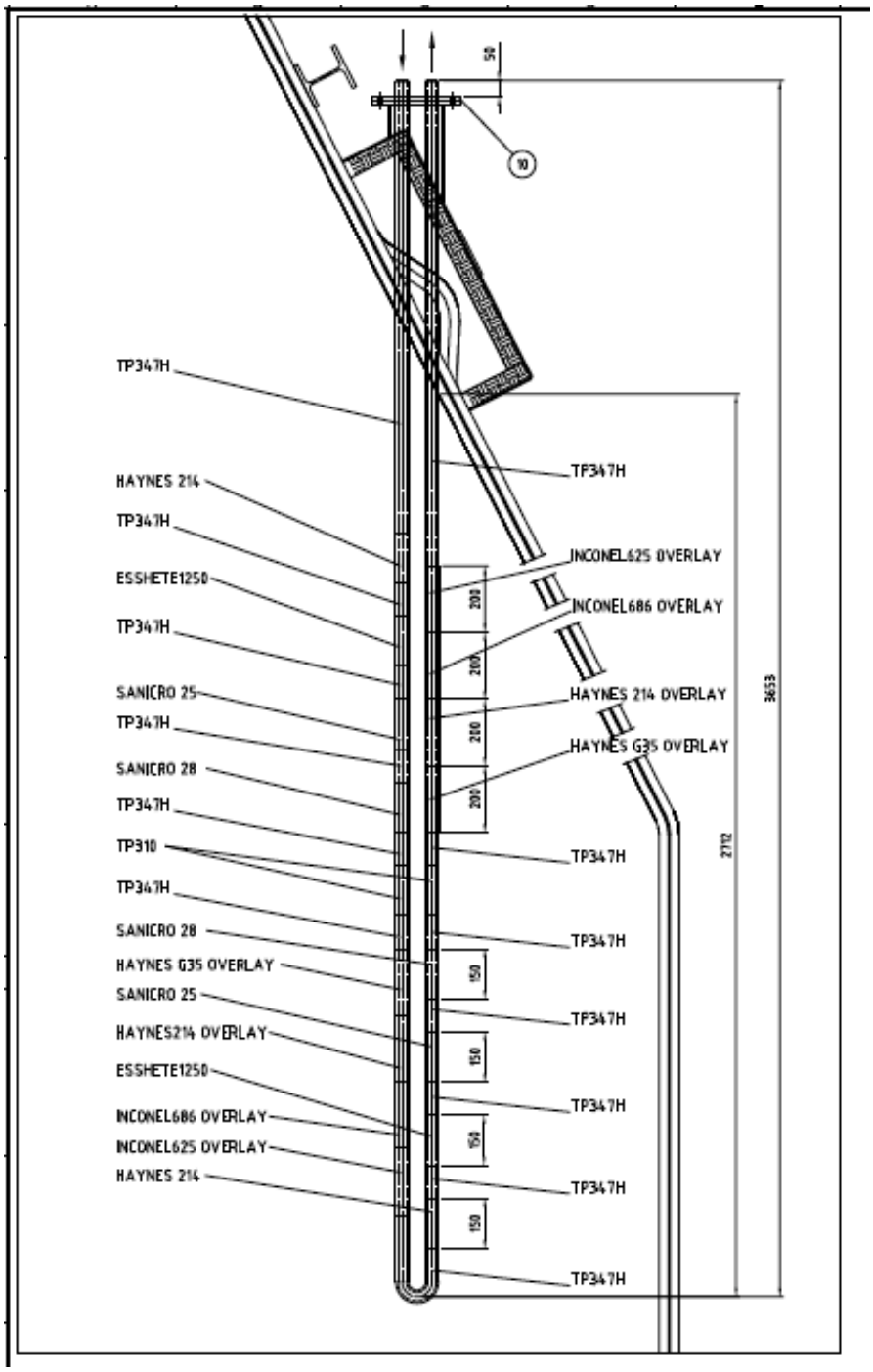

Figure 8: Steamboost drawing showing the different materials. Three similar tubes were coupled in series.

Nine materials were tested in each of the three tubes. Fourteen material sections of the materials were welded together giving in total 84 samples, see Figure 8. An overview of the

tested materials and their chemical composition are given in Table 5. The boiler was cleaned prior to removal of the first set of fixed installed materials.

Table 5: Composition of tested materials during fixed installation test at steamboost position.

Material	% C	% Fe	% Al	% Cr	% Ni	% Mo	% Si	% Mn	Others
Esshete1250	0.093	bal		14.72	9.31	0.92	0.45	6.22	P, S, Nb, V, B
Haynes 214	0.05	3.59	4.19	16.12	bal	<0.1	0.09	0.23	P,S,Nb,Co,Zr,Mg,Y,Ti,W,B
Sanicro 25	0.064	bal	0.023	22.35	25.36		0.18	0.51	P, S, Nb, Co, W, B, N, Cu
Sanicro 28	<0.020	bal		27	31	3.5	<0.6	<2.0	P, S, Cu
TP347H	<0.1	bal		9-12;	17 - 19		1	2	P,Nb
310	<0,25	bal		24-26	19-22			<2.0	P, S
Inconel 625	<0.1	<5	<0.4	20-23	58	8-10	<0.50	<0.50	P, S, Nb, Co, Ti
Inconel 686 (to be added)	<0.010	<5		19-23	59	15-27		<0.75	P, S, W, P
Haynes G35 (to be added)f	<0.05	<2	<0.4	33.2	58	8.1	<0.6	<0.5	W

Figure 9. Photo showing of two of the three Steamboost tubes removed from the boiler

Table 6: Materials exposed in second fixed installation.

Material
Esshete1250
Haynes 214
Sanicro 25
Sanicro 28
TP347H x 4
TP310
Inconel 625 overlay
Inconel 686 overlay
Haynes 214 overlay
Haynes G35 overlay

The second exposure of fixed installed material consisted of the same setup with 14 materials, see Table 6.

4.3.2 Un-cooled FeCrAl tube installation

The corrosion properties of FeCrAl was investigated as an alternative to the steel tubes. The alumina-forming FeCrAl solid tube without cooling was inserted at the Steamboost position. This alternative solution would need a co-axial superheater with an inner super heater tube

with the steam inside, and an outer corrosion resistant material (in this case FeCrAl) explaining the higher exposure temperature.

The tube was loosely centered into the hatch opening flange with four bolts. A fiber blanket was used to fill the gap closest to the tube. To the inside of the hatch, two 10 cm thick Rockwool pieces were cut to fill the gap between tube and tunnel in the boiler wall. The tube gets support from the bolts in the hatch, and from the bottom of the tunnel. Distance between points of support about 70 cm, (the thickness of the boiler wall including insulation and hatch. The tube extends 70 cm outside the flange in the hatch. Figure 10 shows a drawing of the inserted Kanthal APMT tube.

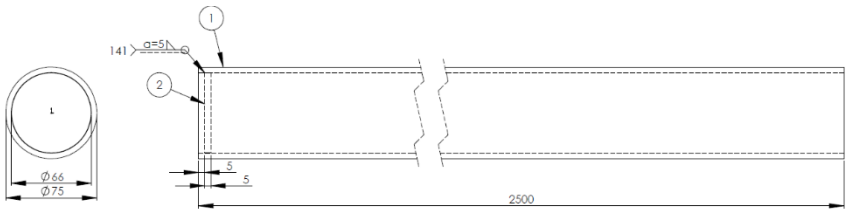

Figure 10. Inserted Kanthal APMT tube. The tube was preoxidized 1050°C 8 hours before shipment

The tube consisting of the commercial Kanthal APMT FeCrAl material was positioned inside the furnace near the Steamboost superheater during several steps of the project. The first exposure lasted for 4500h. Figure 11 shows the tip of the tube after being cut for analysis. The temperature of the tube was measured to be about 900 °C and recorded during the exposure with a thermocouple. The commercial Kanthal® APMT FeCrAl alloy was in addition tested on a corrosion probe along with FeCrAl model alloys, see section 3.2.4.

Figure 11. Tip of the FeCrAl tube after cut for analysis

During each corrosion probe test the FeCrAl tube was removed and then after the test inserted again in the Steamboost region. After 12000h the material failed and was removed for analysis. Figure 12 shows the tube after being removed due to failure.

Figure 12. FeCrAl tube after being removed

4.3.3 Deposit investigation with air-cooled probe at the Steamboost position

A deposit test was carried out while running the boiler with a large number of different settings in order to investigate the influence of different settings on the deposit formation and in order to be able to select the least corrosive setting.

A total of 29 different settings were investigated. The adjustments were made on the air supply and the boiler conditions was established 1 h prior to each of the 2h deposit exposures. An air-cooled probe which holds 3x3 samples in three temperature zones was used, see Figure 13. The selected temperatures for the deposit test were 525 and 700 °C.

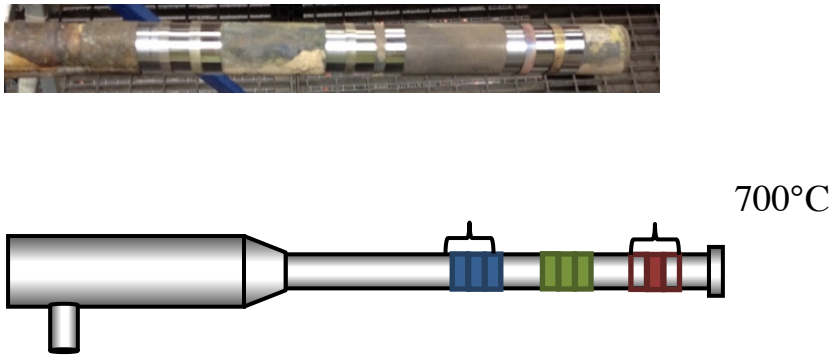

Figure 13: Photo and schematic drawing of the samples placed on the air-cooled probe.

After 2h inside the boiler the probe was removed and all the samples were changed. The exposed samples were handled with care and stored in desiccators in order to avoid of moisture until analysis. Table with deposit test results will be compiled.

4.3.4 Corrosion investigation with air-cooled probe at the Steamboost position

A short term 24h exposure and a long term 1000h exposure were carried out during the winter/spring 2016. A newly designed air-cooled probe with two temperature zones was used. The probe can hold 8 samples, 4 samples in each zone (Figure 14). The temperatures selected for this test were 525 and 700 °C. Seven materials were produced in the shape of sample rings, see table.

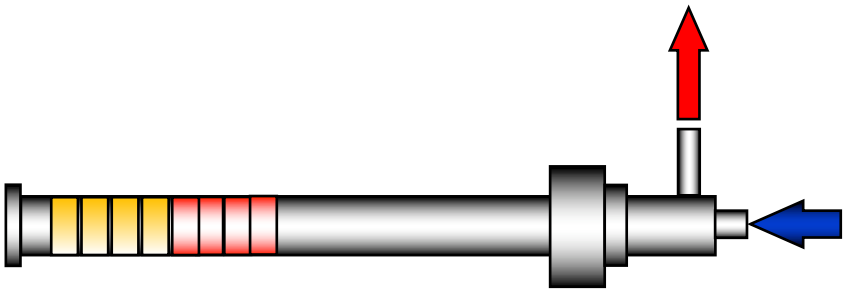

Figure 14: Two temperature zones air-cooled probe used for the corrosion test

Material	% C	% Fe	% Al	% Cr	% Ni	% Mo	% Si	% Mn	Others
TP347H	<0.1	bal		9 - 12	17 - 19				P,Nb
310	<0,25	bal		24-26	19-22			<2.0	P, S
Inconel 625	<0.1	<5	<0.4	20-23		8-10	<0.50	<0.50	P, S, Nb, Co, Al, Ti
Kanthal® APMT	<0.08	bal					<0.7	<0.4	
Nikrothal PM58									To be added
Model Alloy	0,025		3	10			2		Si, Zr
Sanicro 33									[SMT]

Table 7: The materials tested at 525°C were TP347H, 310, Sanicro 33 (newly developed austenitic stainless steel from SMT) and Inconel 625 (overwelded). For 700 °C the Kanthal® APMT, Nikrothal PM58, a Model Alloy and Inconel 625 (overwelded) were tested.

An air-cooled probe was used for the 1000-hour field exposure of five FeCrAl model alloys, selected from the matrix of the lab exposures, as well as an Inconel 625 over weld as reference material. The two zones were both set so that the material temperature of the sample rings would be 600 °C. Prior to exposure, the thickness of all sample rings was measured by using ultrasound. Before the corrosion test, a deposit test was performed in order to analyse the composition of the deposit formed under the corrosion test conditions. As in the previous deposits tests, the material used was Sanicro 28 and the exposure time was 2 hours.

Due to a scheduled shutdown, the air-cooled corrosion test lasted 672 hours instead of the planned 1000h. After the exposure, the sample rings were removed from the probe and individually analysed using SEM to measure the thickness and, in turn, calculate the material loss.

Table 8: Matrix for the corrosion test of FeCrAl model alloys.

ref	1	2	3	4	5
Alloy 625	5 3 2	10 3 2	15 3 2	20 3 2	10 3 0
	Cr Al Si				

4.4 ANALYTICAL TECHNIQUES

4.4.1 Qualitative analysis

All samples were investigated by visual inspection after exposure and documented by photographs. The colour, thickness and adherence of the deposit/corrosion product layer give rough information of the overall condition and performance of the exposed sample. All samples were stored in desiccators together with phosphorous pentoxide drying agent awaiting their analysis.

4.4.2 Scanning Electron Microscopy/Energy Dispersive X-Rays (SEM/EDX)

After the boiler exposure, the samples taken from Steamboost were cast in epoxy, cut and polished prior to the SEM/EDX investigation. The rings were casted by first immersing them in epoxy resin. Both sample and mould were then subjected to a 10-bar pressure to avoid the formation of bubbles during the hardening of the resin. The hardening time was fixed in 24 hours. After the hardening of the epoxy resin was complete, the samples were cut using a silicon carbide disc and a lubricant without any water due to the delicate corrosion products. The samples were then polished dry with Silicon Carbide P4000. The cross-section was coated with gold to avoid charging in the SEM. The polished cross-sections of the samples were investigated by scanning electron microscopy, SEM. The SEM is equipped with an Energy Dispersive X-ray system enabling analysis of the elemental composition in small areas of the sample. In this study, a FEI 200 Quanta FEG ESEM was used. It is equipped with a field emission electron gun (FEG) and an Oxford Inca energy dispersive X-ray (EDX) system. SEM/EDX was used for imaging, elemental mapping and quantification. An accelerating voltage of 20kV was used for all analysis.

4.4.3 Material loss measurements

The samples were evaluated by means of metal loss determination, performed with an Olympus 38DL Plus ultrasonic thickness gage with a 0.01mm resolution.

4.4.4 Ion Chromatography (IC)

To determine the amount of water-soluble anions (Cl^-, SO_4^{2-}) on the exposed samples, a Dionex ICS-90 system was used. The anions were analysed with an IonPac AS4A-SC analytic column and 1.8mM NaHCO3/1.7mMNaHCO3 was used as solvent. The flow rate was 2ml/min.

A representative and known amount of deposit was removed from the samples and dissolved in 100 mL distilled water. A 5 mL sample of this prepared solution was inserted into the IC

column in order to know the amount of chlorine and sulfate ions (ppm). The results are presented as mass percentage (amount of ions/100 g deposit).

4.4.5 X-Ray Diffraction (XRD)

In order to determine the crystalline phases in the deposit and corrosion product layer XRD was used. The diffractometer was a Siemens D5000 powder diffractometer, equipped with grazing-incidence beam attachment and a Göbel mirror. Cu-Kα radiation was used and the angle of incidence was 2°. The measuring range of the detector was $10° < 2\theta < 65°$.

5 Results - Laboratory investigation of FeCrAl alloys

It is well known that KCl is corrosive and present in the environment where the steamboost will be positioned. The laboratory investigation of the corrosion mechanisms of FeCrAl alloys was therefore investigated in the presence of KCl.

5.1 THE EFFECT OF KCL ON COMMERCIAL FECRAL ALLOYS

The influence of preoxidation of commercial FeCrAl alloys on the corrosion resistance in a KCl containing environment was studied in the laboratory at 600 °C up to 168 h. The work includes kinetic behaviour with and without pre-oxidation as well as a detailed microstructural investigation as described below.

5.2 INFLUENCE OF PRE-OXIDATION ON THE EFFECT OF KCL ON COMMERCIAL FECRAL ALLOYS

Pre-oxidation was performed in a tube furnace at 700 °C in 20% O_2 +80% N_2 for 24 h. After pre-oxidation 0.1 mg/cm^2 KCl was deposited onto the samples by spraying before additionally exposing the samples for 1h, 24h and 168h in 5% O_2 + 40% H_2O (N_2 in balance) at 600 °C. Exposures of samples that had not been pre-oxidized were also sprayed with the same amount of KCl and exposed in the same environment and for the same amount of time except that these were also exposed at 72h.

The beneficial effect of pre-oxidation is illustrated in Figure 15 where mass gains versus exposure time for both pre-oxidized and untreated samples along with reference exposures without the presence of KCl. The exposure of the untreated samples in the presence of KCl resulted in a rapid increase in mass gain. After 10 hours, no further corrosion attack occurred as the last of the KCl evaporates (see mass loss). Exposing the pre-oxidized samples did not result in a mass gains but instead a mass loss due to the evaporation of KCl.

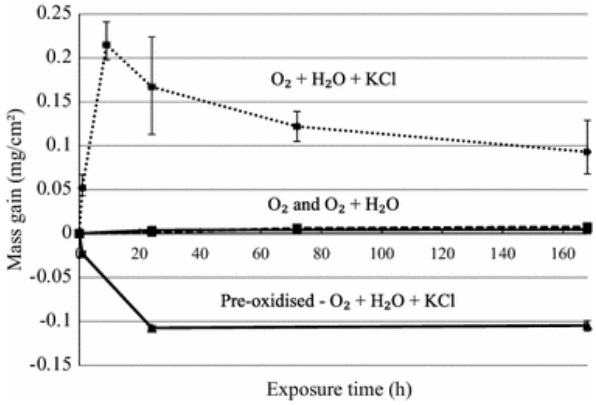

Figure 15: Mass gain versus exposure time for untreated and pre-oxidized Kanthal APMT in the presence of KCl (0.1 mg/cm2). The samples were exposed in an environment consisting of 5% O_2 + 40% H_2O at 600 °C. Also, the mass gains of two exposures without the presence of KCl, in dry and wet O_2, are shown as reference

In Figure 16 plan view SEM/BSE images are shown of untreated samples exposed in the presence of KCl after different amount of times. Already after one hour of exposure K_2CrO_4 particles are found around partly unreacted KCl particles and in some areas K_2CrO_4 particles formed a layer that tend to crack (might be due to large expansion coefficient of K_2CrO_4). Some KCl particles are already at this stage overgrown by iron-rich oxide.

After 24 hours, most of the surface consisted of iron oxide and no KCl crystals were left unreacted. K_2CrO_4 has grown in size and tend to agglomerate in certain areas, especially at former KCl crystals. Morphological features with similar distribution and shape as that of the K_2CrO_4 particles after one hour could be seen but now seems to have been decomposed.

After 168 hours the entire surface was overgrown by iron-rich oxide with ridges of iron-rich oxide surrounding the former KCl crystals.

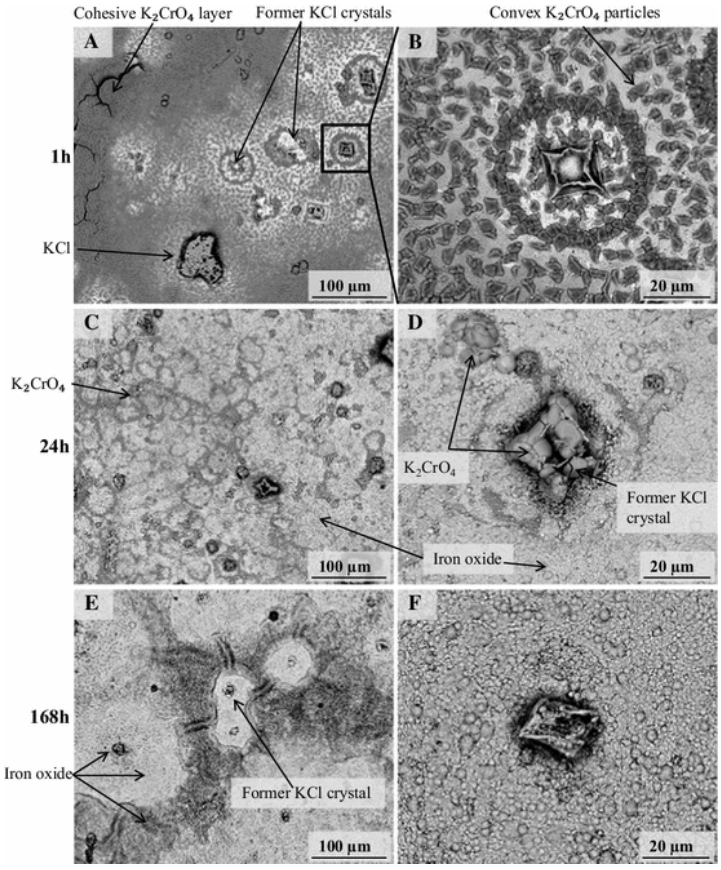

Figure 16: SEM/BSE images of Kanthal APMT exposed in 5% O_2 +40% H_2O in the presence of KCl (0.1 mg/cm2) for 1h (a,b), 24h (c,d) and 168h (e,f)

In Figure 17 plan view SEM/BSE images are shown of pre-oxidized samples exposed in the presence of KCl after different amount of times and can be compared to the case with untreated samples. After one-hour surface morphology has barely changed and shows a large difference from the case without pre-oxidation. Just a few K_2CrO_4 particles can be found and the KCl particles are less reacted than in the case without pre-oxidation.

After 24 hours, no indication KCl crystals on the surface could be detected and no morphological traces were left either (probably KCl was evaporated). The amount of K_2CrO_4 particles increased compared to after 1 hour (can be seen as dark spots in the image) but was much less than in the case without pre-oxidation.

After 168 hours the surface morphology looks similar to that after 24 hours with the only actual difference being that the K_2CrO_4 particles had been replaced with porous agglomerates of similar size and distribution. This is assumed to be remnants of decomposed K_2CrO_4 particles.

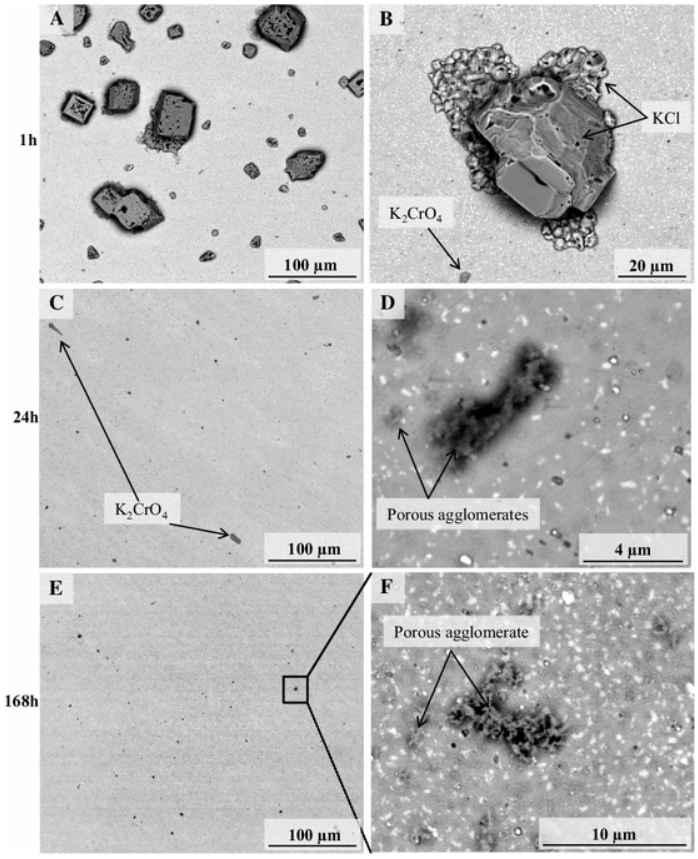

Figure 17: SEM/BSE images of pre-oxidized Kanthal APMT exposed in 5% O_2 +40% H_2O in the presence of KCl (0.1 mg/cm2) for 1h (a,b), 24h (c,d) and 168h (e,f)

5.3 THE INFLUENCE OF ALLOYING ELEMENTS ON THE CORROSION PROPERTIES OF FECRAL MODEL ALLOYS

The focus of the investigation of the model alloys was put on two alloying elements, i.e Cr and Si. This gave in total seven model alloys as described in section 4.2.

5.3.1 Alloy microstructure

Heat treatments of FeCrAl model alloys were performed in order to minimize the grainsize distribution of the as-received alloys. Figure 18 shows an example of the as received microstructure. Large elongated grains could in addition be observed in the cross sections of the as-received alloys due to insufficient heat treatments, see Figure 19.

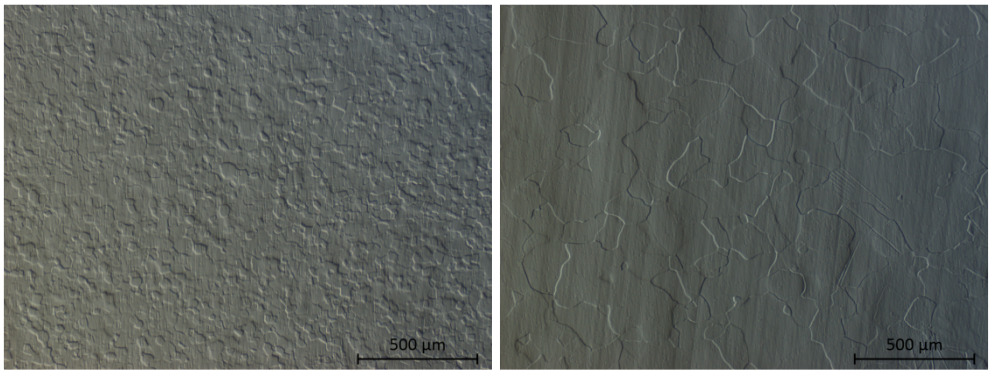

Figure 18: Images from optical microscope on two different areas of the surface of one of the as-received FeCrAl model alloys.

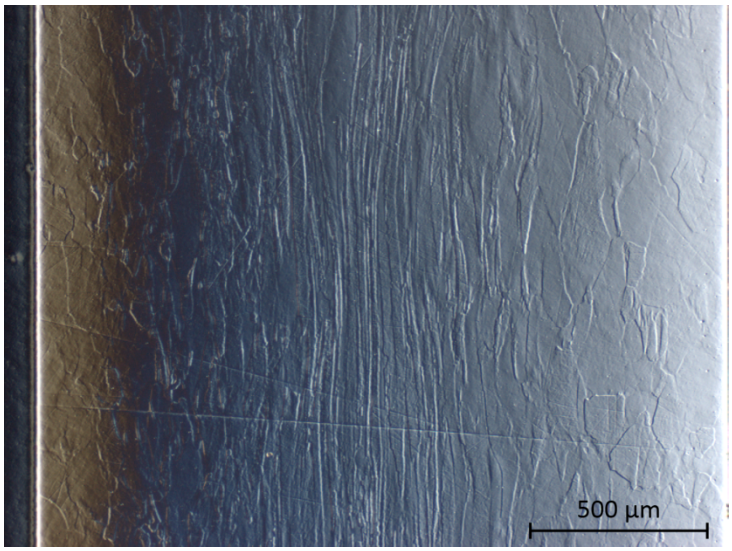

Figure 19: Image from optical microscope on the cross section of one of the as received FeCrAl model alloys.

Heat treatments were performed at 950 °C for 1h and 22h in a box furnace with the samples laying in alumina boats. The results of these heat treatments varied where some samples showed an even grain size distribution while others showed larger variation of grain sizes. Even within the same batch of alloys heat treated at the same time, differences in the resulting grain size distribution were found. However, the elongated grains seen in the cross section of the as-received alloys were removed by the heat treatment already after one hour.

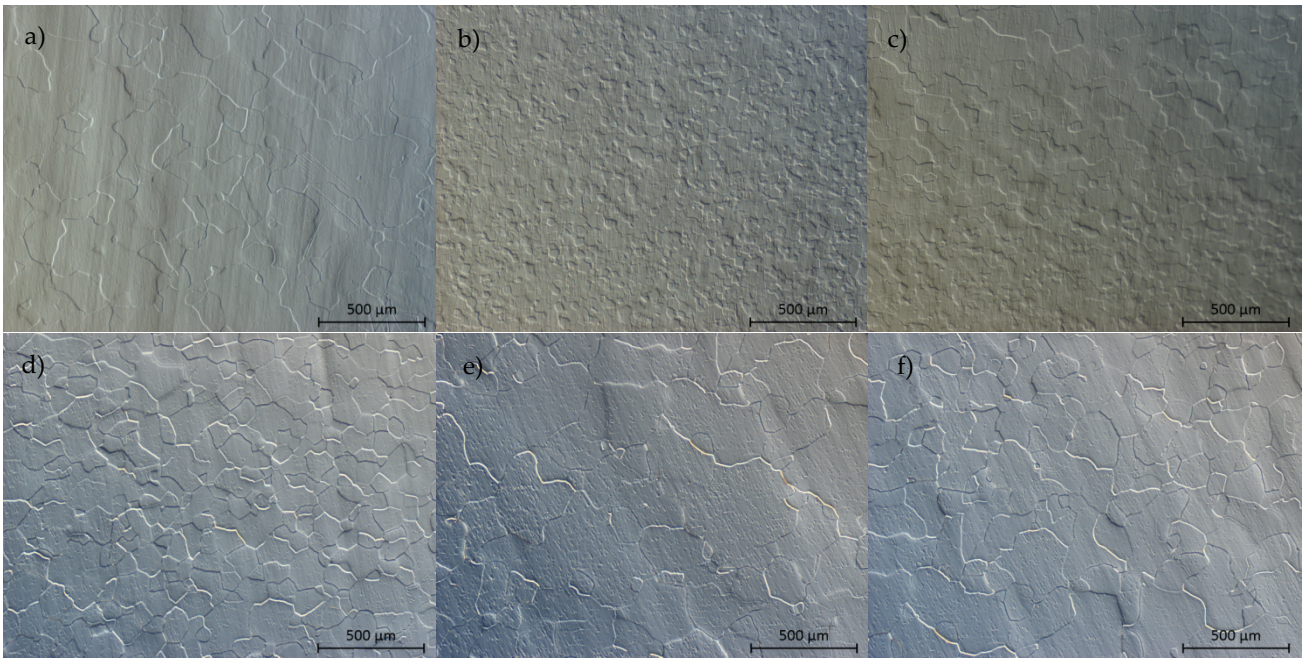

Figure 20: Images from optical microscope of a FeCrAl model alloy before (a,b,c) and after (d,e,f) heat treatment at 950°C for 22 hours.

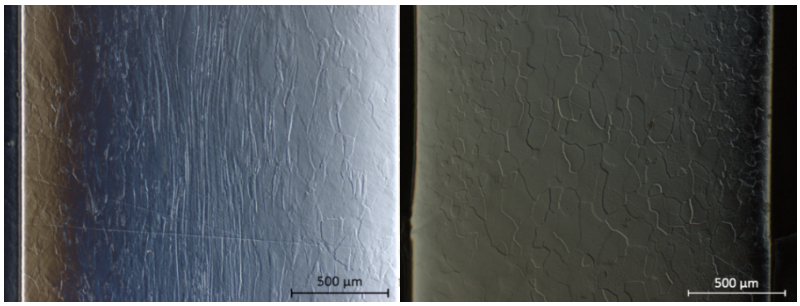

Figure 21: Images from optical microscope of the same FeCrAl model alloy before (left) and after (right) heat treatment at 950°C for 1 hour.

It may be possible to further improve the heat treatments to have an even more uniform grain size. However, this was discussed within the project group and determined to be satisfactory at this point and the microstructure variation influence would be considered in the corrosion response.

5.3.2 Reference exposures in O2 + H2O at 600 °C for 168h

In order to investigate the oxidation behaviour without KCl present reference exposures were performed in 5% O_2 + 20% H_2O + 75% N_2 at 600 °C for 168 hours.

5.3.2.1 The influence of Cr

The mass gains of the model alloys with varying Cr content are displayed in Table 9.

Alloy	Mass gain average (mg/cm2)
Fe**5Cr**Al2Si	0,025273
Fe**10Cr**Al2Si	0,008336
Fe**15Cr**Al2Si	0,002340
Fe**20Cr**Al2Si	0,003288

Table 9: Average mass gain of FeCrAl model alloys reference exposures in which **Cr** content is varied.

The resulting mass gains were low for all of the different alloys shown in Table 9. The resulting oxide layers on the samples were in the nanometre range, which could be concluded from the surface morphology/colour and mass gain of the samples after exposure. The oxide surface morphology was further studied with SEM, see Figure 22. In the image to the left, the grains of the alloy are visible, indicating that the oxide layer is very thin. As can be observed, small dark spots, corresponding to iron oxide, are scattered evenly on the surface. When looking at the right image (with higher magnification) smaller bright particles can also be observed which corresponds to zirconia particles. When taking a closer look at the larger of the dark iron oxide spots, zirconia particles can be seen in the centre of the spot. Similar features are observed in most of the other iron oxide crusts on the surface.

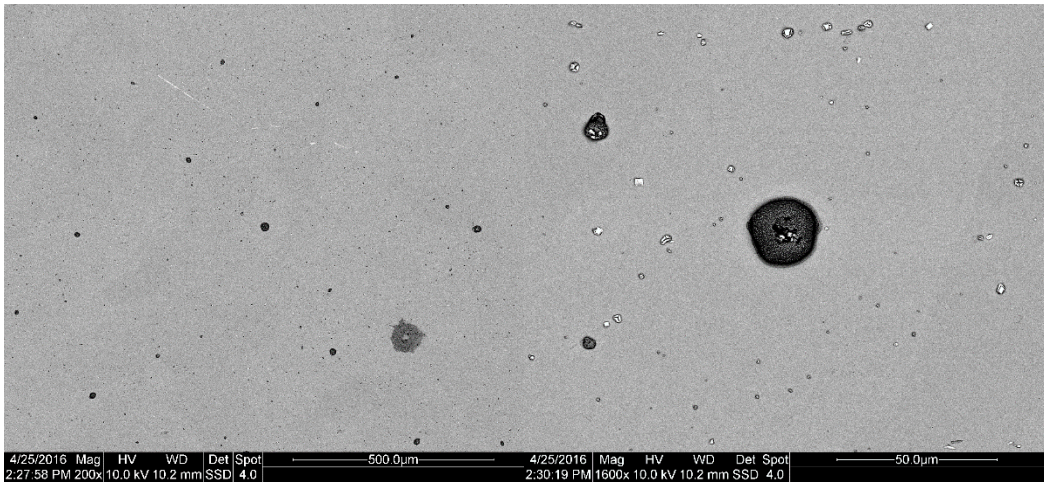

Figure 22: SEM BSE plan view images of Fe**5Cr**Al2Si sample exposed in 5% O_2 + 20% H_2O + N_2 at 600°C for 168h.

Figure 23 shows SEM/BSE images of two different alloys. The alloy grains of the sample with lowest mass gain can be observed indicating an even thinner oxide layer. Also, no dark iron oxide spots can be seen in either of the magnifications. In the image to the right bright zirconia particles can be observed.

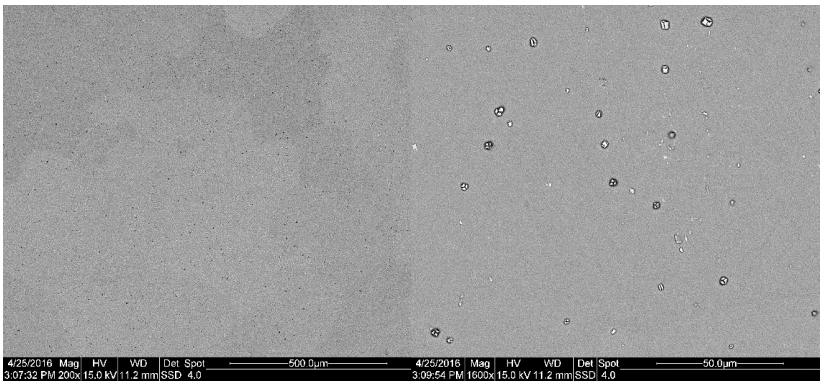

Figure 23: SEM/BSE plan view images of Fe**20Cr**Al2Si sample exposed in 5% O_2 + 20% H_2O + N_2 at 600°C for 168h

The higher magnification SEM/BSE image (Figure 24) indicates that the zirconia particle opens up in the centre. This may indicate that the spots of iron oxide originate from zirconia particles.

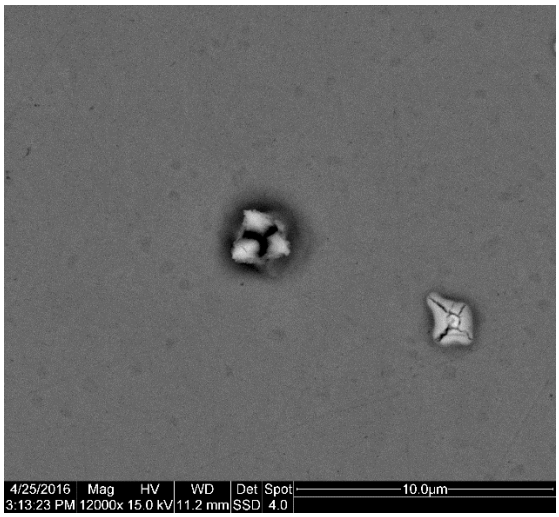

Figure 24: SEM BSE plan view image of Fe**20Cr**Al2Si sample exposed in 5% O_2 + 20% H_2O + N_2 at 600°C for 168h. Image shows a zirconia particle that have "opened up".

5.3.2.2 *The influence of Si*

The mass gains of the model alloys with varying Si content are displayed in Table 10.

Alloy	Mass gain average (mg/cm2)
FeCrAl**0Si**	10.14336
FeCrAl**1Si**	0.004530
FeCrAl**2Si**	0.000108

Table 10: Average mass gain of FeCrAl model alloys reference exposures in which **Si** content is varied.

The resulting mass gains differed drastically. FeCrAl**0Si** has formed a very thick oxide while FeCrAl**1Si** and FeCrAl**2Si** have formed thin protective oxides which is shown in Figure 25. The much thicker oxide of FeCrAl**0Si** is indicated by the rough surface morphology (Figure 25(a)).

A cross-section image of FeCrAl**0Si** is presented in Figure 26, i.e. the only alloy that had a high mass gain in the reference environment. It shows a thick oxide of about 85 µm thickness. It has formed an outward growing oxide consisting of an upper hematite layer, followed by a magnetite layer. Underneath the magnetite it has formed an Fe-, Cr-, Al-spinel followed by a reaction zone. The thickness is in good agreement with the reported mass gain.

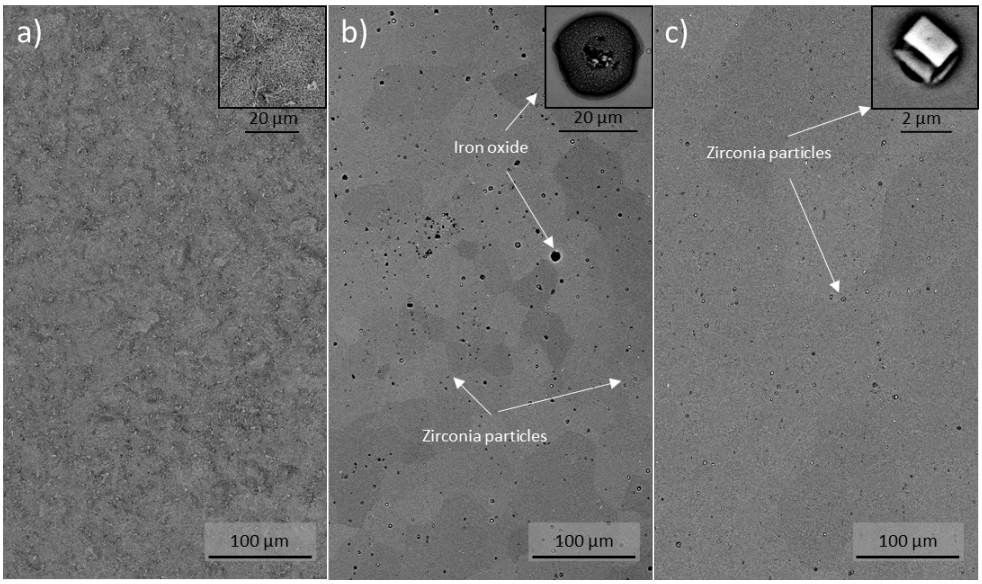

Figure 25: SEM BSE plan view images of (a) FeCrAl0Si, (b) FeCrAl1Si and (c) FeCrAl2Si exposed in 5% O_2 + 20% H_2O + N_2 at 600°C for 168h.

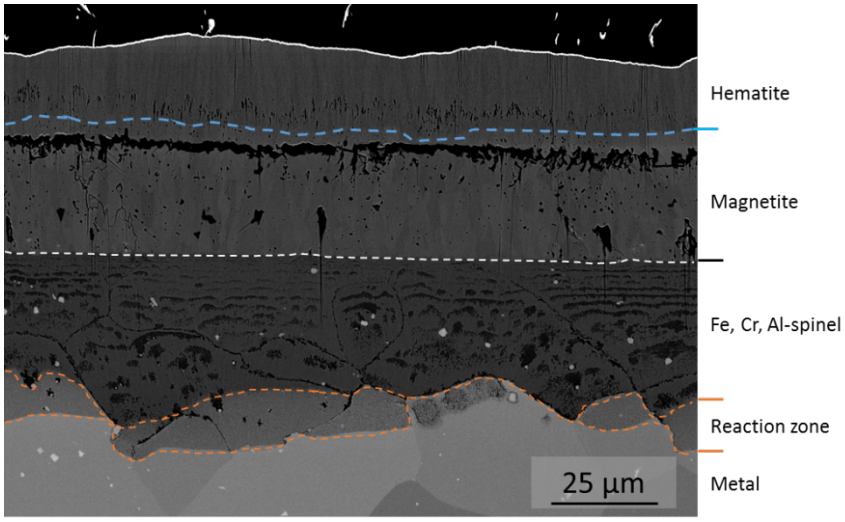

Figure 26: SEM-BSE cross section image of FeCrAl0Si after exposure in 5% O_2 + 20% H_2O + N_2 at 600°C for 168h

5.3.3 Exposures in O2 + H2O + KCl(s) at 600 °C for 168h

The exposures with KCl present, were performed in the same environment as the reference exposures, see section 4.2.1.

5.3.3.1 The influence of Cr

The average mass gains after 168h of the samples in which the Cr content is varied are shown in Table 11. The results show a decreased corrosion rate with increased Cr content. Fe**20Cr**Al2Si exhibit a mass loss due to the mass gain from the formation of corrosion products is lower than the weight of evaporated KCl.

Alloy	Mass gain average (mg/cm^2)
Fe**5Cr**Al2Si	3,173578
Fe**10Cr**Al2Si	0,945177
Fe**15Cr**Al2Si	0,433743
Fe**20Cr**Al2Si	-0,06053

Table 11: Average mass gain of FeCrAl model alloys in which **Cr** is varied in the presence of KCl

The samples were analysed with SEM/EDX both in plan view and in cross section. Figure 24 shows plan view images of the different model alloys. Figure 27(a) corresponds to Fe**5Cr**Al2Si. A porous upper oxide layer can be seen consisting mainly of iron oxide. Figure 27(b) corresponds to Fe**10Cr**Al2Si. The surface morphology is different and no porous oxide such as in (a) can be observed. When performing an EDX-mapping, indications of K_2CrO_4 was observed evenly distributed across the surface. Figure 27(c) corresponds to Fe**15Cr**Al2Si. K_2CrO_4 was distributed in a similar way but more and larger dark regions was observed on Fe**10Cr**Al2Si. Finally, Figure 27(d), corresponding to Fe**20Cr**Al2Si, shows less dark areas but large amounts of K_2CrO_4 appear distributed over the whole surface.

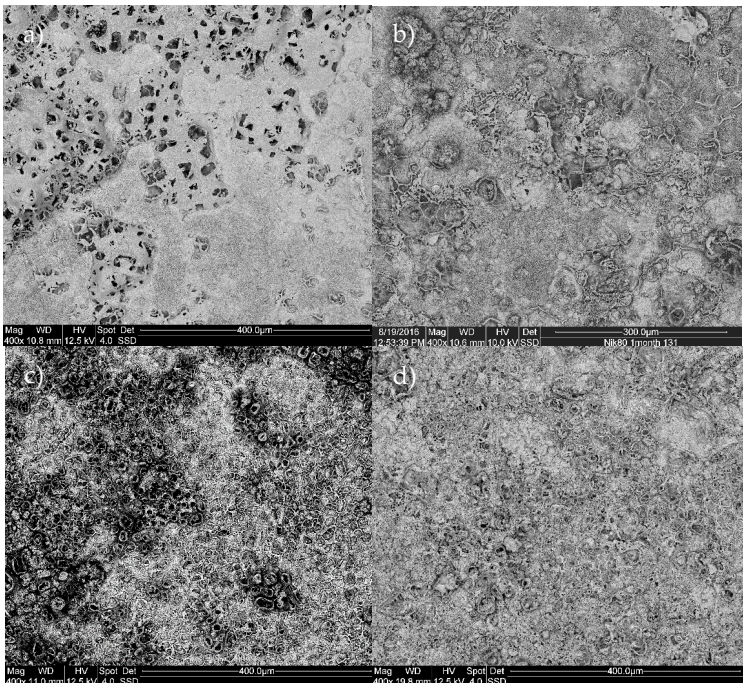

Figure 27: SEM BSE plan view images. (a) Fe**5Cr**Al2Si, (b) Fe**10Cr**Al2Si, (c) Fe**15Cr**Al2Si and (d) Fe**20Cr**Al2Si after 168 hours exposure in 5% O_2 + 20% H_2O + N_2 + 1.0 mg/cm^2 with KCl present at 600°C

In Figure 28 the decrease in oxide thickness with an increase in Cr in the alloy can be observed. The oxide scales are well adherent to the substrate in all the alloys. The oxide thickness corresponds well with the mass gains (Table 11), neglecting the crusts of K_2CrO_4 on top of the base oxide on Fe**15Cr**Al2Si and Fe**20Cr**Al2Si. The oxides on Fe**5Cr**Al2Si to Fe**15Cr**Al2Si consist of an outward growing iron oxide and an inward growing spinel oxide. It is difficult to distinguish the original metal surface on Fe**20Cr**Al2Si and therefore it is unclear if it has both an inward and outward growing oxide. However, chromium-rich oxide grows inward in the alloy on some parts indicating metal grain boundary attack. This phenomenon was also observed for Fe15CrAl2Si but not to the same extent as Fe20CrAl2Si. A nitridation zone beneath the oxide scale was observed on all of the model alloys.

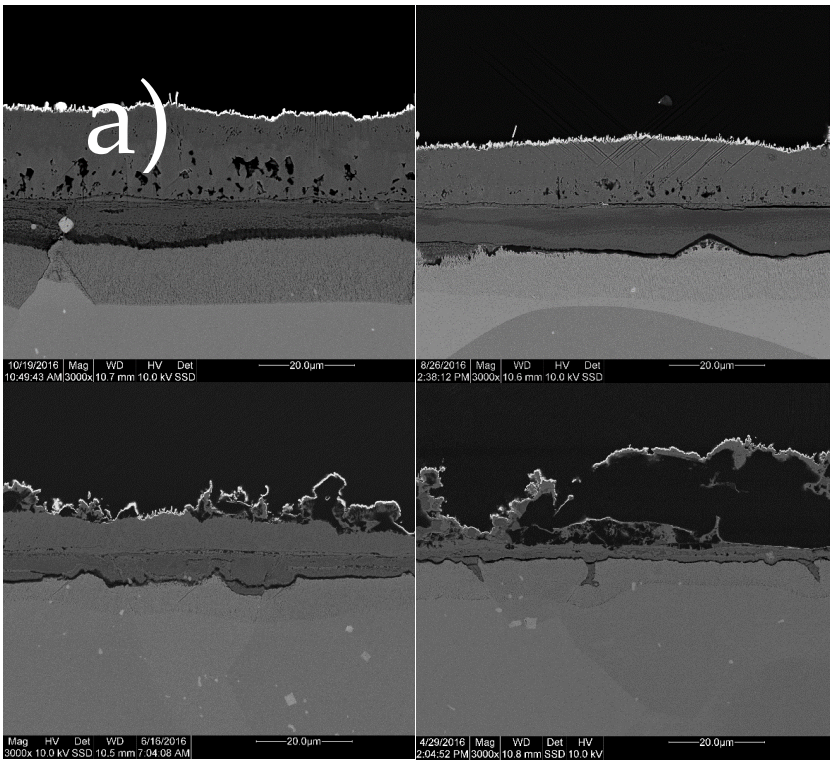

Figure 28: SEM BSE cross section images of a) Fe**5Cr**Al2Si, b) Fe**10Cr**Al2Si, (c) Fe**15Cr**Al2Si and (d) Fe**20Cr**Al2Si after 168 hours exposure in 5% O_2 + 20% H_2O + N_2 + 1.0 mg/cm^2 KCl at 600°C.

5.3.3.2 *The influence of Si*

The average mass gain of the samples in which the Si content is varied and are shown in Table 12. The mass gain data after 168h shows a large decrease in the corrosion rate by adding small amounts of Si. Higher levels gives lower corrosion rate.

Alloy	Mass gain average (mg/cm2)
FeCrAl**0Si**	9,50769
FeCrAl**1Si**	2,356443
FeCrAl**2Si**	0,945177

Table 12: Average mass gains of FeCrAl model alloys in which **Si** is varied in the presence of KCl.

The plan view images in Figure 29 indicate that all three alloys have formed thick oxides, indicated by the rough surface morphology with K_2CrO_4 spread out all over the surface, in good agreement with the mass gains. The thin protective scale formed in the reference environment with oxygen and water vapor has broken down at an earlier stage or not formed at all.

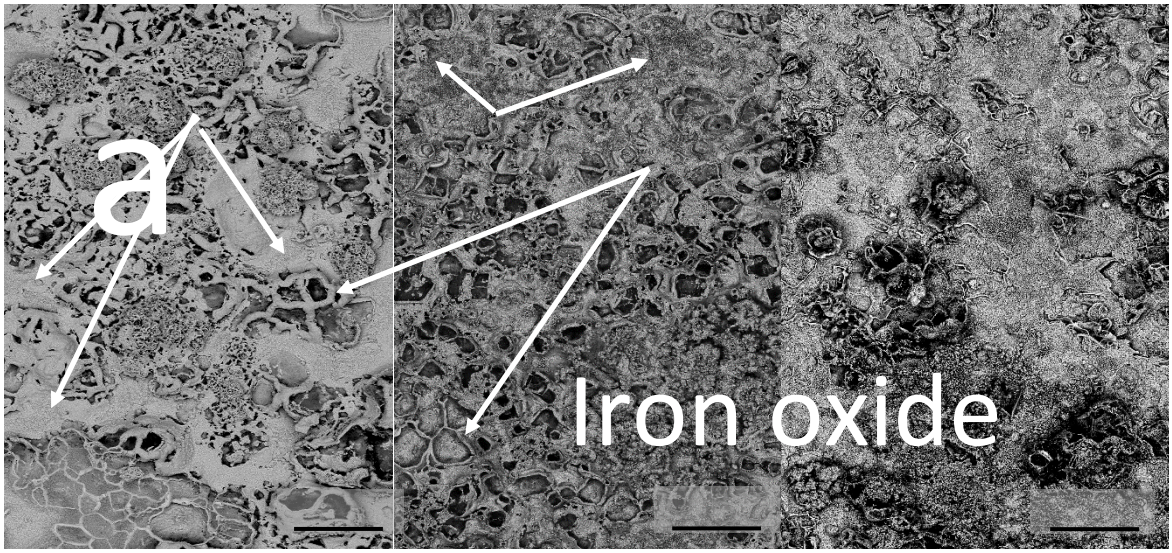

Figure 29: SEM-BSE plan view image of a) FeCrAl**0Si**, b) FeCrAl**1Si** and c) FeCrAl**2Si** after being exposed with KCl present for 168 hours at 600 °C.

Figure 30 shows all the cross sections and the beneficial effect of adding Si could be observed as well as the effect of amount of Si.

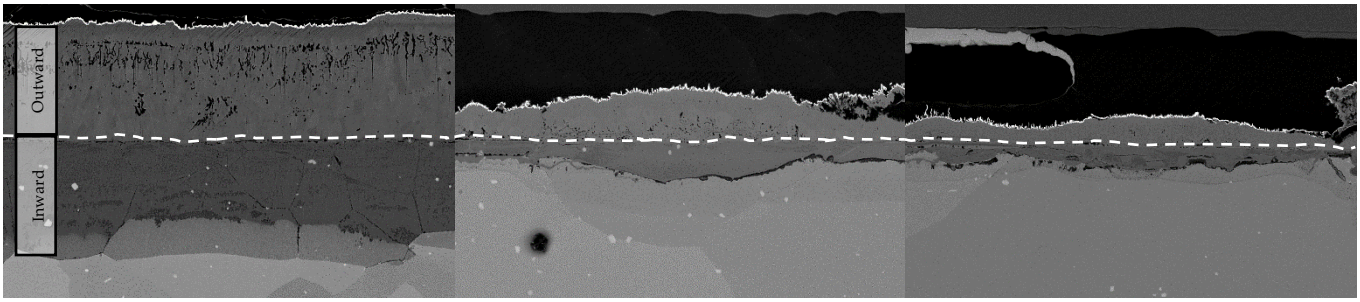

Figure 30: SEM-BSE cross section images of a) FeCrAl**0Si**, b) FeCrAl**1Si** and c) FeCrAl**2Si** after exposure with KCl present for 168 hours at 600 °C.

Figure 31 shows the oxide layer formed on FeCrAl0Si. An outward growing oxide consisting of a thin upper hematite layer followed by a much thicker magnetite layer, has grown. Underneath the magnetite layer it was found an inward growing oxide consisting of an Fe-, Cr-, Al-spinel followed by a reaction zone, indicated by the brighter contrast compared to the spinel (darker compared to the bulk).

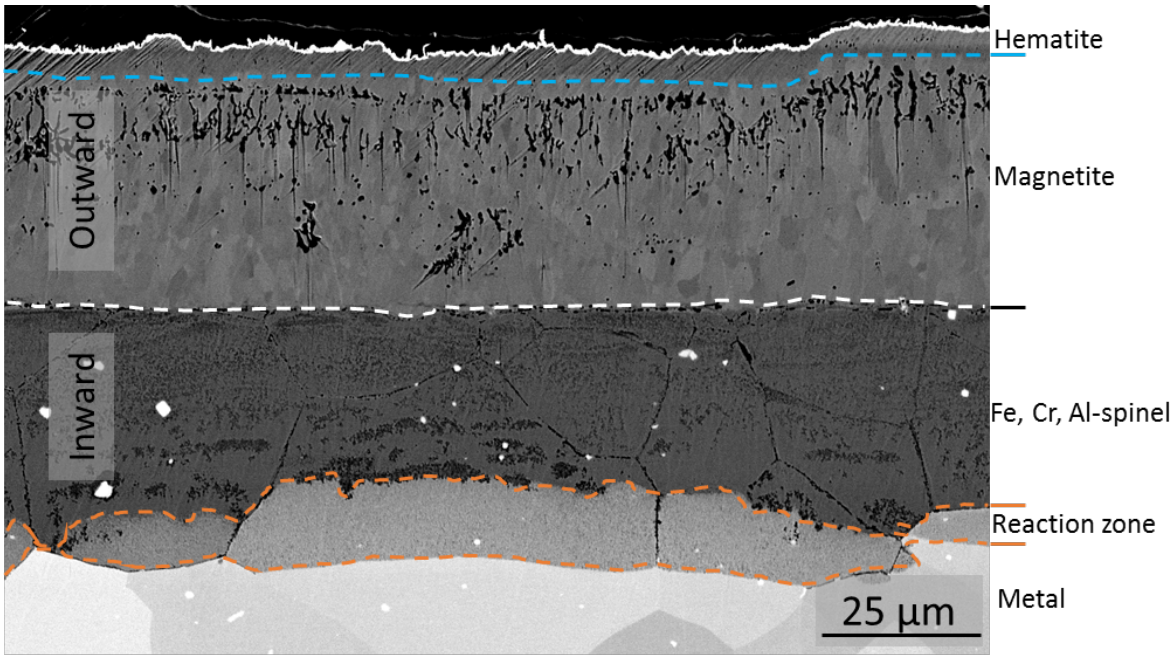

Figure 31: SEM-BSE cross section image of FeCrAl**0Si** after exposure with KCl present for 168 hours at 600 °C.

Figure 32 shows the different oxide layers of FeCrAl**1Si** in cross-section. It has formed an outward growing oxide consisting of an upper hematite layer followed by a magnetite layer. It has also formed an inward growing Fe-, Cr-, Al-spinel. Underneath the spinel, instead of a reaction zone, a nitridation zone has formed.

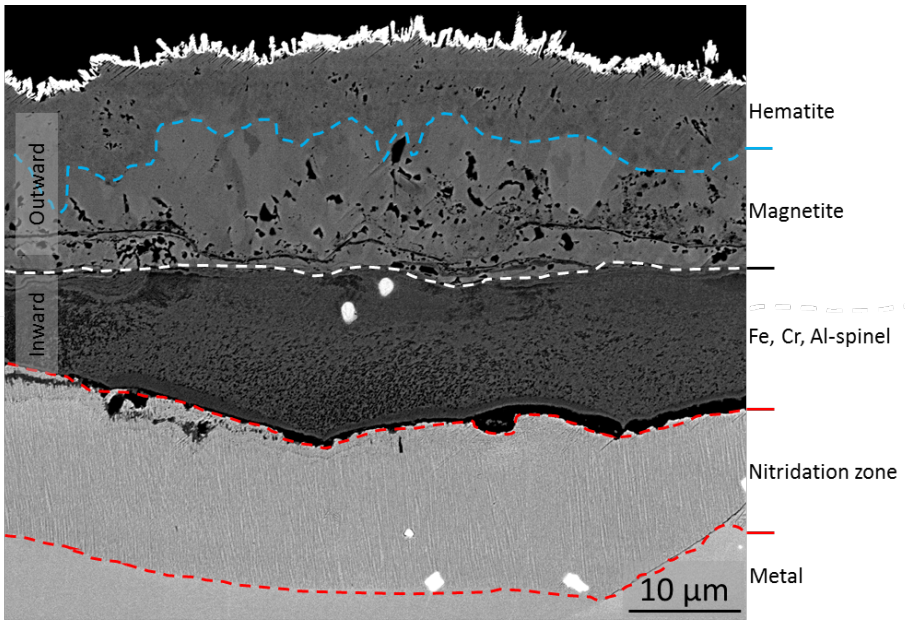

Figure 32: SEM-BSE cross section image of FeCrAl**1Si** after exposure with KCl present for 168 hours at 600 °C.

Figure 33 shows the different oxide layers of FeCrAl**2Si** in cross-section. It has formed an outward growing oxide but it only consists of a thicker hematite layer and no magnetite. Underneath the hematite it has formed an Fe-, Cr-, Al-spinel, followed by a nitridation zone.

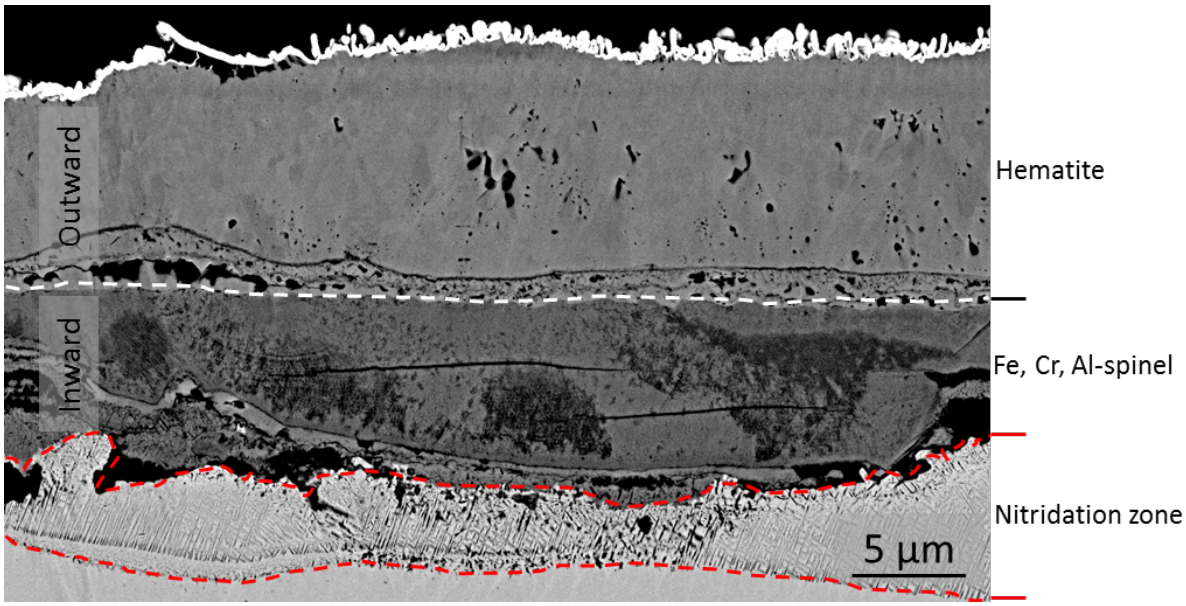

Figure 33: SEM cross section image of FeCrAl**2Si** after exposure with KCl present for 168 hours.

Short time exposures have been performed in the HTC project critical corrosion phenomoneon and shows a very similar incubation time to breakaway oxidation on all samples exposed in the presence of KCl.

6 Results – Investigation of the Steamboost position at AffaldPlus

The environment of the Steamboost position at the AffaldPlus boiler was investigated through a deposit test. The corrosion resistance of commercial stainless steels, state of the art stainless steels and FeCrAl alloys were in addition investigated at the Steamboost position. This was done through both fixed installations and air-cooled probe tests.

6.1 ENVIRONMENT INVESTIGATION - DEPOSIT PROBE INVESTIGATION

The environment at the Steamboost position was investigated through deposit probes. Specially the influence of the boiler settings was investigated. This was done during one campaigns as described in section 4.3.3. The exposures generated 29 samples. Deposits were in addition collected from the fixed installed material after removal.

6.1.1 Optical inspection

The air-cooled probe was inserted at the Steamboost position 1h after the settings were changed which was time enough for the boiler to be stable with the new settings. After 2h exposure in the boiler, the samples were removed for analysis and pictures were taken for optical inspection. Figure 34 shows three different deposits formed at three different settings (setting K22, S22 and C11 in Figure 35). The amount of deposit is different for every setting going from very small amounts (Figure 34 (b)) to extremely thick deposits (Figure 34 (c)).

(a) (b) (c)

Figure 34. Images of three different deposits after 2 hours of exposures from the settings (a) K22, (b) S22 and (c) C11. 29 different conditions were set up in the boiler in order to find out the less corrosive one. All the deposits from the 29 settings were analysed to select the one to run the corrosion test

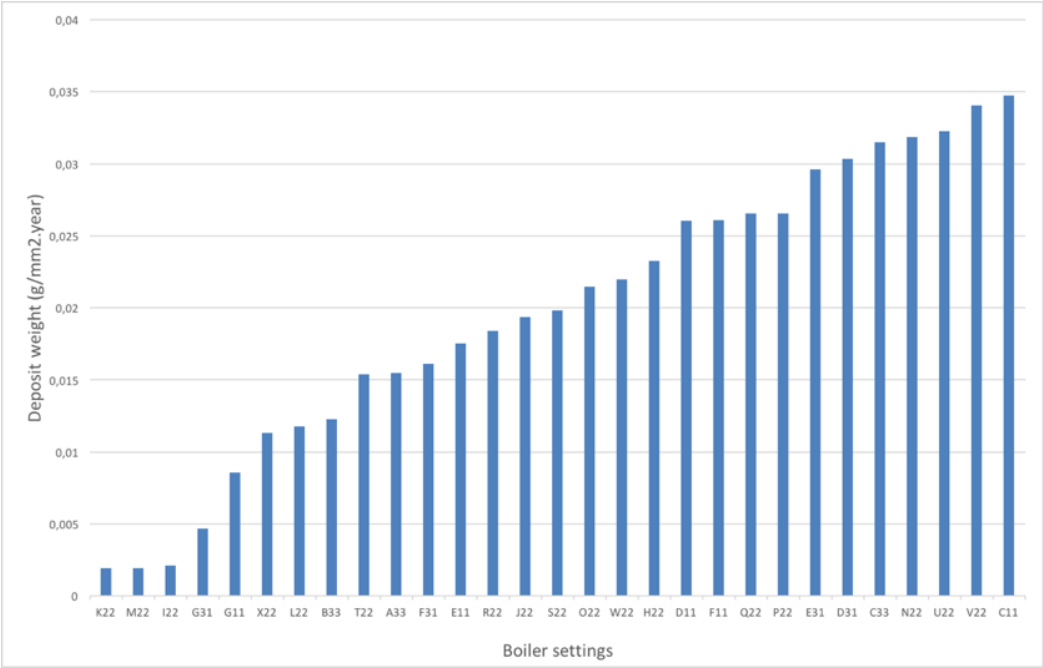

Figure 35. Amount of deposit in grams of the 29 settings tested in the boiler

6.1.2 Scanning Electron Microscopy (SEM)

A selected reference sample was cast and cut in order analyse the deposit in cross-section with SEM/EDX. The aim was to check the amount of deposit and its composition and compare this with the IC results. After 2h exposure the amount of deposit was limited in this setting (setting C33 in Figure 35) and according to EDX it is mainly composed of silicon with some calcium and sodium (Figure 36).

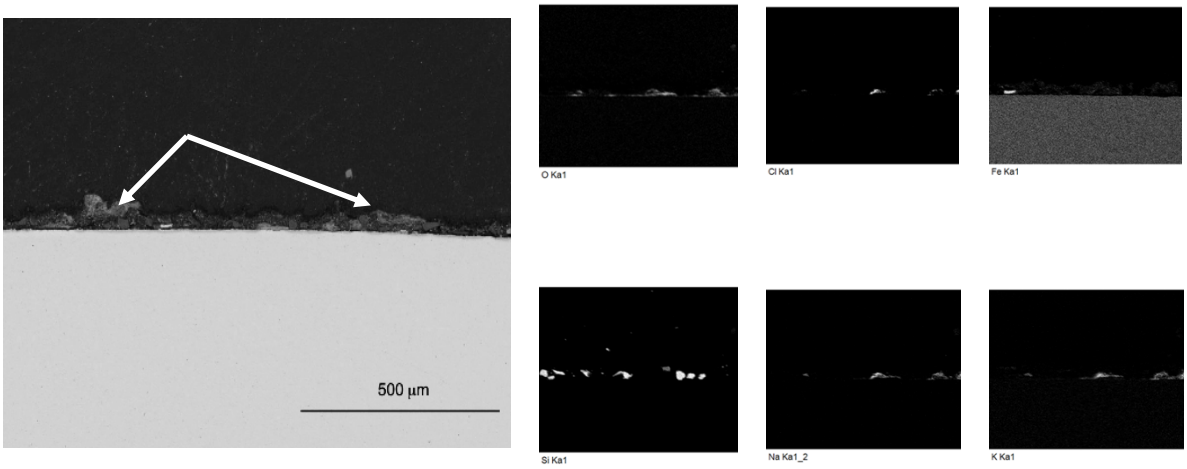

Figure 36. Scanning Electron Microscopy backscattered image of a Sanicro 28 material exposed 2h in the Steamboost region

6.1.3 X-Ray Diffraction (XRD)

The reference sample from the commercially used setting of the boiler was in addition analysed by XRD in order to confirm the composition of the deposit given by the EDX. The XRD diffractogram showed a deposit composed mainly by silicates and also some hematite (Fe_2O_3) is present (not shown). The amount of chlorine for this deposit was very low and no KCl was detected during the XRD analysis.

6.1.4 Ion Chromatography (IC)

The deposits generated during the 29 2h exposures with different settings of the boiler were analysed with Ion Chromatography. The amount of deposit, the chlorine content and the S/Cl ratio were calculated for all the settings. Figure 37 shows the different settings ordered by the chlorine content while the Figure 38 represents the settings ordered by the S/Cl ratio. The results were evaluated and the heat transfer was considered in order to decide on one setting for the corrosion test. The setting K22 (marked in red in Figure 37 and Figure 38) was selected for the corrosion test. The chlorine content is mild (around 6,5 % in weight) and the amount deposited is very low with a value of 0,002 g/mm^2.year, see Figure 35.

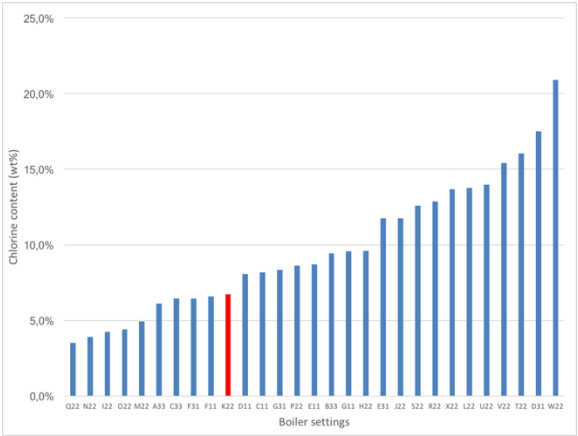

Figure 37. Chlorine content in the deposit of the 29 settings tested in the boiler

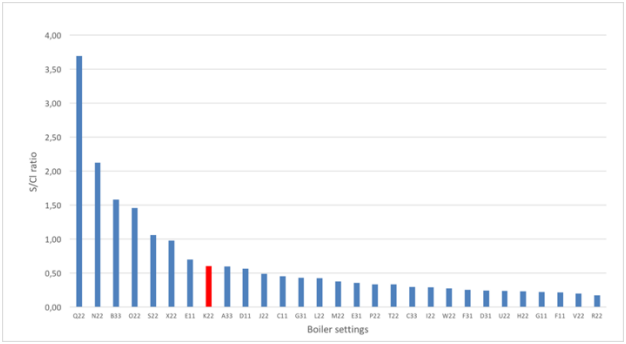

Figure 38. S/Cl ratio obtained from the deposits of the 29 settings of the boiler

6.1.5 Deposit from fixed installed material

The deposit taken from the fixed installed Steamboost tubes (first installation) was analysed by using Ion Chromatography and the results are shown in Figure 39.

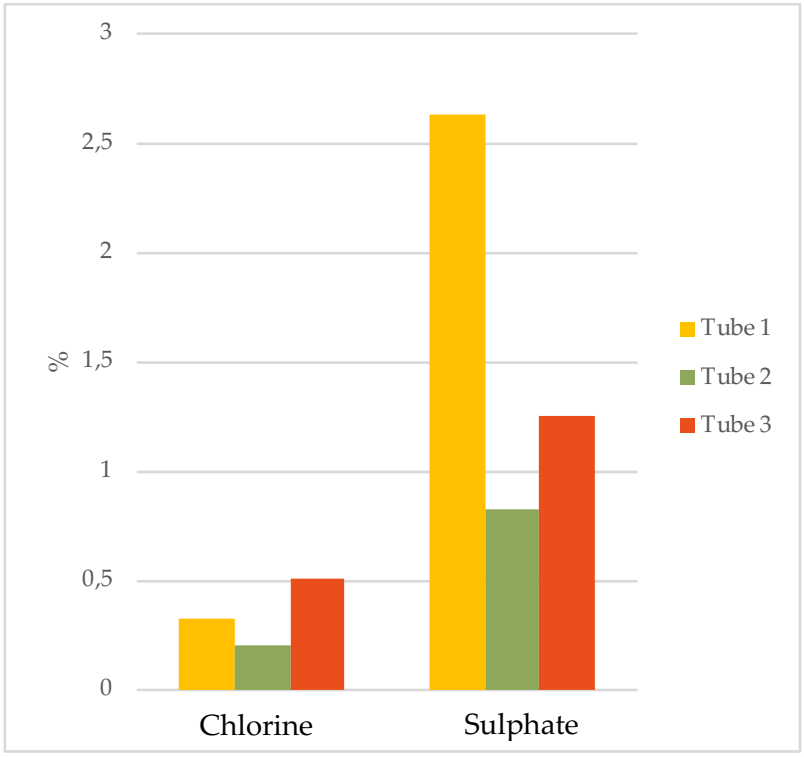

Figure 39. Ion Chromatography results show the percentage of chlorine and sulphate in the deposit of the three different tubes.

The chlorine content was very low in all the collected samples and lower than the sulphate content in all the cases. This could be caused by the fact that the boiler was cleaned before the collection of the samples.

6.2 MATERIAL INVESTIGATION - FECRAL TUBE INSTALLATION

The pre-oxidized (8h and 1050°C) Kanthal APMT FeCrAl tube was inserted at the Steamboost position in the AffaldPlus boiler and exposed for 4500h. After each exposure, a sample was cut and analyzed as described in section 4.3.2.

6.2.1 First FeCrAl tube sample - 2016

After 4500h a part of the tip from the FeCrAl tube was cut and analysed with SEM. The investigation showed that approximately 50% of the tube still had the pre-oxide formed protective alumina oxide remaining (Figure 40). The scale thickness is in thickness is in the µm range thick and aluminium rich. In the bulk, some inner Cr rich regions could be observed.

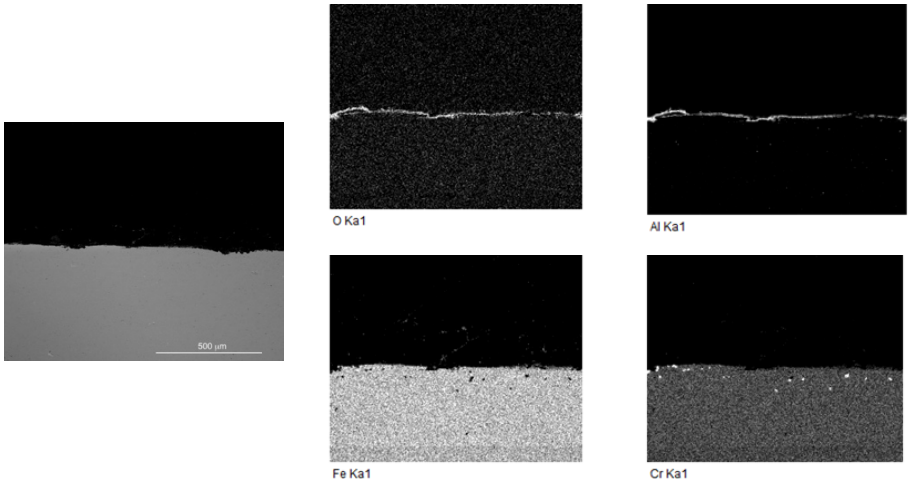

Figure 40. Backscattered SEM image and EDX analysis of the FeCrAl tube placed at Steamboost area 4500h. This area represents the 50% of the tube where the protective alumina was not damaged

However, in the remaining 50% of the tube the alumina layer was damaged/absent and the material is covered by thick iron and chromium oxide scales. Indications of nitrides inside the bulk material could also be observed (Figure 41).

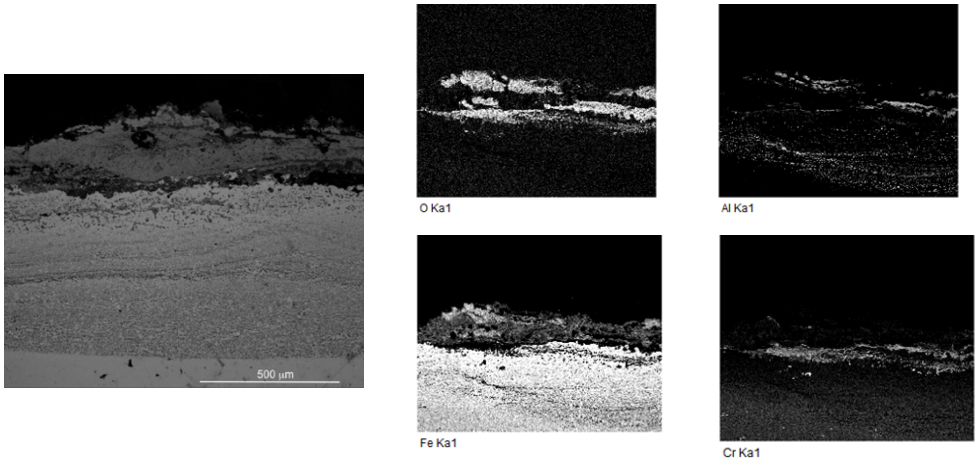

Figure 41. Backscattered SEM image and EDX analysis of the FeCrAl tube placed at Steamboost area 4500h. This area represents the 50% of the tube where the protective alumina was cracked and corrosion occurred

6.2.2 Second FeCrAl tube sample - 2017

After analysing the 2016 sample, the tube was inserted and exposed in the same position at the Steamboost region. After approximately 12000h the change in shape was observed. The bent tube was then removed for analysis, see Figure 12.

Figure 42 shows a SEM/BSE images of the top part of the tube. The sample was very corroded and indications of nitrides could be found all the through the sample, see EDX analysis. No traces of an alumina scale were observed on any part of the sample. Figure 43 shows the bottom part of the tube which had a similar microstructure and corrosion attack.

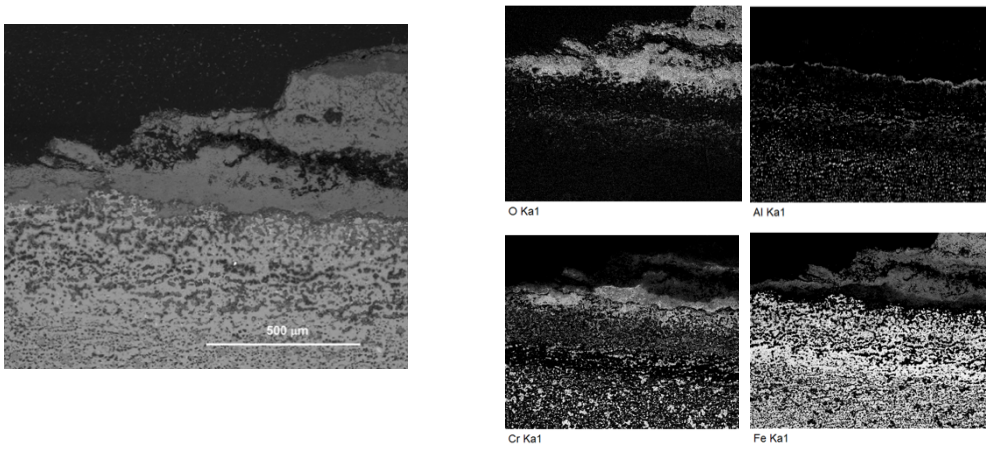

Figure 42. Backscattered SEM image and EDX analysis of the top of the FeCrAl tube

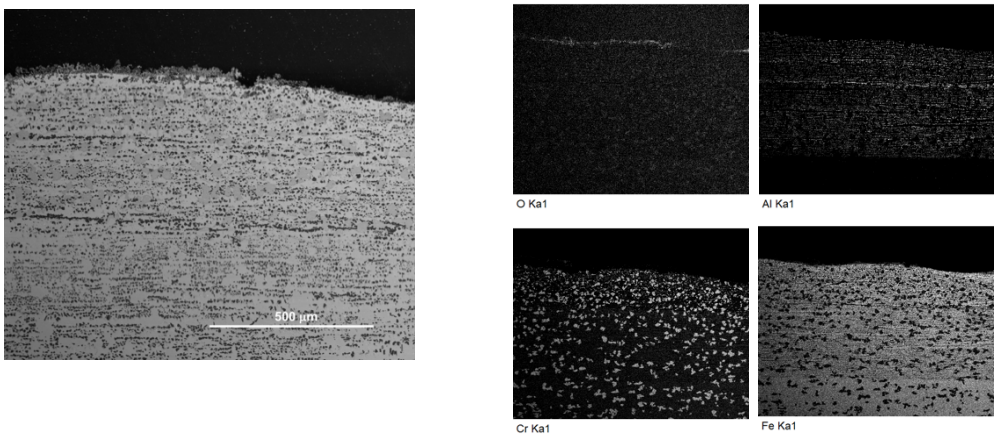

Figure 43. Backscattered SEM image and EDX analysis of the bottom of the FeCrAl tube

6.3 MATERIAL INVESTIGATION - CORROSION PROBE INVESTIGATION

The air-cooled probe corrosion investigation was performed during winter 2016 in the AffaldPlus boiler in Naestved (Denmark). The aim was to investigate the initial corrosion attack and the oxidation propagation of seven different materials at the Steambost position. The boiler settings had been optimized during the deposit test and was run with setting K22. The exposures consisted of a 24 hours exposure followed by a 1000 hours exposure in the Steamboost superheater region. The over weld Inconel 625 was selected as reference in all exposures with an as received surface. The investigation generated a large set of samples and analysis results. Selected parts are shown below and some are appended in appendix I.

6.3.1 Initial corrosion attack – 24h exposure

Figure 44 shows the probe (a) before and (b) after the 24h exposure. The probe has two temperatures zones, i.e. 525 °C and 700 °C. After the exposure, limited amount of deposit could be observed on the samples in good agreement with the deposit found after this setting of the boiler. However, some spallation could be observed on the samples.

(a)

(b)

Figure 44. (a) Probe with the samples before exposure (b) Probe with the samples after 24 h exposure in the Steamboost region

The materials exposed at 525 °C were 347H, 310, Sanicro 33 and Inconel 625 overweld. The selected materials for 700°C were Kanthal APMT, Nikrothal PM58, Inconel 625 over weld and a FeCrAl model alloy (Fe10Cr3Al2Si). After the 24h exposure all the samples were removed and stored in desiccators awaiting analyses. In order to study the corrosion attack of the different materials, cross-sections of the samples were prepared and investigated by SEM/EDX. The main aim was to investigate the initial corrosion attack in order to better understand the long-term behaviour.

6.3.1.1 *Initial corrosion attack - SEM/EDX analysis*

Polished cross-sections of all samples were analyzed with SEM/EDX except the 625 over weld. In general, the corrosion attack was affecting several 100µm of the each of the alloy after the 24h exposure. In many cases the oxide and deposit spalled off during handling of the samples or during cooling the samples after the exposure. The results from three materials, i.e. 347H exposed at 525 °C, Kanthal APMT and the FeCrAl model alloy exposed 700 °C, are shown below. SEM/EDX results from the other materials could be found in appendix I.

- **347H exposed at 525 °C for 24h**
  The SEM/EDX investigation of the cross-section shows that only small amounts of deposit are left on the sample, see Figure 45. The remaining deposit consist of K, Ca, Na and S while very little/no chlorine could be found in the deposit. The oxide scale is approximately 250 µm and composed of an outward growing Fe rich oxide of about 100 µm, and an inward growing Fe-Cr-Ni oxide. In the inner part of the oxide scale chlorine could be detected indicating the presence of metal chlorides, see Figure 46. Indications of alloy grain boundary attack could be observed on some positions.

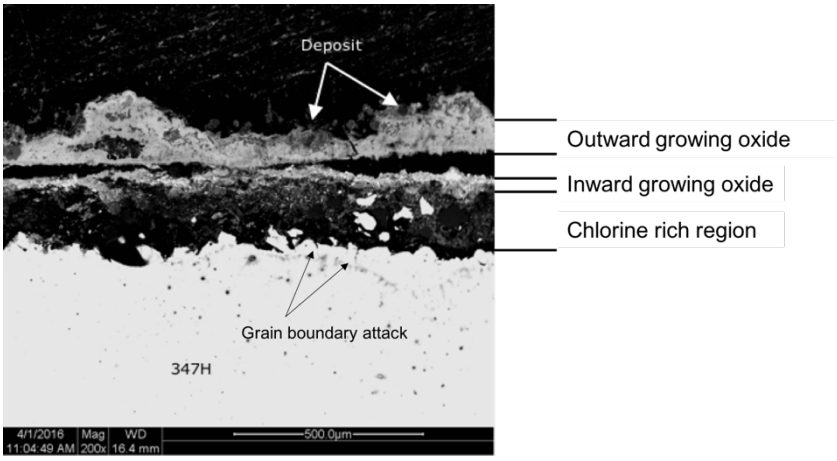

Figure 45. Backscattered SEM image of the 347H sample after 24h exposure

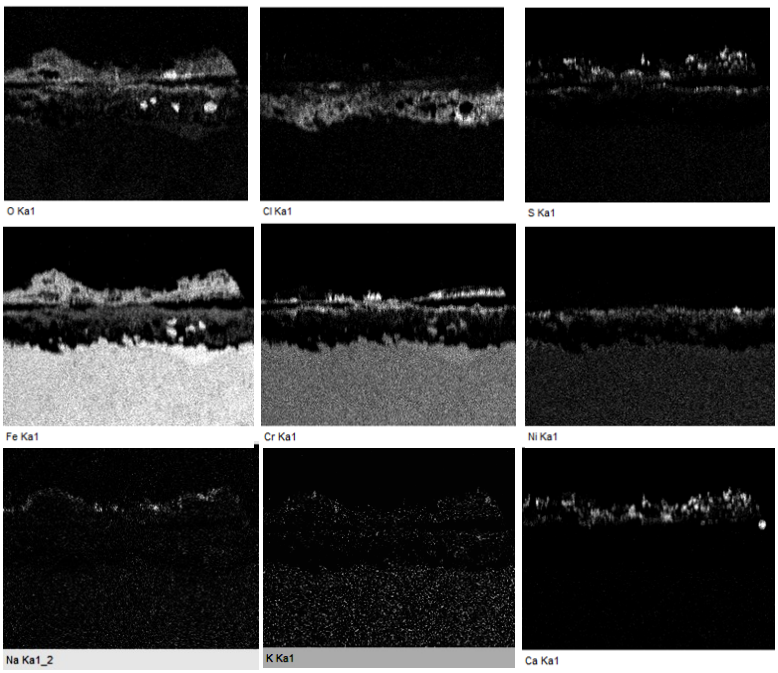

Figure 46. EDX mapping analysis of the 347H sample after 24h exposure

- **Kanthal APMT exposed at 700°C for 24h**
  The SEM/EDX investigation of the Kanthal APMT alloy exposed at 700 °C also shows that only small amounts of deposit are left on the sample, see Figure 47. The remaining deposit consists of K, Ca, Na and S while very little/no chlorine could be found in the deposit also at 700 °C. The oxide scale is approximately 50 µm and composed of an outward growing Fe rich oxide of about 25 µm, and an inward growing Fe-Cr-Al oxide. A discontinuous aluminium oxide was found at the metal/oxide interface. SEM/EDX quantification showed that it was pure alumina. Indications of the formation of a Cr rich phase along alloy grain boundary could be observed in the bulk material, see Figure 48. No indications of any nitridation could be observed.

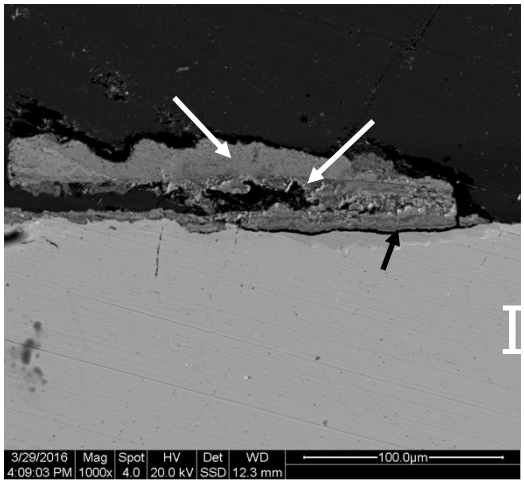

Figure 47. Backscattered SEM image of the Kanthal APMT sample after 24h exposure

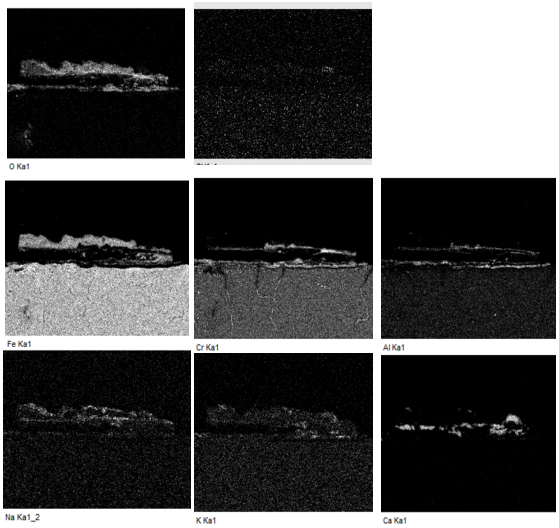

Figure 48. EDX mapping analysis of the Kanthal APMT sample after 24h exposure

- **Model Alloy exposed at 700 °C for 24h**
  A representative image from the model alloy after 24h exposure is presented in Figure 49. The EDX analysis presented in Figure 50 shows that no or very little deposit was left after the handling of the sample. A chromium and aluminium oxide appears covering the whole surface of the sample and an approximately 100 μm layered iron, chromium and aluminium oxide is formed over it.

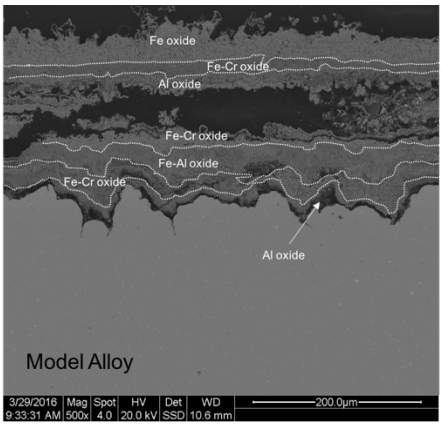

Figure 49. Backscattered SEM image of the model alloy after 24h exposure

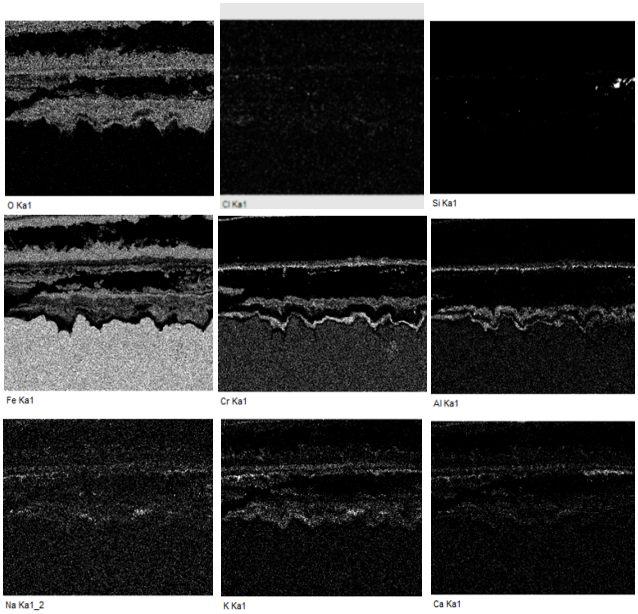

Figure 50. EDX analysis of the model alloy sample after 24h exposure

6.3.2 Corrosion propagation - 1000h exposure

The 24 hours exposure was followed by a 1000h exposure of the same material matrix, i.e. the materials exposed at 525 °C were 347H, 310, Sanicro 33 and Inconel 625 over weld. The selected materials exposed at 700 °C were Kanthal APMT, Nikrothal PM58, Inconel 625 over weld and a the FeCrAl model alloy (Fe10Cr3Al**2Si**). In order to study the corrosion attack after 1000h material loss measurements as well as cross-sections investigations by SEM/EDX analysis were conducted. Figure 51 shows the probes with the samples before and after the exposure. After 1000h exposure a thick deposit covers the probe. The sample closest to the probe tip, i.e. the model alloy sample ring broke due to mechanical failure during mounting on the probe. It was still possible to mount the sample and start the exposure (no extra sample was available). After 500 h exposure one part of the ring was lost exposing the thermocouple to the hot flue gas. This affected the thermocouple controlling of the 700 °C temperature zone for approximately 100 h of the exposure.

(a)

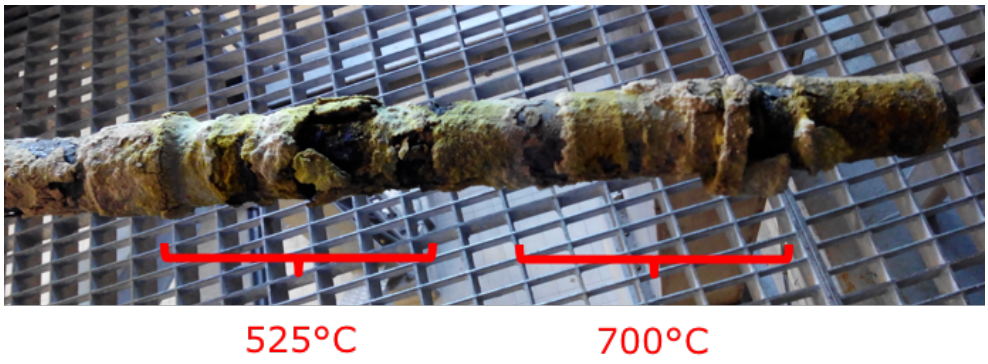

(b)

Figure 51. (a) Probe with the samples before exposure (b) Probe with the samples after 1000 h exposure in the Steamboost region

6.3.2.1 *Corrosion propagation – material loss measurements*

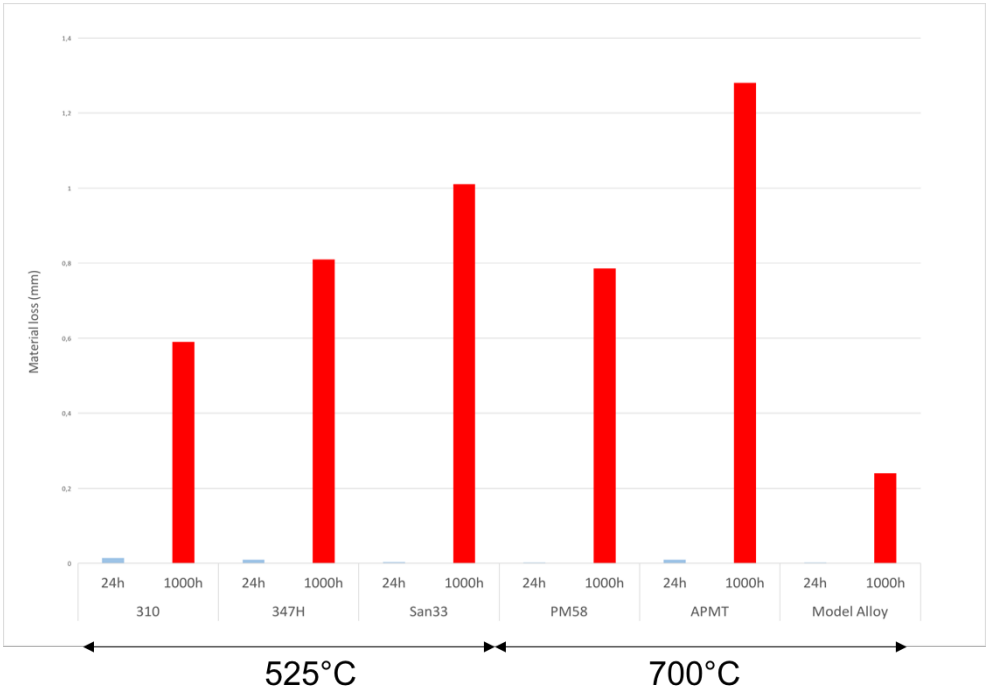

Figure 52 shows the material loss calculated for the materials exposed 1000h in the Steamboost region compared to the 24h exposure. The analyses were carried out as described in 3.2.6.3. The over welded materials were not included in the material loss measurements due to the high error that the shape of the weld seam introduces. It should be pointed out that the temperature control of the 700 °C temperature zone was lost for about 100h of the exposure. The corrosion rates are high and in line with the fast-initial corrosion attack observed on the 24 h samples. The two alumina forming alloys represent the highest material loss (Kanthal APMT) and the lowest material loss (Model alloy).

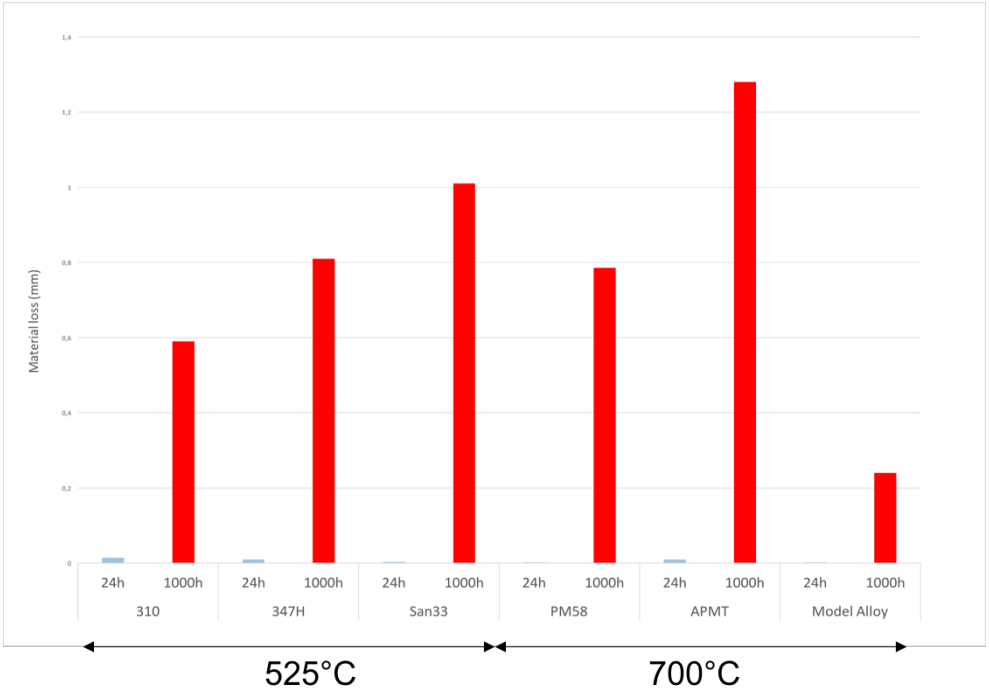

Figure 52. Material loss of the different materials exposed 24h and 1000h in the Steamboost region.

6.3.2.2 Corrosion propagation – SEM/EXD analysis

Polished cross-sections of all samples were prepared for SEM/EDX. In many cases the oxide and deposit spalled off during handling of the samples or during cooling the samples after the exposure. The results from three materials, i.e. 347H exposed at 525 °C, Kanthal APMT and the FeCrAl model alloy exposed 700 °C, are shown below. All other SEM/EDX results could be found in appendix I.

- **347H exposed at 525 °C for 1000h**
  The cross section of the sample presented in Figure 53 shows that no deposit is left on the sample after 1000h exposure on the 347H sample. The thick deposit formed over the samples during the exposure was lost during the removal of the samples from the probe.

  The SEM/EDX results show that very little of the oxide scale remains while a deep grain boundary attack could be observed. The attack penetrates about 300 µm deep into the alloy. The EDX maps (Figure 54) shows that the oxide scale is formed mainly by chromium oxide at the grain boundaries and a nickel enriched metal close to the Cr rich oxide. Very little chlorine was detected and, when detected, it was at the outside of the alloy indicating spallation at the oxide/chloride/metal interface.

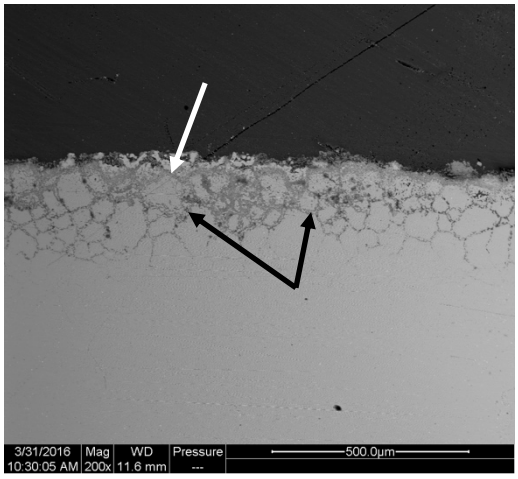

Figure 53. Backscattered SEM image of the 347H sample after 1000 h exposure

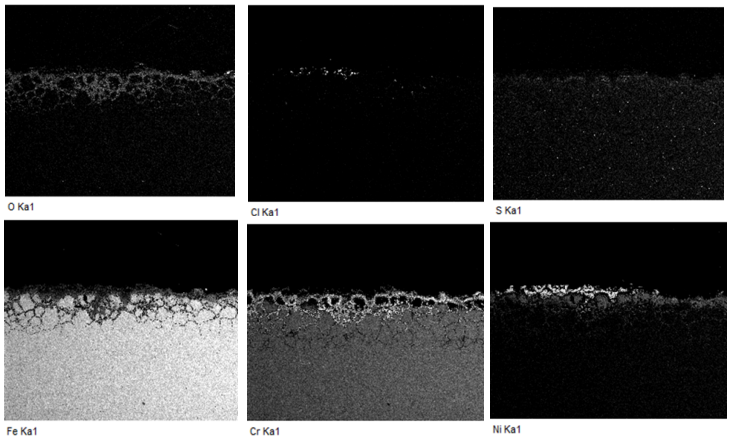

Figure 54. EDX mapping analysis of the 347H sample after 1000 h exposure

- **Kanthal APMT exposed at 700 °C for 1000h**
  A cross-section of the Kanthal APMT sample exposed 1000h at 700°C is presented in Figure 55. The material is heavily corroded with a corrosion product layer thicker than 500 µm. The EDX analysis (Figure 56) shows that the outer part of the corrosion products consists of an about 150 µm iron-chromium oxide layer. This is followed by a very thick and non-continuous and non-protective aluminium oxide. A large nitridation zone could be observed as well as the formation of a Cr rich phase in the bulk.

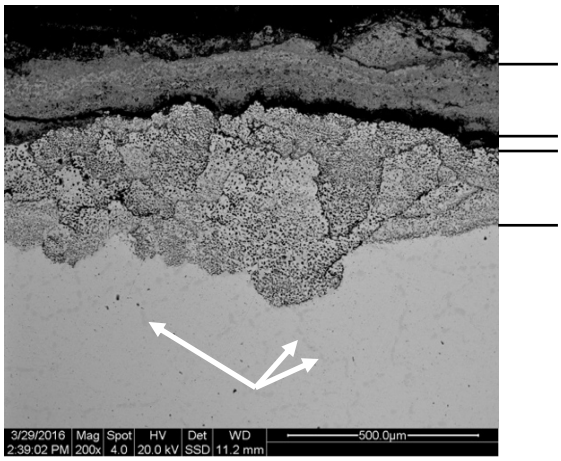

ɟure 55. Backscattered SEM image of the Kanthal APMT sample after 1000h exposure

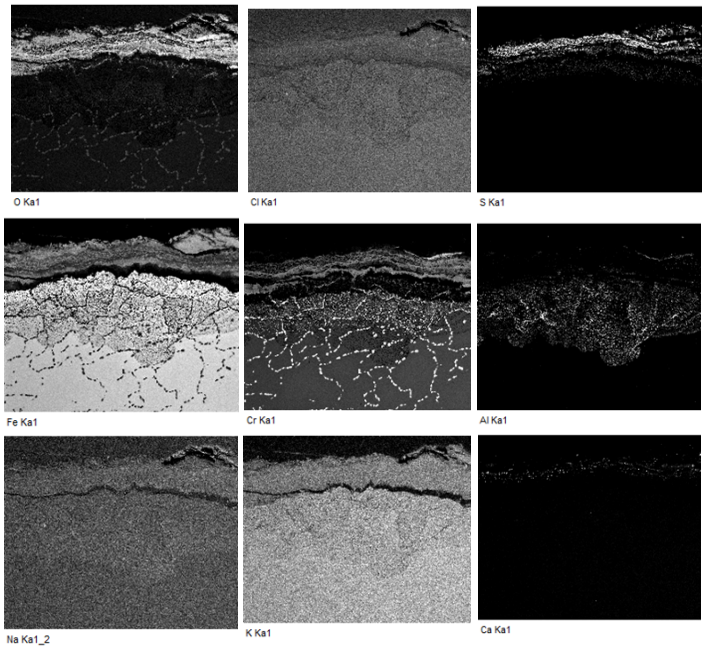

Figure 56. EDX mapping analysis of the Kanthal APMT sample after 1000h exposure

- **FeCrAl model alloy exposed at 700 °C for 1000h**
  Figure 57 shows two cross-sections of the model alloy sample after 1000h exposure. Due to mechanical failure, the sample was cracked when inserted. During the exposure half of the sample ring fell off, leaving the thermocouple exposed during approximately 100h until a deposit covered the area again. The failure makes the temperature profile during the exposure uncertain.

  The Figure 57(a) shows the surface of the non-broken remaining part. The SEM/EDX analysis presented in Figure 58 indicates that an alumina oxide has formed at the metal/oxide interface all over the sample. No signs of nitridation could be observed beneath the alumina scale. Figure 57(b) shows a part of the sample near the crack of the sample which is heavily corroded where homogeneous alumina was formed on the surface.

  These results have to be taken in account when looking at the material loss of this sample as it was calculated only region far from the crack/lost part which is just the 25% of the sample. Unfortunately, the other 75% of the sample was lost inside the boiler during the exposure making the material loss calculation impossible after that.

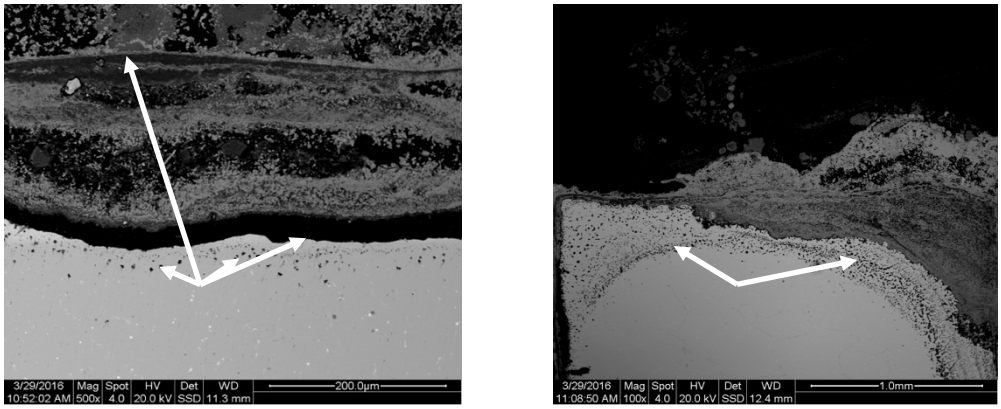

(a)

Figure 57. Backscattered SEM image of the model alloy sample after 1000h exposure (a) non-broken part (b) broken part

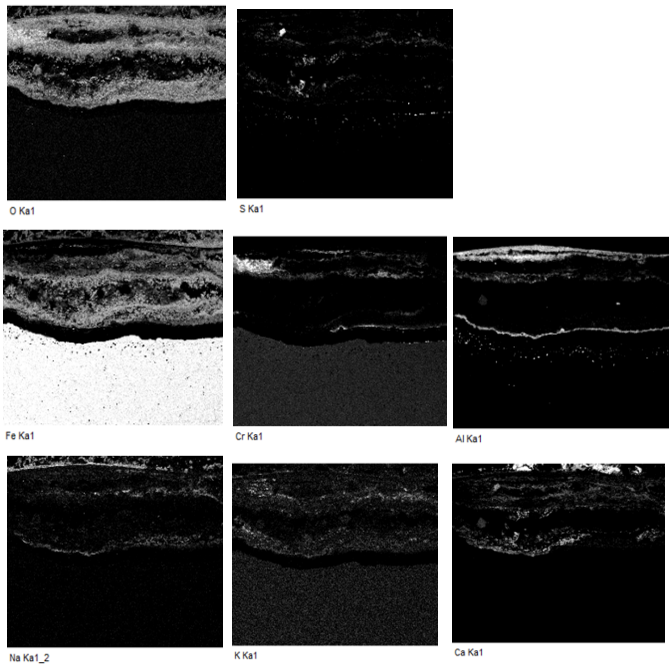

Figure 58. EDX mapping analysis of the model alloy sample after 1000h exposure (non-broken part)

- **Inconel 625 exposed at 700 °C for 1000h**

Figure 59 shows an image of the Inconel 625 over welded material. After 1000h exposure at 700 °C the surface is covered by a 20 µm thick chromium rich oxide.

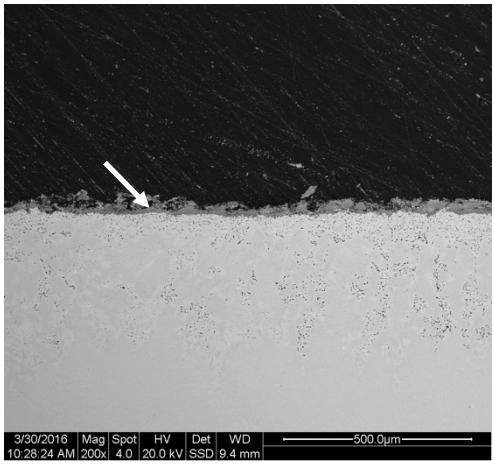

Figure 59. Backscattered SEM image of the Inconel 625 overwelded sample after 1000 h exposure

6.3.3 Corrosion propagation - FeCrAl model alloys

The aim of the corrosion test of the FeCrAl model alloys (described in section 4.3.4) was to investigate trends discovered in the lab on FeCrAl model alloys in at the Steamboost position. The aim was in addition to follow up on the FeCrAl alloy corrosion rates and the possibility to form an alumina layer. A sample with both as-received surface and partly turned surface was produced but unfortunately the air supply failed during a first attempt for this exposure and it was interrupted. All the samples were replaced and the exposure was started from the beginning with exactly the same conditions as planned.

6.3.4 Material loss of FeCrAl model alloys

The material loss was calculated and is presented in Figure 60. It has also been illustrated in 7 different diagrams (one for each sample ring, except for the over weld). From alloy 1 to alloy 4, the Cr content is varied. An increased corrosion resistance is observed by terms of reduced material loss. However, for alloy 4, two of the measuring points after exposure is set to zero. This result is due to the ring breaking when trying to remove it from the probe. This indicates an embrittlement of the material as the Cr content is increased. For alloy 3, the material loss is close to zero all over the ring except for one of the measuring point in which the corrosion attack was more severe (see Figure 62). This is due to this part of the ring being situated on the flue gas side, causing a much harsher environment.

The difference in composition between alloy 2 and alloy 5 is the silicon content. Alloy 2 demonstrates a much higher corrosion resistance compared to alloy 5, in which large parts of the ring has been corroded all the way through.

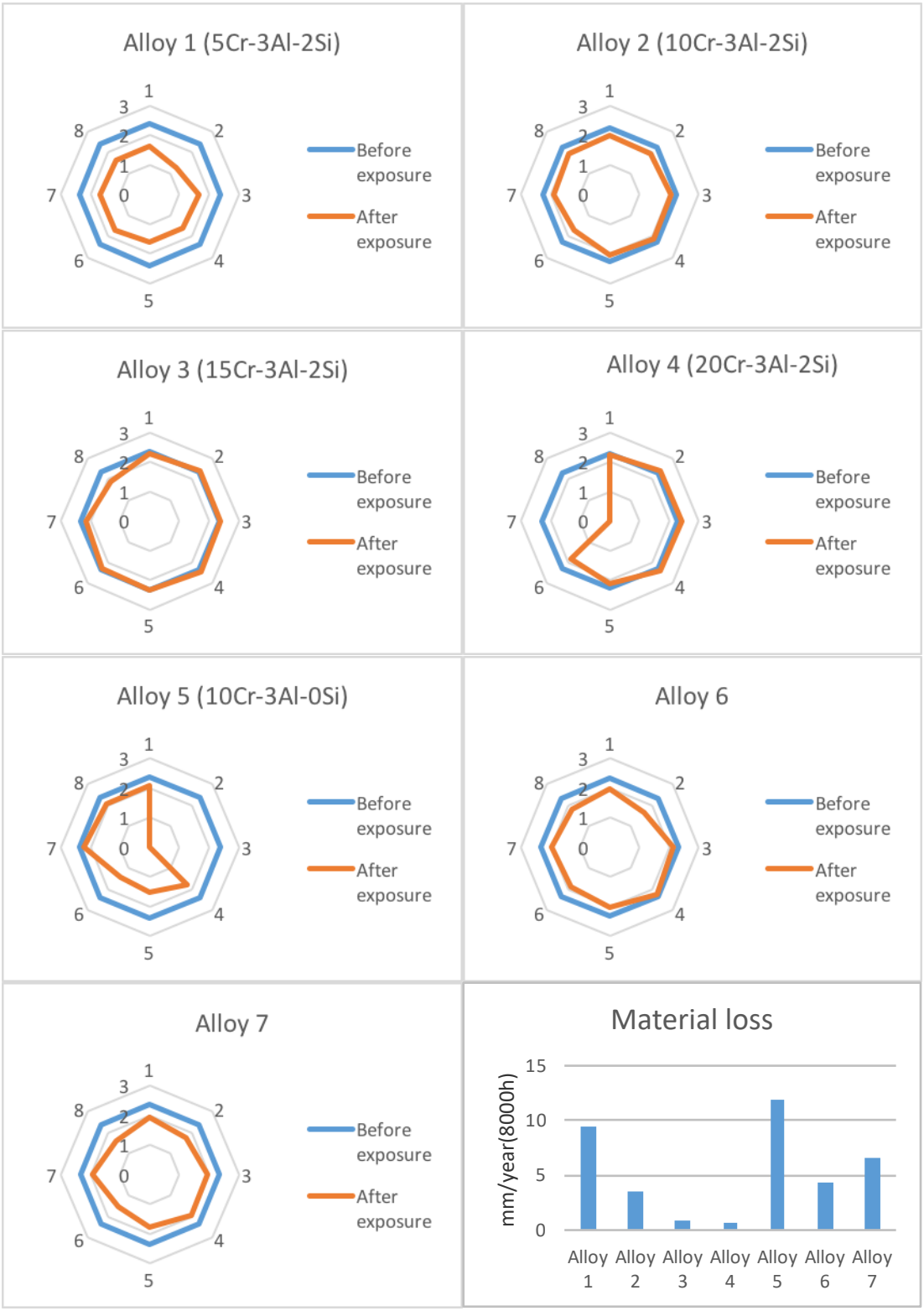
Alloy 1 (5Cr-3Al-2Si)
Alloy 2 (10Cr-3Al-2Si)
Alloy 3 (15Cr-3Al-2Si)
Alloy 4 (20Cr-3Al-2Si)
Alloy 5 (10Cr-3Al-0Si)
Alloy 6
Alloy 7
Material loss
Before exposure
After exposure
mm/year(8000h)
Alloy 1
Alloy 2
Alloy 3
Alloy 4
Alloy 5
Alloy 6
Alloy 7

Figure 61 shows two different cross section images of alloy 1. As can be seen, the material loss is roughly the same all over the ring. Figure 62 shows SEM cross sections of the alloy 3 sample ring which is the sample that performed the best. In the left image a cross section from the least corroded area is shown. Barely any oxide is visible and the material loss is close to zero. This is the case for the majority of the sample ring surface. The exception is the part of the ring that was on the flue gas side which has corroded much more severely. This can be seen in the left image of Figure 62 as the oxide is reaching into the material.

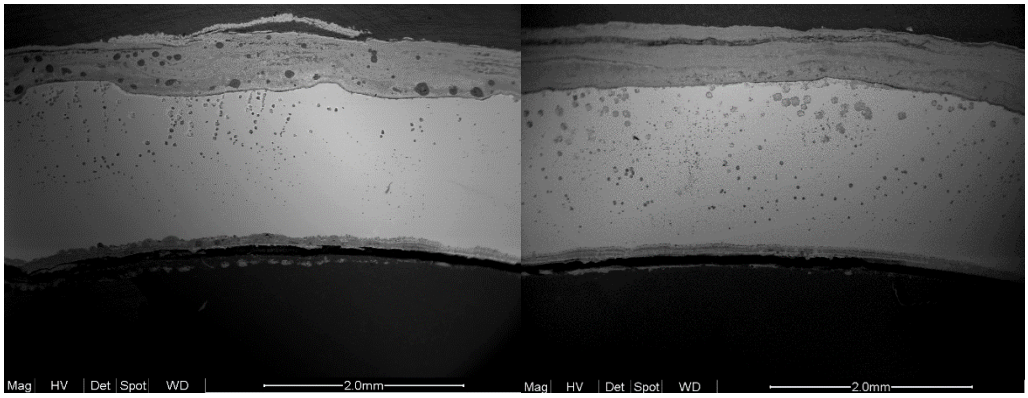

Figure 61: SEM cross section images of two different points of the **alloy 1** sample ring.

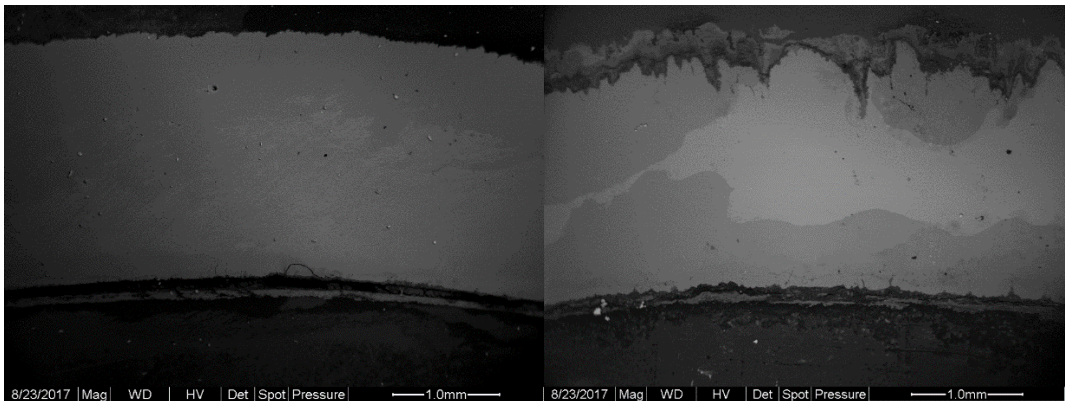

Figure 62: SEM cross section images of the least severely corroded (left) and the most severely corroded (right, flue gas side) point on the **alloy 3** sample ring.

Figure 63 and Figure 64 shows SEM cross section images of alloy 2 and alloy 5 in which the silicon content is varied from 2 to 0 wt-%. The material loss for alloy 2 is quite uniform all along the ring but slightly higher at the flue gas side (see right image in Figure 63). Alloy 5 has only a few areas of the ring which isn't severely corroded (see left image of Figure 64) and on the flue gas side the sample ring has been corroded all the way through the ring (see right image of Figure 64).

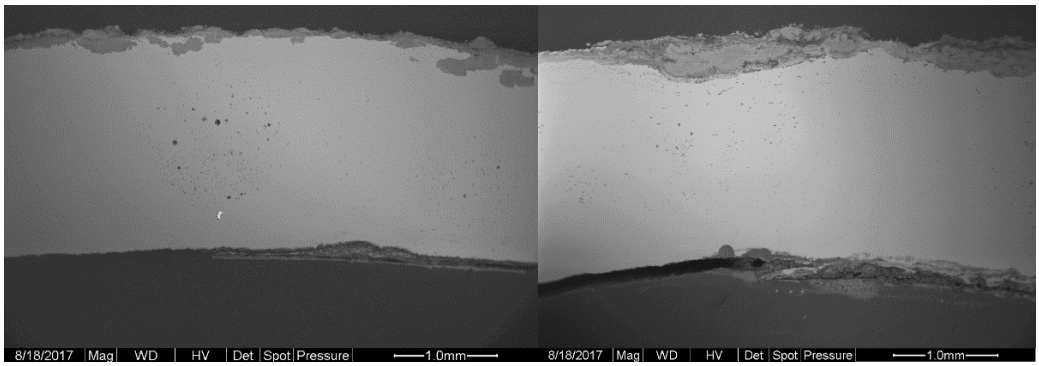

Figure 63: SEM cross section images of the least severely corroded (left) and the most severely corroded (right, flue gas side) point on the **alloy 2** sample ring.

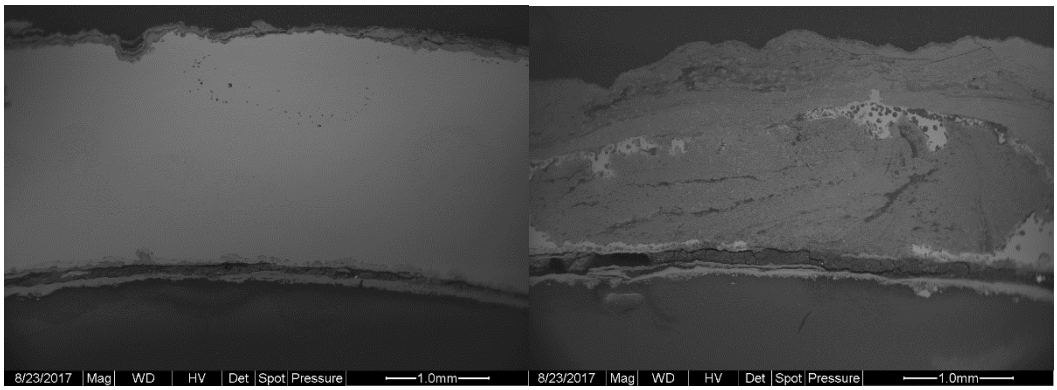

Figure 64: SEM cross section images of the least severely corroded (left) and the most severely corroded (right, flue gas side) point on the **alloy 5** sample ring.

As mentioned earlier a reference ring, consisting of an Inconel 625 over weld was exposed together with the other FeCrAl alloy rings. A non-exposed Inconel 625 ring was analysed with EDX to investigate if Fe from the substrate had diffused into the Inconel over weld during the welding (see figure). The iron content remained constant at 1 at-% throughout the over weld layer.

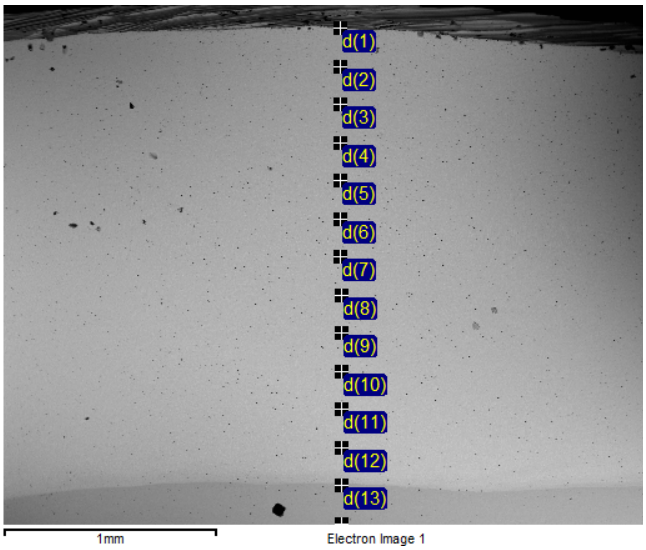

Figure 65: SEM cross-section image of unexposed Inconel 625 over weld showing the points of EDX-analysis

In Figure 66, two SEM cross section images of different locations on the sample ring is shown. These images indicates that the Inconel 625 over weld has been subjected to a quite severe corrosion attack and has formed a porous oxide. The image to the right displays a slightly thicker oxide caused by being positioned on the flue gas side.

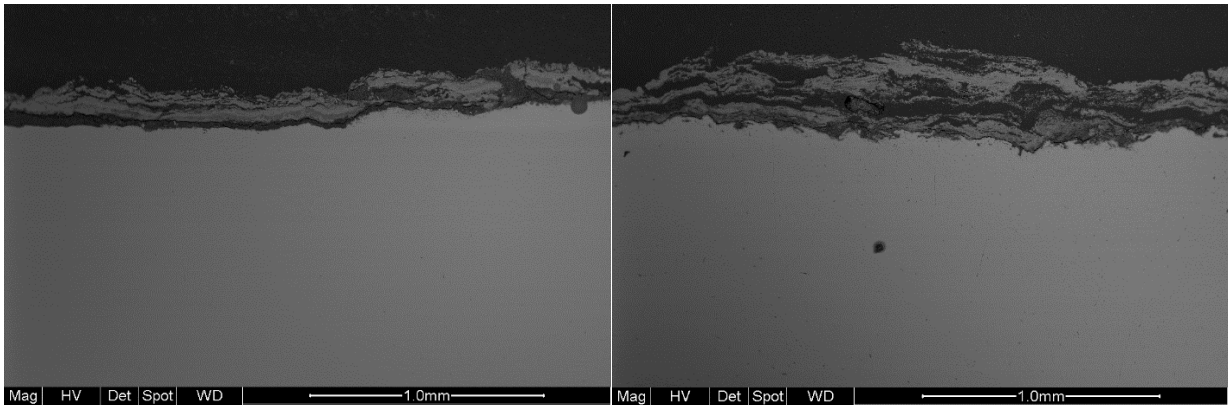

Figure 66: SEM cross section images of the most severely corroded (right, flue gas side) and one of the less corroded (left) points of the Inconel overweld sample ring.

In Figure 67 chlorine attack is indicated by the formation of metal chlorides in the metal. The chlorine appears to have penetrated about 100 µm down into the overweld.

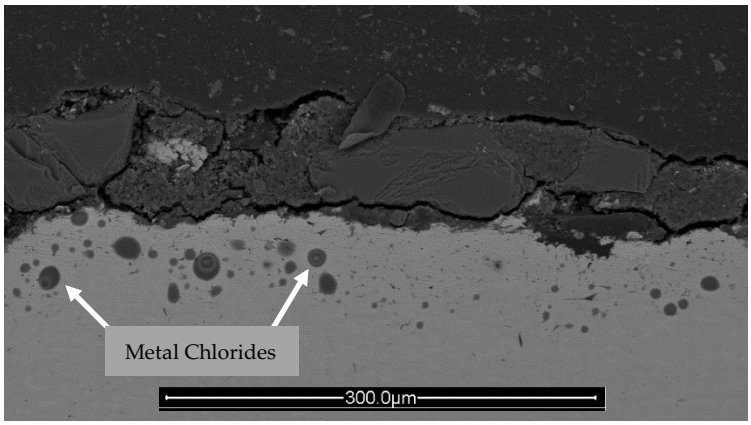

Figure 67: SEM cross section image of Inconel 625 overweld sample ring showing the formation of metal chlorides.

6.4 THE MATERIAL - FIXED INSTALLED STEAMBOOSTMATERIAL

In addition to the air-cooled probes fixed material was mounted at the Steamboost position in AffaldPlus, see section 3.2.1. This installation was performed during the 2015 revision and the material followed the normal start up sequence of the boiler. The analysis was focused on material loss as the material was handled in a way where the deposit/corrosion products may be lost, i.e. cutting down the fixed installation and separating the different material sections.

6.4.1 Corrosion rates - Material loss measurements

6.4.1.1 First installation – 8000h

The first Steamboost installation was removed after being exposed 8000h inside the grate fired boiler and the whole Steamboost installation was taken down. The materials were cut and stored in desiccators awaiting analysis. The material loss analyses were carried out as described in 4.4.3. The over welded materials were not included in the material loss measurements due to the high error that the shape of the weld seam introduces in the surface of the metal. The values of the material loss for the different materials are shown in Figure 68.

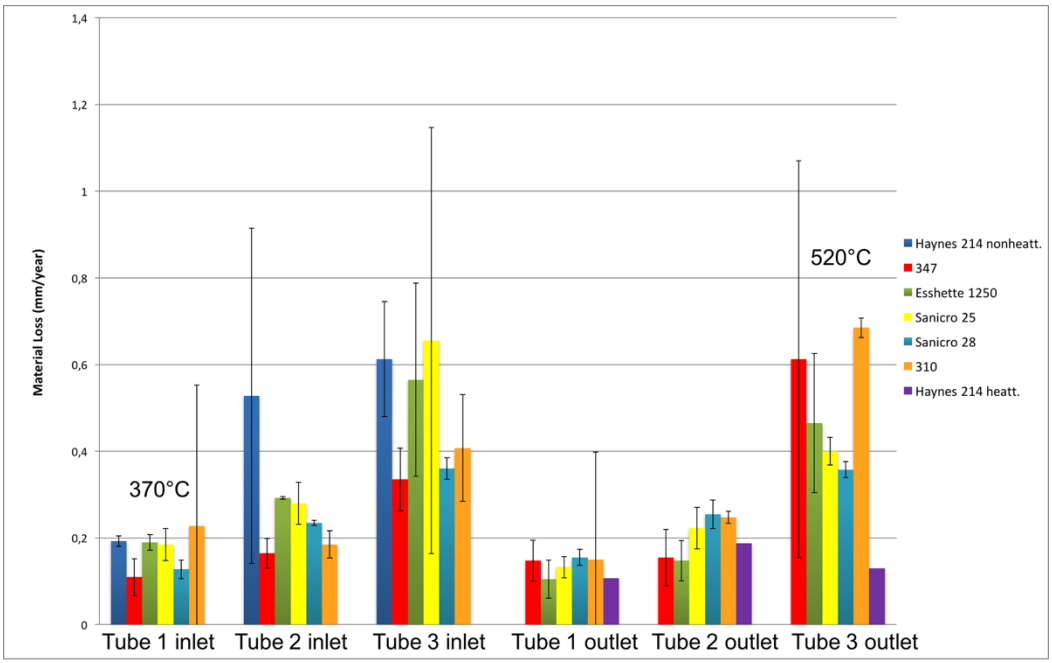

Figure 68: Material loss of the different material of the Steamboost for the different tubes (2015)

The steam enters the tube 1 at 320°C (tube 1 inlet) and leaves the tube 3 at 470°C (tube 3 outlet). The material temperature was estimated to be 50°C higher than the steam temperature. That way, the tube 1 materials were exposed at 370°C in the inlet and the temperature increases until 520°C in the tube 3 outlet. As expected, all the materials show an increase of material loss when increasing the temperature from tube 1 to tube 3.

6.4.1.2 The second installation – 6500h

The second installation of Steamboost was removed after 6500h. This time, the most corroded tube (tube 3 at 520°C) was stored for analysis in the same way as the previous Steamboost. The material loss analyses were carried out as described in 3.2.6.3. The values of the material loss for the different materials and its comparison with the previous Steamboost analyses are shown in Figure 69

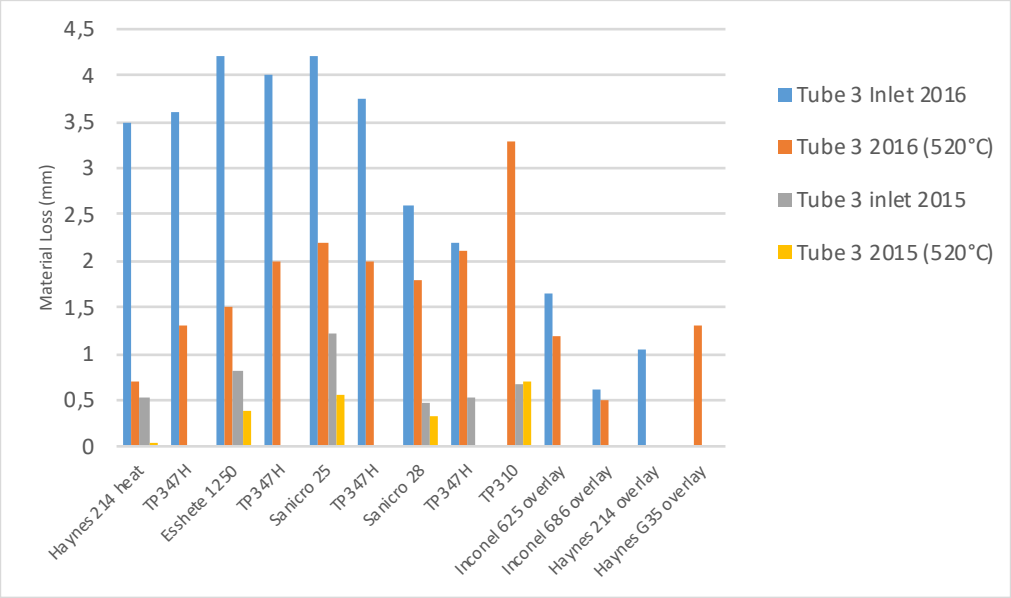

Figure 69. Material loss of the different materials in the tube 3 (520°C) 2016

6.4.2 Microstructure of the corrosion attack – SEM/EDX

After 8000h exposure all the materials which composed the Steamboost were studied with SEM. As an example, a backscattered image of 347H material is presented in Figure 70. It is possible to see the oxide on the top of the alloy and the grain boundary attack. As the boiler was cleaned before the removing of the Steamboost no or very little deposit was observed on the top of the samples.

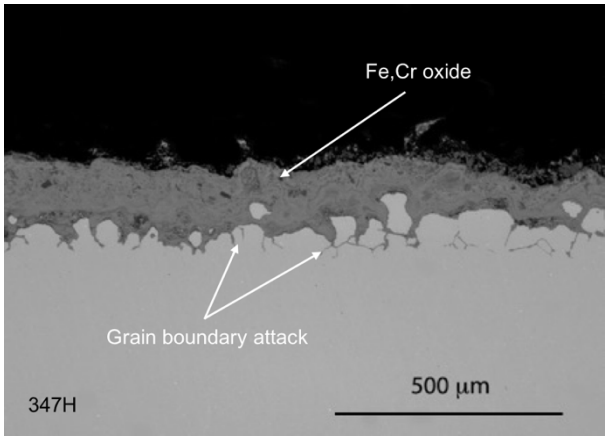

Figure 70: Scanning Electron Microscopy Backscattered image of 347H material exposed 8000h at the Steamboost

7 Analysis of the results

In order to utilize the full potential of renewable energy sources such as biomass and waste in combustion, solutions must be found to meet the corrosiveness of these fuels. The resulting flue gas environment from biomass and waste is more corrosive than fossil fuels and the high temperature corrosion of pressurised part materials is a major challenge in utilisation of the energy. From an energy recovery efficiency point of view, high steam pressure and superheater temperature are of great importance. In order to achieve a thermal efficiency close to other types of boiler fuels, e.g. fossil fuels and clean biomass fuels, the superheater temperature must be increased from the present values.

This project investigates two pathways to reduce the corrosion of the key components in order to utilize higher steam data from these processes. One approach is a new technology proposed by Babcock & Wilcox Vølund aiming to increase the steam temperature. The idea is to utilize CFD modelling in order to use positions where the flue gas from the grate have a high heat flux and a low chlorine concentration [7]. Superheaters may then be positioned in a part of the furnace within the less corrosive flue gas and subsequently increase the steam temperature up towards 500 °C.

A second approach to increase the energy output, i.e. higher operating temperatures, is to utilize new materials that can cope with these aggressive environments. Currently, stainless steels are the material of choice for use in these boilers. A possible strategy to avoid component failure in a power boiler would be to use an alumina-forming alloy such as the well-known FeCrAl.

The investigated position in the boiler in combination with this for these environments new material class opens up for two possible solutions for the FeCrAl alloys. They could be used as traditional superheater materials with a material temperature range of about 500-600 °C or as a coaxial solution with a higher material temperature. The FeCrAl materials were therefore investigated in a temperature span of 600-900 °C. It is in addition very important to investigate the mechanisms of these alloy systems and the impact of key elements. This was accomplished through a detailed laboratory study in parallel to the exposures in the complex environment. The laboratory study was performed in collaboration with the HTC project critical corrosion phenomenon.

7.1 FECRAL ALLOYS IN THE SIMULATED/REAL BOILER ENVIRONMENT

The influence of alkali chlorides and other chlorine-containing species on the high temperature corrosion of different metals/alloys has been investigated in simulated boiler environments in several investigations [6, 12-14]. The strong acceleration of corrosion caused by HCl, KCl and NaCl has been attributed to alloy chlorination, e.g. by the ''chlorine cycle'' mechanism described by Grabke et al. [15] or more recently by an electrochemical mechanism [16]. Attention has also been directed towards the role of alkali in the breakdown of the protective chromia-rich scales on stainless steels. Thus, alkali chloride has been shown to react with the chromia in a scale under oxidizing conditions, forming alkali chromate (VI) according to Reaction (1):

$$^1/_2\, Cr_2O_3(s) + {}^3/_4\, O_2(g) + H_2O(g) + 2KCl \rightarrow K_2CrO_4(s) + 2HCl(g)$$

This process depletes the protective scale of chromium and tends to convert it to a poorly protective iron oxide scale, allowing alloy chlorination to proceed [6, 12].

Alumina forming alloys such as FeCAl alloys may provide a better protection in these environments because the reaction of KCl with Al_2O_3 to produce potassium aluminate ($KAlO_2$) is thermodynamically less favoured than K_2CrO_4 formation at the relevant temperature, it appears that alumina-forming alloys may provide a possible alternative for high temperature applications where materials are exposed to alkali chlorides. Two different strategies have been investigated, i.e. pre-oxidation to form the protective α-alumina or and optimizing the composition to use non-peroxidised alloys. The laboratory work on commercial FeCrAl alloys performed within this project has been a part of N. Israelssons PhD thesis[11].

7.1.1 Commercial FeCrAl alloys – the influence of pre-oxidation in the laboratory

The corrosion behavior of non-preoxidised commercial FeCrAl alloys has previously been investigated in the presence of KCl at 600 °C [17]. This work has been focused on pre-oxidized samples and the corrosion resistance of these in an KCl rich environment at 600 °C. The work included in this report shows the potential of the pre-oxidation even though the fact that the pre-oxidation was performed at 700 °C. Alkali do not react with the pre-formed scale and very little corrosion attack could be observed after 168 hours. This may be compared to the polished sample without pre-oxidation where the sample showed breakaway oxidation sprayed with only 0.1mg/cm^2 prior to exposure. However, the laboratory work performed by N. Israelsson showed that the resistance of the peroxidised scales is limited. More pre-oxidizations were investigated and for longer times [11]. It was concluded that the resistance towards KCl-induced corrosion of the pre-formed alumina scales was: (900 °C, 1 hour), (1100 °C, 1 hour), (900 °C, 24 hours) and (1100 °C, 24 hours). Corrosion and the associated break-up of the alumina scales were initially highly localized and much of the sample surface was seemingly unaffected. However repeated exposures with KCl caused the corrosion to spread laterally over the surface. The lateral movement of the "corrosion front" is assumed to be associated with the spreading of cracks in the alumina scale.

The absence of any corrosive species, e.g. potassium and chlorine at the alumina/alloy interface shows that the pre-formed alumina scale was protective towards KCl-induced corrosion at 600 °C. However, the above results suggest that KCl- induced corrosion is initiated at flaws in the alumina layer and that the intact alumina layer is impermeable to attack since KCl was detected at the alloy/alumina scale interface close to the corrosion front [11].

The results indicate that if the α-alumina scale is intact it constitutes an effective barrier towards the diffusion of ions (Fe^{2+}, Cl^-). However, once the scale cracks, the situation changes. It is suggested that, when a crack or similar flaw in the alumina scale is present, KCl immediately enters it by surface diffusion, forming an adsorbed layer on the exposed alumina in the crack [11].

7.1.2 Model alloys – influence of alloy elements Si and Cr in the laboratory

Another strategy to utilize FeCrAl alloys is to optimize the alloy composition for lower temperatures as the commercial alloys are optimized for higher temperatures. This strategy has been investigated through model alloys since it is important to get a better understanding

of how the protectiveness of these vary with different compositions. Through this strategy the limitation with working with commercial alloys that contains a lot of different element additions may be avoided. Also, when comparing different commercial FeCrAl alloys to study the effect of a certain element, it's most likely several other amounts of elements that are varied as well, making the reason behind the difference in corrosion behaviour difficult to understand. Model alloys were produced, which consist of specific amounts of each element. The focus of this work has been on the effect of small amounts of Si as well as varying the amount of Cr in Si containing FeCrAl alloys.

The results of the laboratory study show a positive effect on the corrosion behaviour upon addition of silicon to the FeCrAl alloys. This is true for both of the investigated environments but to a larger extent in the reference environment (5% O_2 + 20% H_2O + N_2(bal.)), i.e. without KCl. In the reference environment, FeCrAl**0Si** exhibits a high mass gain as a result of the loss of the protective oxide, leading to a rapid formation of iron-rich oxide as shown in Figure 29 (rough surface morphology) and Figure 31 (thick inward and outward growing oxide). Meanwhile, FeCrAl**1Si** and FeCrAl**2Si** still form protective oxides in the nanometer range. These results indicate that silicon has an effect on the chromium evaporation, induced by the water vapour. However, whether this is a direct or indirect effect is not as clear. Silicon may form a thin SiO_2 layer limiting the reaction between chromium and water vapour or have an indirect effect on the corrosion resistance by increasing the activity or diffusivity of aluminium. A more detailed microstructural investigation is planned to investigate this.

When adding KCl to the environment it results in a loss of the primary protection (protective oxide before breakaway oxidation) for all three alloys. FeCrAl**0Si** forms an oxide that is roughly the same thickness as when exposed without KCl present. FeCrAl**1Si** and FeCrAl**2Si** were not affected by the presence of water vapour, but when adding KCl it caused a large increase in corrosivity, resulting in a loss of the primary protection and a rapid formation of iron-rich oxide. Even though none of the alloys have kept the primary protection, the thickness of the formed iron-rich oxide decreases significantly upon addition of silicon. Short term exposures (1-3h, not shown) showed that all three alloys have lost the primary protection already after three hours, which means that a difference in incubation time is not the cause of the large difference in oxide thickness. The results instead indicate that the rate of the oxide growth of the secondary protection is affected by the amount of silicon in the alloy and a better understanding of the kinetics is therefore needed, which can be achieved either by performing shorter intermediate exposures, or by using a thermobalance, in which the samples are continuously weighed while they are being exposed.

All of the silicon containing FeCrAl alloys in which the Cr was varied kept their primary protection when exposed in the reference environment (5% O_2 + 20% H_2O + N_2). In the KCl containing environment however, all of the alloys lost their primary protection and formed thick iron oxide. However, when increasing the amount of Cr in the FeCrAl model alloys, the mass gain as well as the oxide thickness after exposure was reduced significantly. There are two possible reasons behind this reduction in corrosion attack. One of them is that it's possible to form a protective chromia layer in the beginning of the exposure and that this layer is broken down after a certain amount of time when the alloys has been depleted of their Cr. It would then be expected that the incubation time before break is increased with an increased amount of Cr in the alloy. This is however unlikely when looking at FeCrAl**2Si** which, as was mentioned earlier, lost its primary protection already after 3 hours of exposure. The other

possibility would therefore be that the increased amount of Cr reduces the growth rate of the secondary protection. More detailed microscopy is needed to understand the mechanisms.

7.1.3 FeCrAl alloys at the Steamboost position in AffaldPlus

In order to study the FeCrAl materials in a complex environment a pre-oxidized FeCrAl tube was inserted without cooling at the Steamboost position at AffaldPlus. This exposure was interrupted for cutting samples and for air-cooled probes where both commercial FeCrAl alloys, stainless steels and FeCrAl model alloys were exposed in the steambost position. The fixed installed FeCrAl tube was made of Kanthal APMT that was pre-oxidized at 1050 °C for 8 hours before its installation in the boiler. After being exposed for 4500 hours the tube was removed and the tip of the tube was cut for analysis. The tube tip was then welded together again and the tube exposed in the same conditions for 12 000h until it failed, see Figure 12.

After 4500h exposures at about 900 °C the protective pre-oxidized alfa-alumina was still intact on 50% of the sample (Figure 41). This is in line with the laboratory results even though the exposure temperature was much higher and the environment very complex. If the α-alumina remains without cracks it will protect the material from further corrosion. The growth rate of α-alumina is very slow also at high temperatures as 900 °C [9, 18]. This shows the potential of the alumina formers in this corrosive environment. The oxide grows very slowly and does not react with the deposit/environment. However, the other 50% of the sample was corroded and no protective alumina layer could be observed, see Figure 41. This was also the case after second round of exposure where no protective alumina remained and the tube eventually failed due to corrosion.

The results from the air-cooled probes of the alumina forming alloys are in line with the laboratory and FeCrAl tube results. The alloys suffered from severe corrosion in the absence of a protective α-alumina layer. However, the model alloy sample failed mechanically exposing the thermocouple to the hot flue gas during the exposure resulting in no temperature control during the second half of the exposure. Despite this the remaining part of the model alloy showed little material loss and indications of the formation of a healing alumina layer at the metal oxide interface.

In order to further investigate the behavior of the model alloys in boiler conditions, an extra air-cooled probe campaign was designed including over weld Inconel 625 as reference material. This new air-cooled probe test campaign was designed based on the previous stainless-steel campaign (section 6.3). The aim was to investigate the failed model alloy with interesting indications as well as the relevance of the laboratory studies, i.e. if the same trends could be observed in field exposures as well, rings of similar composition as the model alloys in the laboratory studies were made to be exposed at the Steamboost position in AffaldPlus.

The measured material loss of the sample rings with varying Cr (alloy 1-4) showed a clear trend of reduced corrosion rate with increased amount of Cr which correlates well with the results from the laboratory studies. Apart from a reduced corrosion rate with increased amount of Cr, the field studies also show an embrittlement that results from increased Cr content; alloy 4 (20% Cr) broke into two pieces when removed from the probe. The SEM cross sections of the rings show that the severity of the corrosion attack differs significantly between the part of the ring pointing towards flue gas side and the rest of the ring. Even though alloy 3 (15% Cr) has a very low overall material loss it is observed that at the flue gas side the

material loss is actually higher than on the flue gas side for alloy 2 (10% Cr). The pros and cons of the variation of Cr will have to be weighed against each other.

The silicon content is varied between alloy 2 (2% Si) and alloy 5 (0% Si). The material loss varies significantly and shows a clear trend of increased corrosion resistance upon addition of Si. This correlates well with the results from the laboratory study in which small additions of silicon resulted in a large decrease in corrosion rate. The SEM cross section images show that the severity of the corrosion attack doesn't differ to such a large extent between the part of the ring pointing towards the flue gas side and the rest of the ring for alloy 2. But for alloy 5 (0% Si) a large part of the ring is corroded almost all the way through the ring.

This field study has shown two different trends, an increased corrosion resistance when increasing the Cr content in the alloy as well as an increased corrosion resistance when adding a small amount of Si to the alloy. Both of these trends were observed in the laboratory studies as well and shows that performing exposures in a simplified lab environment is relevant to answer important questions regarding the corrosion behaviour of different materials in the real application.

7.1.4 FeCrAl – 625 over weld comparison

In very corrosive environments alloy 625 over weld is commonly used. The aim in this project was therefore to compare with this material and it was included as a reference in all exposures. The project group decided to keep the surface as received as the surface finish is known to influence the corrosion properties. However, this made material loss measurements difficult. The average corrosion attack was instead investigated as shown in section 6.3.4. An attempt was in addition performed to investigate both the general behaviour as well as a smooth pre-measured surface. In this way both the average corrosion attack could be observed and a material loss measurement performed. Half of a ring sample was turned and measured prior to the air-cooled exposure, see Figure 71. However, the compressed air to the probe failed during the exposure and no results could be acquired from the sample. This may be a strategy for future investigations.

Figure 71: Picture of the half turned Inconel 625 over weld ring.

It was due to the failure of the half-turned Inconel 625 ring difficult to compare its material loss to the FeCrAl model alloys. The corrosion attack of the Inconel 625 over weld ring indicates that the exposure environment during this air-cooled probe exposure causes significant corrosion also on alloy 625. The microstructural investigation shows corrosion

products in the range of 150 – 400 um, i.e. in the same range as some of the better performing alloys (alloy 2 and 3). However, the more research is needed to confirm this.

Since the half turned Inconel 625 ring failed, it was difficult to compare its corrosion behaviour to the FeCrAl model alloys. The quite severe corrosion attack of the Inconel 625 overweld ring that was exposed however, indicates that the exposure environment is more severely corrosive than in the majority of probe corrosion tests in which Inconel 625 has been used. Regarding this, some of the better performing alloys (alloy 2 and 3) show promising performance. However, the critical point is the part situated towards the flue gas side at which the corrosion attack is reaching down significantly further in the metal. This effect is observed for the Inconel 625 overweld as well but it's difficult to determine the extent of the effect compared to the FeCrAl model alloys

7.2 THE STEAMBOOST SUPERHEATER POSITION AT AFFALDPLUS

The full-scale experiments were performed on the AffaldPlus plant in Denmark. The aim was to investigate the deposit formation as well as the corrosion behaviour of both stainless steels, state of the art stainless steels and FeCrAl alloys at the potential Steamboost position in a commercial boiler. This section will focus on deposit formation and stainless steels as the FeCrAl alloys were discussed in the previous section.

7.2.1 The Steamboost environment – deposit formation

The environment and especially how the deposit formation on the material positioned at the steamboost position could be controlled was studied during an extensive air-cooled deposit probe campaign. The focus of the analysis was to investigate the amount of the deposit, composition and eventually the corrosiveness of the deposit linked to the settings of the boiler.

The results show that it is possible to influence all aspects of the deposit formation by changing the settings of the boiler and the composition of the deposit amount ranged from 0,02 g - 0,5 g during the 2 h exposure on each ring (recalculated to g/mm2/year in Figure 35) and the Cl load from 3,5% to 21% during the 2h long exposures. Chlorine, alkali metals and sulphur are all known to influence the corrosiveness of the deposit and the analysis was focused on these species [15]. Specially, the formation of alkali and chlorine-induced corrosion is known to increase the corrosion rate and several mechanisms have been suggested to explain the role of alkali [12] and chlorine, see e.g. [6, 19]. Alkali was observed in all deposits and it has been shown that a very small amount is needed to breakdown the protective Cr rich oxide scale on stainless steels. In line with the presence of alkali in the deposit no protective Cr rich scales were observed after exposures on any of the exposed stainless steels, see below. The chlorine content in the formed deposit varied from 3.5% in the setting with less amount to 20.9% (mass) in the setting with most chlorine, see Figure 37. The selected setting for the corrosion investigation resulted in a deposit with approximately 6,5% Cl. There is a large difference in fuel mixes and boiler designs and it is therefore difficult to compare the Cl load with a deposit formed at the normal superheater position in the same boiler or any other boiler as no data is avalible from the normal superheater position in the AffaldPlus boiler. The levels are in the same range as in the KME711/KME714 projects [20, 21]. However, the very high flue gas temperature in combination with the direct heat radiation from the grate makes it difficult to directly compare positions/deposits and more work is needed. One option to

lower the corrosiveness of the flue gas in the steamboost position would be to insert a ceramic shield, separating the most corrosive species from the position. As the results of the deposit formation investigation that showed Cl levels in the same range as in a normal superheater position this strategy was not pursued. The deposit investigation in addition shows that it is possible to influence all aspects of the deposit formation at the steambost position, i.e. there is a potential to further optimize the deposit formation and reduce the corrosiveness.

7.2.2 The Steamboost - corrosion attack of stainless steels

The deposit investigation was followed by different investigations of the corrosion at the steamboost position at AffaldPlus. A fixed FeCrAl tube was inserted, seven different materials (at two temperatures) were investigated through air-cooled probes together will a large number of FeCrAl model alloys and nine materials were investigated through two sets of fixed installed materials (the materials were repeated two times in three loops). During the second Steamboost campaign the tube exposed under the most severe conditions (highest temperature) failed due to a leakage after 6500h. The tube was removed from the boiler and stored in desiccators for analysis and comparison with the first Steamboost. It should be noted that the fixed installed materials were exposed during the deposit tests, i.e. exposed also to settings generating large amount of very corrosive deposits, see Figure 34. The corrosion investigation generated a very large set of samples. The FeCrAl alloys have been discussed in section 7.1.1 and this part is focused on stainless steels.

The material loss measurements were carried out on all samples. The results from the air-cooled probes showed an increase in corrosion resistance with higher Cr/Ni content in the alloy, see Figure 52. Including all samples, i.e. samples from fixed installed materials, no clear trend between material loss and composition of the alloys could be observed, see Figure 68 and Figure 69. It may in addition be noted that there is a large difference between the fixed installed samples and the samples exposed on the air-cooled probes. The probe exposed samples experience higher material loss at the same exposure temperature compared to the fixed installed samples. The microstructural investigation also shows very corroded microstructures after only 24 hours exposures on the air-cooled probes, see e.g. Figure 45. It is well known that air-cooled probes result in higher corrosion rates. This may in this case be explained by the very rapid temperature ramp in the hot flue gas/direct radiation heat from the grid and exposure to corrosive species as the probe is inserted. The temperature of the clean material surface will be exposed to the 900 °C hot flue gas resulting in the initially fast-growing oxide scale. More Cl was in addition found in the corrosion products on the probe samples exposed for short times, compare Figure 45 and Figure 53. The fixed installed material will follow the normal start-up procedure of the boiler. This will result in a slower temperature ramp and a build-up of less corrosive deposits and this will also be the case for Steamboost superheater. A positive corrosion memory effect has been reported, i.e. a protective deposit may delay/limit the corrosion attack in a more corrosive flue gas [20].

In general, the stainless steels show relatively high corrosion rates at 525 °C (0.6-1mm/1000h probes, 0.35-0.6mm/8000h first fixed installation, 3-4mm/8000h second fixed installation). The discussion of stainless steels will be focused on one representative material, i.e. the material 347H. The material loss from the first fixed installation is shown in Figure 66. The steam entered tube 1 at 340 °C and leaved tube 3 at 470 °C (tube 3 outlet). The material temperatures are estimated to be 395 °C (tube 1 inlet) and 525 °C (tube 3 outlet) for the 347H samples. As expected, the material loss increases with an increased temperature, i.e. ranging from 0.1

mm/8000h (tube 1) to 0.6 mm/8000h (tube 3). The increased material loss during the second fixed installation may be a result of the investigation of differently settings or as indicated by the air-cooled probe exposures different start-up conditions.

The results from the detailed microstructural investigation is in line with the material loss measurements. The 347H samples from the first fixed installation exposed at the highest material temperature showed an approximately 250 µm thick scale, see Figure 68. This sample was exposed in tube 3 outlet at approximately 525 °C material temperature during 8000h. The oxide scale consists of a complex layered scale. The outer part consists of a fully oxidized Fe-Cr scale while some regions in the middle part still remains un-oxidized. Closest to the alloy, indications of an alloy grain boundary attack could be observed while no or only very low chlorine concentrations were detected. The microstructural investigation shows that the stainless steel 347H is in breakaway mode in good agreement with the material loss measurements. This is expected in the presence of alkali metals, such as potassium, that have been reported to react with the protective Cr rich scale normally formed on stainless steels. The product, i.e. potassium chromate, depletes the oxide in Cr transforming it to a fast-growing iron rich scale [22]. However, very little metal chlorides were observed in the metal oxide interface, which are in line with the relatively low material loss results for this material/exposure.

The microstructural investigation of the air-cooled exposed 347H sample shows an extensive corrosion attach already after 24 hours exposure, see Figure 45. This may be caused by the rapid temperature ramp and the exposure of a clean metal surface in the hot flue gas initially building a very corrosive deposit, described above. Higher amounts if chlorine indicates the formation of metal chlorides at the metal/oxide interface and indications of an alloy grain boundary attack. However, the microstructure still indicates an ion diffusion controlled growth mode as the outward growing part consists of pure iron oxide/mixed with some deposit [22]. After 1000h exposure very little oxide could be observed on the sample while instead an extensive alloy grain boundary attack could be seen. This indicates a scale with low adhesion caused by metal chlorides at the metal/oxide interface and is concluded that the scale spalled of during sample preparation. The results from the microstructure investigation is in line with the fixed installed 347H sample where an alloy grain boundary attack also could be observed. The results indicate that the alloy grain boundary attack is driven by the corrosion and not changes (aging) of the alloy microstructure as has been reported in similar environments [20].

The results from the corrosion investigation of stainless steels are in line with the deposit investigation and the corrosion rates in the same range as expected in a normal superheater position. However, as with the deposit formation more work is needed.

8 Conclusions

- This project investigates two pathways to reduce the corrosion of the key components in order to utilize higher steam data from these processes. The results show that both the use positions where the flue gas over the grate have a high heat flux/low chlorine concentration and to utilize new materials (FeCrAl) that can cope with these aggressive environments are promising.
- The laboratory results from the pre-oxidized FeCrAl alloys indicate that if the α-alumina scale is intact it constitutes an effective barrier towards the diffusion of ions (Fe^{2+}, Cl^-). This shows the potential of the alumina formers in this corrosive environment. The oxide grows very slowly and do not react with the deposit/environment.
- The pre-oxidized FeCrAl exposed in the boiler for 4500h at about 900 °C had a protective pre-oxidized α-alumina still intact on 50% of the tube material. This result is in line with the laboratory results even though the exposure temperature was higher and the environment very complex and shows the potential of the alumina scale in these environments.
- The laboratory and field study of the FeCrAl model alloys without pre-oxidation has shown two different trends, an increased corrosion resistance when increasing the Cr content in the alloy as well as an increased corrosion resistance when adding a small amount of Si to the alloy. Both of these trends were observed both in the laboratory and the boiler. The performance of the best model alloys is in the same range as over weld alloy 625. However, more work is needed to confirm this as direct material loss measurements were not possible to perform within the scope of this project. It should also be noted that an increased amount of Cr also showed an embrittlement of the samples.
- The results of the deposit formation investigation at the AffaldPlus boiler showed Cl levels in the same range as in a normal superheater position. The deposit investigation in addition shows that it is possible to influence all aspects of the deposit formation at the steamboost position, i.e. there is a potential to further optimize the deposit formation and reduce the corrosiveness. Due to these results, the option to lower the corrosiveness of the flue gas in the steamboost position by inserting a ceramic shield, separating the most corrosive species from the position, was not investigated.
- The corrosion investigation of the stainless steels showed no clear trend between material loss and composition of the alloys. Large difference between the fixed installed samples and the samples exposed on the air-cooled probes was observed. The microstructural investigation shows that the stainless steels are in breakaway mode. This is expected in the presence of alkali metals, such as potassium, that have been reported to react with the protective Cr rich scale normally formed on stainless steels.
- The results from the corrosion investigation of stainless steels are in line with the deposit investigation. The results indicate that it is possible to reach corrosion rates in the same range as expected in a normal superheater position. However, as with the deposit formation more work is needed to utilise the steamboost position.

- The project has generated knowledge about the new superheater position (Steamboost). This includes knowledge about deposit/corrosion formation which has already been used to rule out the need for a ceramic shield planned to separate some of the most corrosive gases in the furnace. Large amounts of corrosion/deposit data have in addition been generated to be used in order to select material in the future. All this knowledge will be used in the next step towards a superheater in the new Steamboost position.
- The project has generated knowledge regarding the corrosion mechanisms of the FeCrAl alloys. This knowledge will be used to identify where these materials can be used (temperature and environment) or how they could be modified in order to become more corrosion resistant in these environments.

9 Goal fulfilment

The overall goal of the project is to improve plant economy by enabling an increased electricity production.
This goal has been achieved by:

- Generating new knowledge to facilitate the implementation of CFD modelling, deposit test and corrosion tests.

The project has generated knowledge about the new superheater position (Steamboost). This includes knowledge about deposit/corrosion formation (linked to CFD modeling performed prior to the project start). The knowledge has already been used to rule out the need for a ceramic shield planned to separate some of the most corrosive gases in the furnace. Large amounts of corrosion/deposit data have in addition been generated to be used in order to select material in the future. All this knowledge will be used in the next step towards a superheater in the new Steamboost position.
This goal is considered as fulfilled.

- Find suitable materials in terms of corrosion for a Steamboost superheater positioned within the furnace.

Large amounts of corrosion/deposit data have in addition been generated to be used in order to select material in the future. All this knowledge will be used in the next step towards a superheater in the new Steamboost position.
This goal is considered as fulfilled.

- Understand the usefulness and limitations of aluminum oxide forming materials as components for biomass- and waste-fired boilers.

The project has generated knowledge regarding the corrosion mechanisms of the FeCrAl alloys. This knowledge will be used to identify where these materials can be used (temperature and environment) or how they could be modified in order to become more corrosion resistant in these environments.
This goal is considered as fulfilled.

This new knowledge will contribute to the following KME goals:

- Higher steam parameters and thereby higher electrical efficiency.
- Development of novel solutions where steam is superheated in the furnace.
- Develop improved material solutions – including alumina forming alloys.

10 Suggestions for future research work

This project investigates two pathways to reduce the corrosion of the key components in order to utilize higher steam data from these processes. The results show that both the use positions where the flue gas over the grate have a high heat flux/low chlorine concentration and to utilize new materials (FeCrAl) that can cope with these aggressive environments are promising. The steamboost materials were exposed during all different test campaigns. More work remains to better understand the impact of the deposit for longer exposures without the variations. The material at the steamboost position also experiences direct radiation from the grid as well as very high temperature flue gas. The impact of these factors on the corrosion of different materials needs further investigation. The performance of the best model alloys is in the same range as over weld alloy 625. However, more work is needed to confirm this as direct material loss measurements were not possible to perform within the scope of this project. It should also be noted that an increased amount of Cr also showed an embrittlement of the samples and more work is needed in order to find good mechanical properties or other ways to apply the material e.g. as a coating. A more detailed investigation of the model alloys is in additioon needed in order to understand the mechanisms behind the Cr/Si effect on the corrosion resistance of FeCrAl alloys in these complex environments.

11 Literature references

1. Nielsen, H.P., *The Implications of Chlorine-associted Corrosion on the Operation of Biomass-fired Boilers.* Progress in Energy and Combustion Science, 2000. **26**: p. 283 - 298.
2. Sroda, S., et al., *The effect of ash deposition on corrosion behaviour of boiler steels in simulated combustion atmospheres containing carbon dioxide (CORBI PROJECT).* Materials and Corrosion-Werkstoffe Und Korrosion, 2006. **57**(2): p. 176-181.
3. Uusitalo, M.A., P.M.J. Vuoristo, and T.A. Mantyla, *High temperature corrosion of coatings and boiler steels in oxidizing chlorine-containing atmosphere.* Materials Science and Engineering a-Structural Materials Properties Microstructure and Processing, 2003. **346**(1-2): p. 168-177.
4. al, M.O.e. *High Electrical Efficiency by Dividing The Combustion Products*. in *16th Annual North American Waste-to-Energy Conference*. 2008. Philadelphia, Pennsylvania, USA.
5. Bøjer, M., et al. *Release of Potentially Corrosive Constituents from the Grate of a Waste-to-Energy boiler*. in *IT3'07*. 2007. Phoenix, AZ, USA.
6. Pettersson, J., et al., *KCl Induced Corrosion of a 304-type Austenitic Stainless Steel at 600°C; The Role of Potassium.* Oxidation of Metals, 2005. **64**(1-2): p. 23-41.
7. Asteman, H., et al., *Oxidation of stainless steel in H2O/O-2 environments - Role of chromium evaporation*, in *High Temperature Corrosion and Protection of Materials 6, Prt 1 and 2, Proceedings*, P. Steinmetz, et al., Editors. 2004, Trans Tech Publications Ltd: Zurich-Uetikon. p. 775-782.
8. Kofstad, P., *High temperature corrosion*. 1988, London; New York, N.Y.: Elsevier applied science.
9. Götlind, H., et al., *The Effect of Water Vapor on the Initial Stages of Oxidation of the FeCrAl Alloy Kanthal AF at 900 °C.* Oxidation of Metals, 2007. **67**(5): p. 251-266.
10. Völund, B.W., *Waste to Energy plant AffaldPlus, line 4, Naestved, Denmark (Plant Fact Sheet)*. 2006, Babcock § Wilcox Völund A/S: Denmark.
11. Israelsson, N., et al., *High temperature oxidation and chlorination of FeCrAl alloys*. 2014, Chalmers University of Technology: Göteborg.
12. Karlsson, S., et al., *Alkali Induced High Temperature Corrosion of Stainless Steel: The Influence of NaCl, KCl and CaCl2.* Oxidation of Metals, 2012. **78**(1): p. 83-102.
13. Pettersson, J., et al., *The Effects of KCl, K2SO4 and K2CO3 on the High Temperature Corrosion of a 304-Type Austenitic Stainless Steel.* Oxidation of Metals, 2011. **76**(1): p. 93-109.
14. Pettersson, C., L.G. Johansson, and J.E. Svensson, *The Influence of Small Amounts of KCl(s) on the Initial Stages of the Corrosion of Alloy Sanicro 28 at 600 °C.* Oxidation of Metals, 2008. **70**(5): p. 241-256.
15. Grabke, H.J., E. Reese, and M. Spiegel, *The effects of chlorides, hydrogen chloride, and sulfur dioxide in the oxidation of steels below deposits.* Corrosion Science, 1995. **37**(7): p. 1023-1043.
16. Folkeson, N., L.-G. Johansson, and J.-E. Svensson, *Initial stages of the HCl-induced high-temperature corrosion of alloy 310.* journal of the electrochemical society, 2007. **154**(9): p. C515-C521.
17. Israelsson, N., et al., *KCl-Induced Corrosion of the FeCrAl Alloy Kanthal ® AF at 600 °C and the Effect of H2O.* Oxidation of Metals, 2015. **83**(1): p. 1-27.
18. Liu, F., et al., *TEM investigation of the oxide scales formed on a FeCrAlRE alloy (Kanthal AF)*

at 900°C in dry O2 and O2 with 40% H2O. Materials at High Temperatures, 2005. **22**(3-4): p. 521-526.

19. Pettersson, C., et al., *KCl-induced high temperature corrosion of the austenitic Fe-Cr-Ni alloys 304L and Sanicro 28 at 600 °C.* Corrosion Science, 2006. **48**(6): p. 1368-1378.
20. Vinter Dahl, K., et al., *Sulfur recirculation and improved material selection for high temperature corrosion abatement*, in *KME report*. 2018.
21. Paz, M.D., et al., *Combating high temperature corrosion by new materials and testing procedures - The effect of increased fractions of waste wood on water wall and superheater corrosion*. 2018.
22. Jonsson, T., et al., *The influence of KCl on the corrosion of an Austenitic stainless steel (304L) in oxidizing humid conditions at 600°C: A microstructural study.* Oxidation of Metals, 2009. **72**(3-4): p. 213-239.

12 Publications

Increased steam temperature with Steamboost superheater in grate fired boilers- linking deposit formation and high temperature corrosion. Proceedings Impact of Fuel Quality on Power Production and the Environment, Prague 19-23 September 2016.

Increased steam temperature with Steamboost superheater – The effect of the combustion in deposits and high temperature corrosion. Proceedings Nordic Flame Days 2017, Stockholm 10-11 September 2017.

High temperature oxidation and chlorination of FeCrAl alloys

Niklas Israelsson

PhD thesis 2014

"No title yet"

Johan Eklund

Lic. thesis 2018

13 Appendix I

13.1 24H

- 310 (525°C)

No deposit was found over the 310 sample after 24h. That was due to falling off of the deposit while removing the samples from the probe (Figure 72).

The EDX maps presented in Figure 73 show a layer of chromium rich oxide present on the top of the sample, all over the surface, followed by a 150 – 200 ◎m nickel rich oxide. Small amounts of chlorine were detected on the top of the sample which are remains of the fallen deposit.

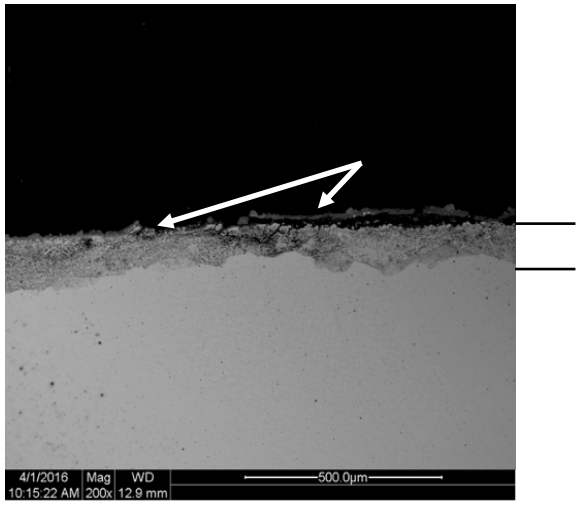

Figure 72. Backscattered SEM image of the 310 sample after 24h exposure

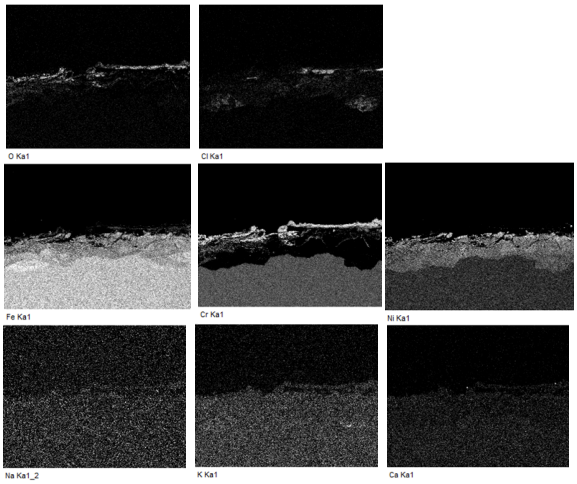

Figure 73. EDX mapping analysis of the 310 sample after 24h exposure

- Sanicro 33 (525°C)

The Sanicro 33 sample presents a chromium oxide layer all over the surface (Figure 74). On the top of this layer, a Fe-Cr rich non-homogeneous outward growing oxide was found. A 50 ◎m nickel rich oxide is present under the chromium oxide.

Some traces of the deposit formed during the exposure still present over the oxide. As an effect of cutting and polishing of the samples, the EDX analysis presented in Figure 75 shows some calcium mixed within the oxide.

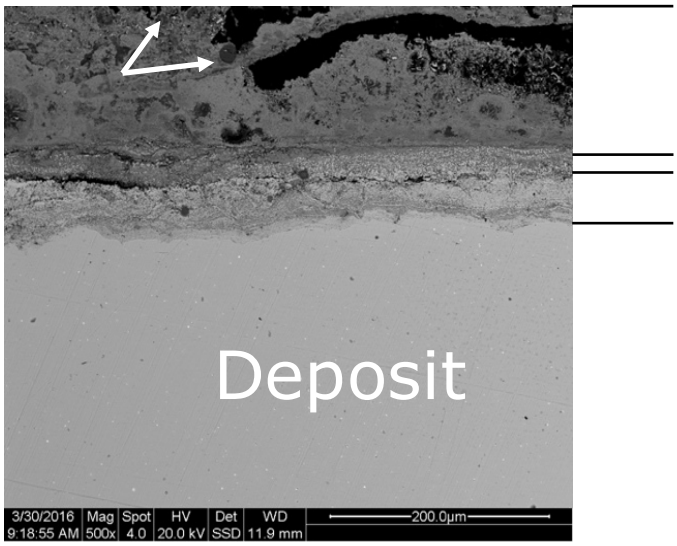

Figure 74. Backscattered SEM image of the Sanicro 33 sample after 24h exposure

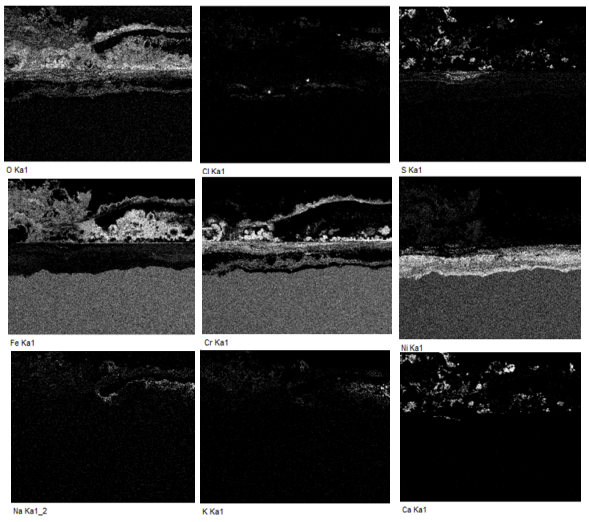

Figure 75. EDX mapping analysis of the Sanicro 33 sample after 24h exposure

- Nikrothal PM58 (700°C)

The Nikrothal PM58 presents a smooth surface with very little corrosion after the 24h exposure at 700°C (Figure 76). A very thin chromium-aluminium oxide is found all over the surface and a nickel enrichment is found under. The traces of the deposit over the surface are mainly potassium and calcium (Figure 77).

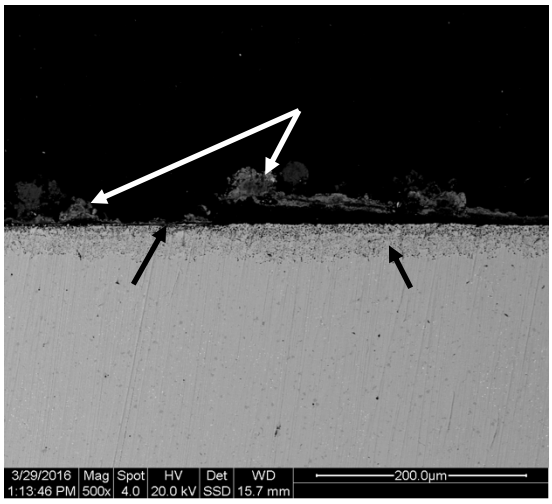

Figure 76. Backscattered SEM image of the Nikrothal 58 sample after 24h exposure

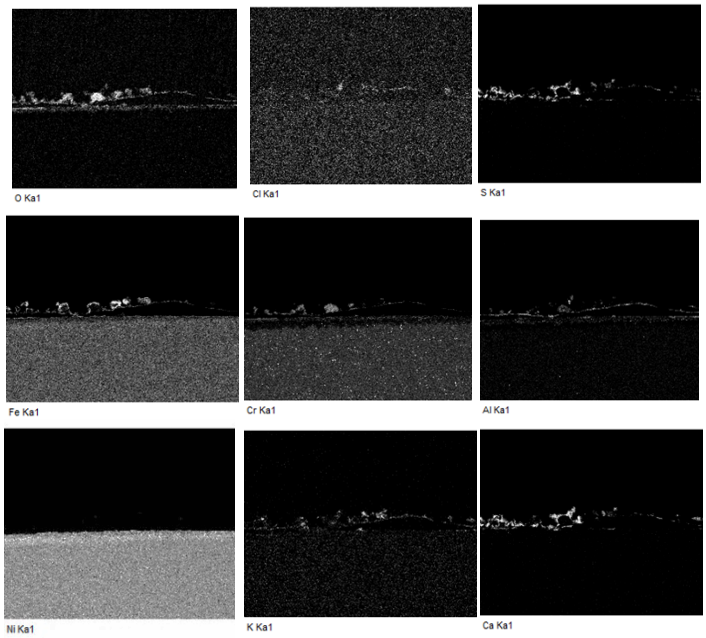

Figure 77. EDX mapping analysis of the Nikrothal 58 sample after 24h exposure

- Inconel 625 (700°C)

Due to the very little corrosion observed in the Inconel 625°C overwelded sample after 1000h exposure (chapter 6.3.2) it was considered that no extra information would be obtained by analysing the sample after 24h in the same conditions.

13.2 1000H

- 310 (525°C)

A cross section of the 310 sample after 1000h is presented in Figure 78. The corrosion products layer found is around 500 ◎m. According to the EDX analysis (Figure 79) it is composed by an outer iron oxide layer followed by a thick chromium oxide of about 50-80 ◎m. A thick and porous nickel rich oxide was found under that, followed by a deep grain boundary attack with mainly iron oxide in the grain boundaries and nickel enriched oxide when reaching the surface of the sample.

No deposit remains were found over the sample.

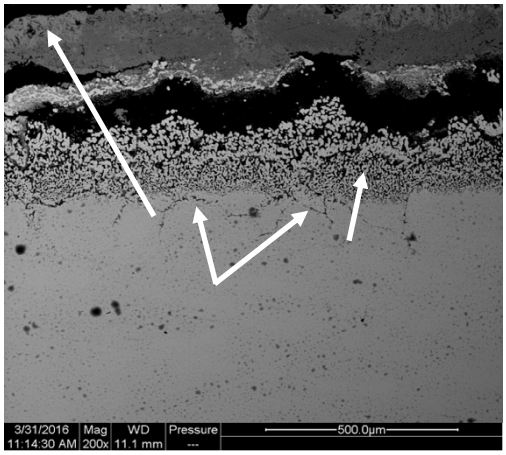

Figure 78. Backscattered SEM image of the 310 sample after 1000h exposure

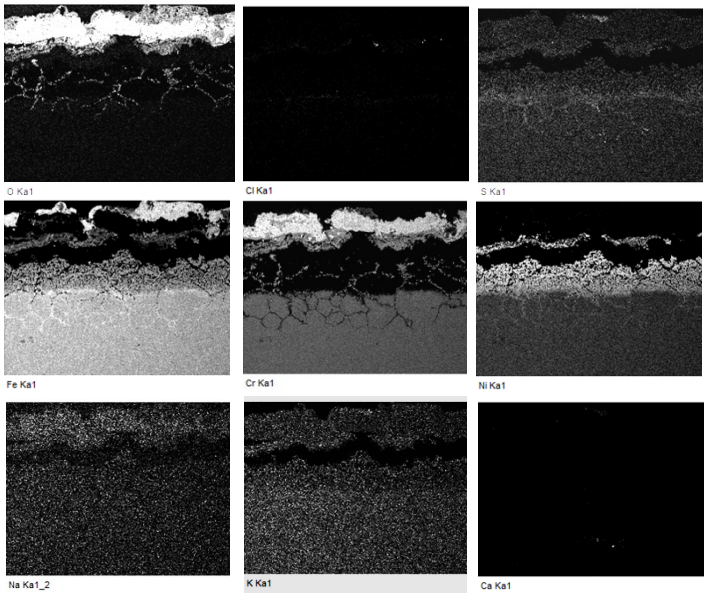

Figure 79. EDX mapping analysis of the 310 sample after 1000h exposure

- Sanicro 33 (525°C)

The Sanicro 33 sample cross-section is presented in Figure 80. After 1000h exposure at 525°C it presents corrosion products thicker than 500 ◎m.

The most remarkable corrosion effect for this material, showed in the EDX analyses of Figure 81 is the effect of the chlorine penetration. Very big rounded-size chromium chlorates were found up to 500 ◎m deep into the material. Some chlorine is still present on the surface of the sample and chromium enrichments were found all the way until the big chromium chlorates. This indicates that the chlorine was able to travel through the grain boundaries deep into the material causing a big corrosion attack.

A thin nickel-rich oxide layer was found on the top of the sample but no deposit was left after the sample preparation.

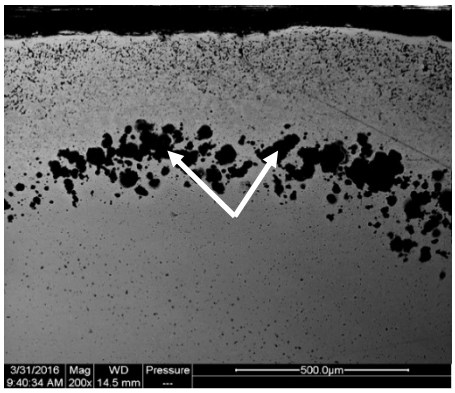

Figure 80. Backscattered SEM image of the Sanicro 33 sample after 1000h exposure

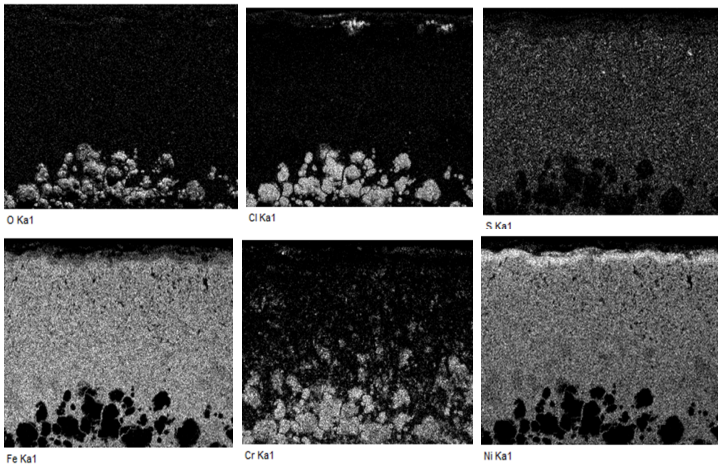

Figure 81. EDX mapping analysis of the Sanicro 33 sample after 1000h exposure

- Nikrothal PM58 (700°C)

A cross-section of the Nikrotal PM58 sample after 1000h exposure is presented in Figure 82. It presents a very thick layer of corrosion products of around 1mm which has been separated from the surface due to sample preparation. It is possible that the corrosion products are even thicker than those shown in the figure as some parts could have been lost during the handling of the samples after the exposure. The EDX analysis presented in Figure 83 shows that the corrosion products are formed by non-homogeneous layers of different oxides. An aluminium oxide layer is covering the whole surface of the sample, followed by a chromium-nickel oxide. Another alumina layer has grown over that followed by a thicker chromium oxide. Over those oxide layers a thick layer of iron oxide has grown. The rest of the corrosion products over are a mix of nickel, iron and aluminium oxides.

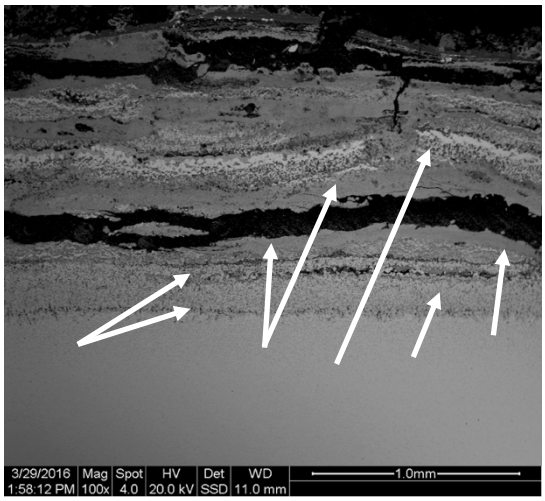

Figure 82. Backscattered SEM image of the Nikrothal PM58 sample after 1000h exposure

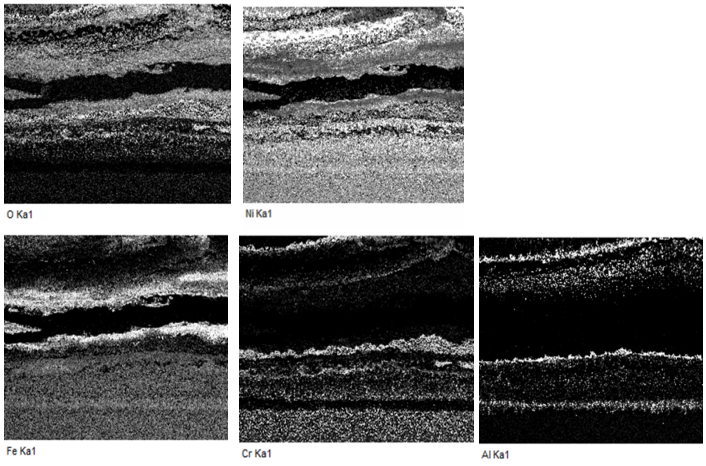

Figure 83. EDX mapping analysis of the Nikrothal PM58 sample after 1000h exposure

14 Appendix II

- 347 (520°C)

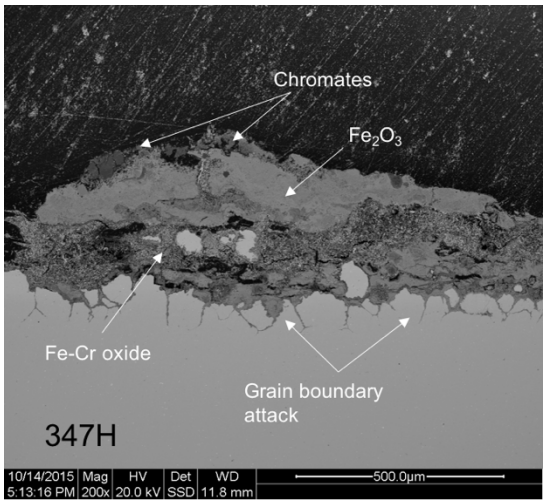

Figure 84. Backscattered SEM image of the 347H sample after 8000h exposure in Steamboost

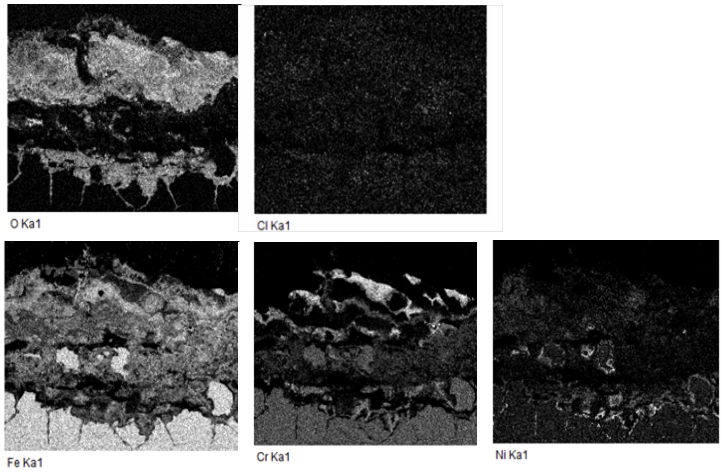

Figure 85. EDX analysis of the 347H sample after 8000 h exposure in Steamboost

- 310 (520°C)

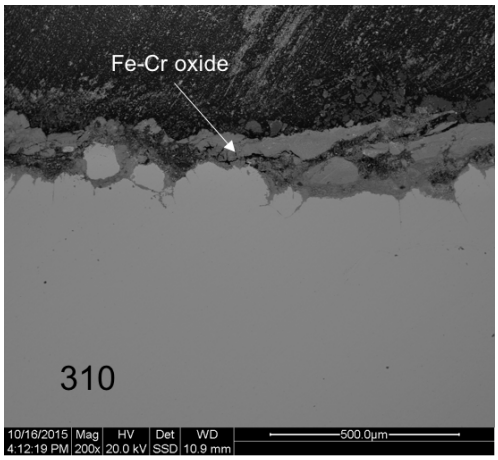

Figure 86. Backscattered SEM image of the 310 sample after 8000h exposure in Steamboost

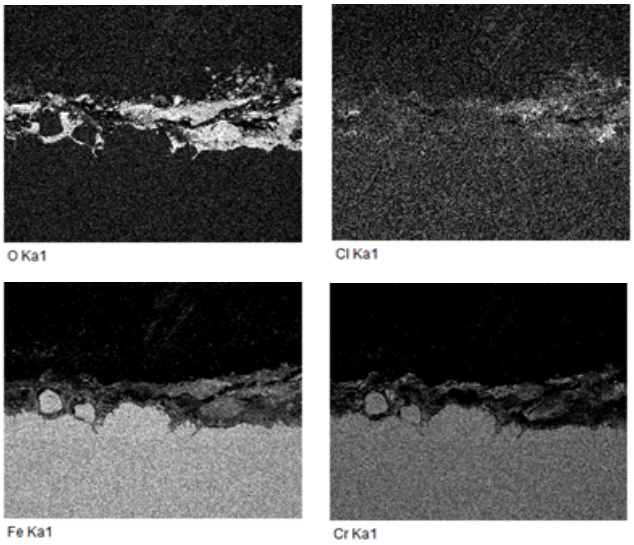

Figure 87. EDX analysis of the 310 sample after 8000 h exposure in Steamboost

- Sanicro 28 (520°C)

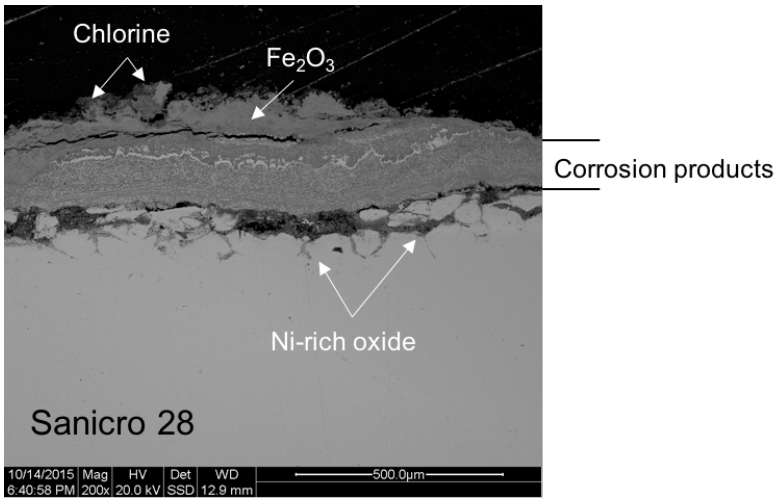

Figure 88. Backscattered SEM image of the Sanicro 28sample after 8000h exposure in Steamboost

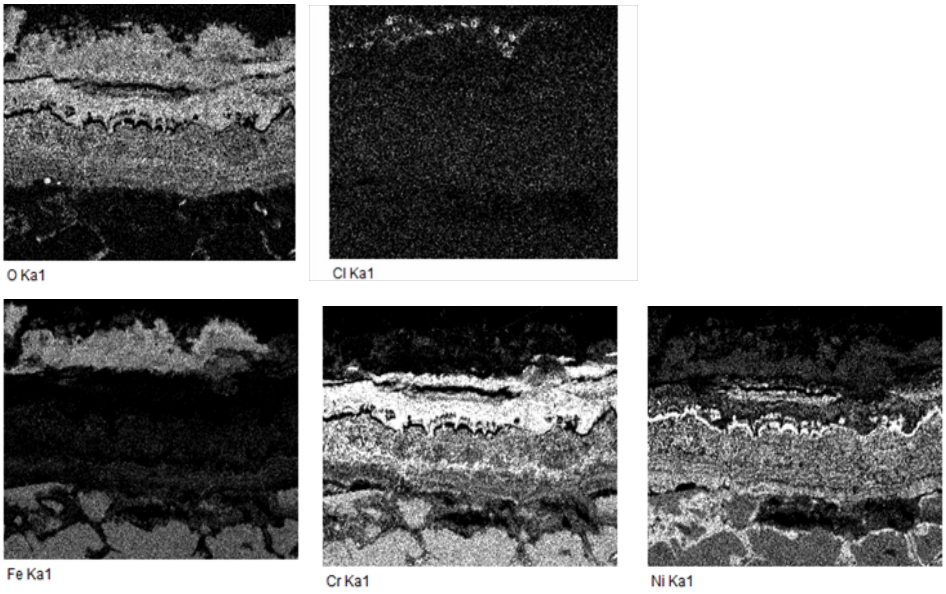

Figure 89. EDX analysis of the Sanicro 28sample after 8000 h exposure in Steamboost

- Esshete 1250 (520°C)

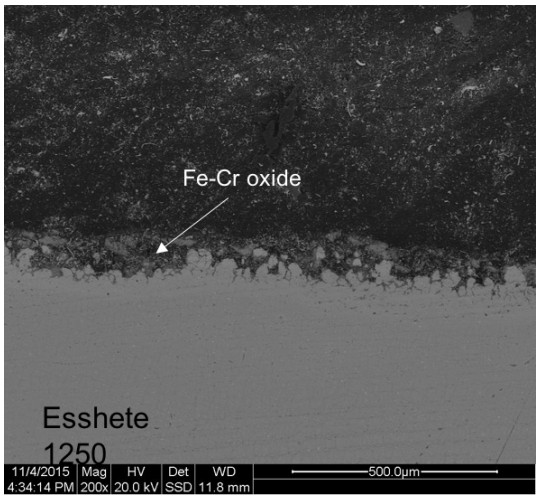

Figure 90. Backscattered SEM image of the Esshete sample after 8000h exposure in Steamboost

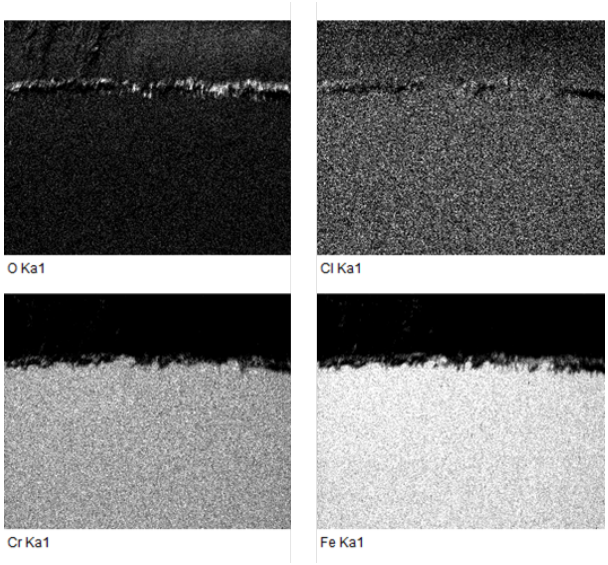

Figure 91. EDX analysis of the Esshete 1250 sample after 8000 h exposure in Steamboost

- Inconel 625 overweld (520°C)

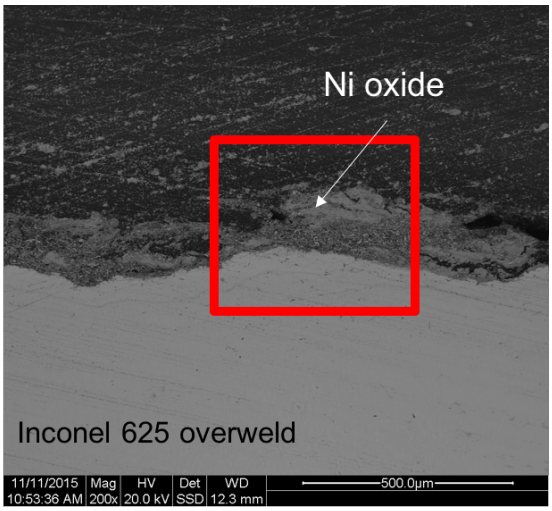

Figure 92. Backscattered SEM image of the Inconel 625 sample after 8000h exposure in Steamboost

Inconel 686 (520°C)

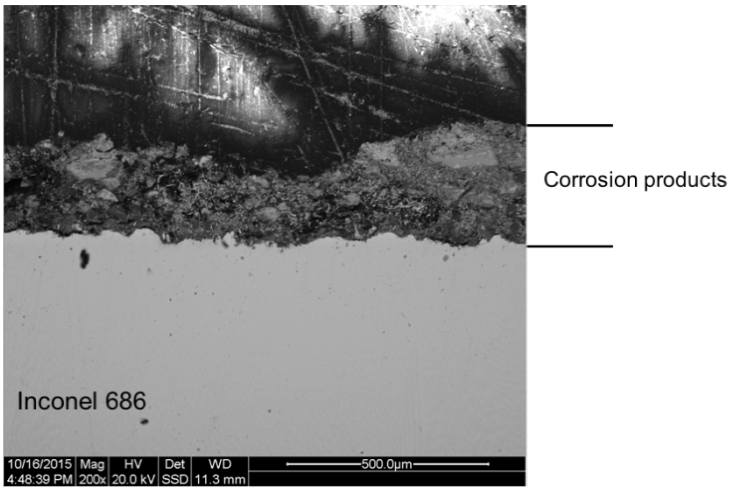

Figure 93. Backscattered SEM image of the Inconel 625 sample after 8000h exposure in Steamboost

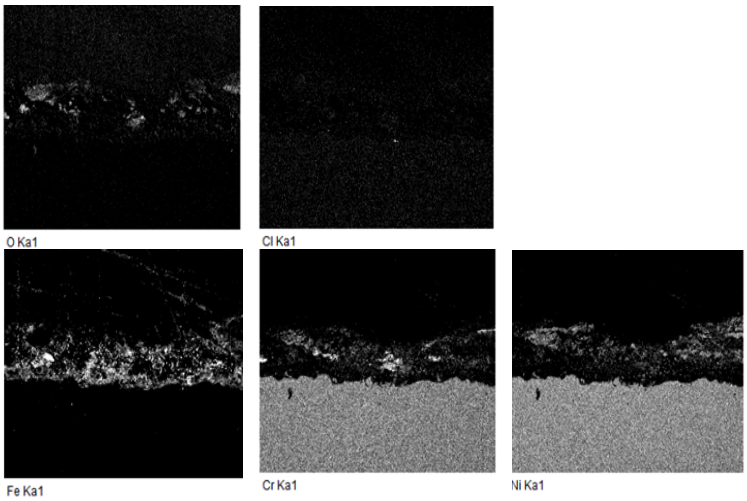

Figure 94. EDX analysis of the Inconel 686 sample after 8000 h exposure in Steamboost

- Haynes 214 – non heat treated (520°C)

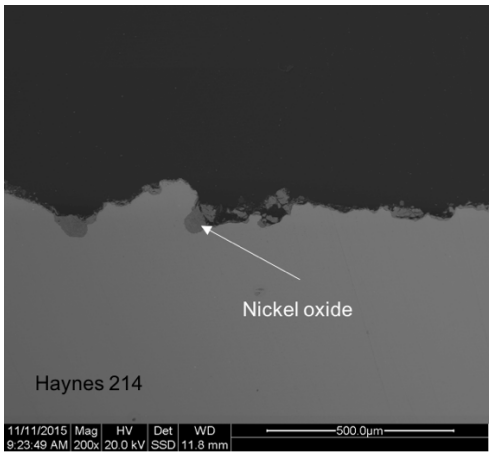

Figure 95. Backscattered SEM image of the Haynes 214 sample after 8000h exposure in Steamboost

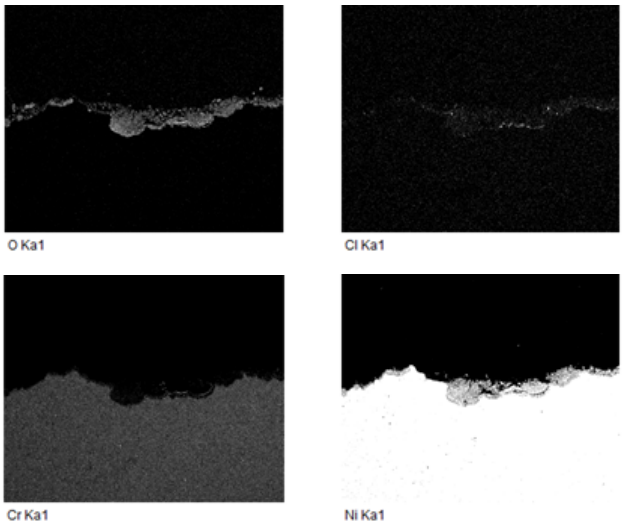

Figure 96. EDX analysis of the Haynes 214 sample after 8000 h exposure in Steamboost

- Haynes 214 – heat treated (520°C)

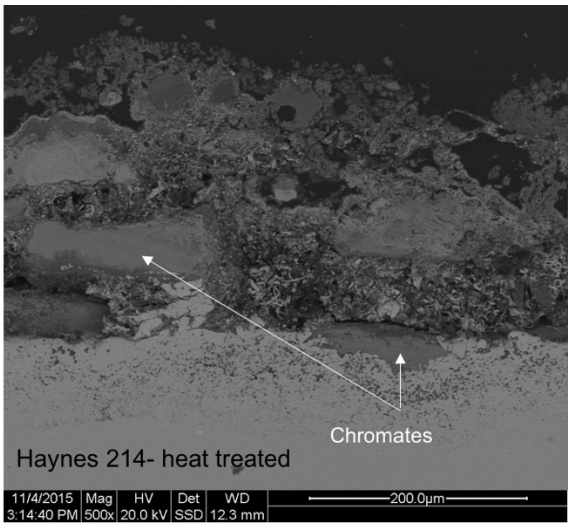

Figure 97. Backscattered SEM image of the Haynes 214 heat treated sample after 8000h exposure in Steamboost. OBS: Magnification 500X

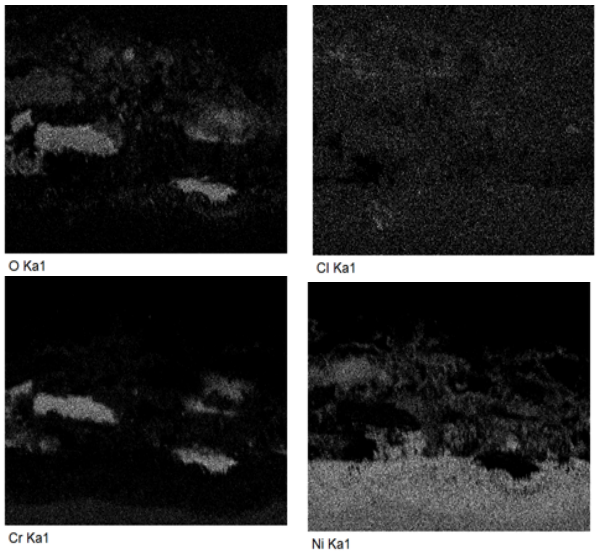

Figure 98. EDX analysis of the Haynes 214 heat treated sample after 8000 h exposure in Steamboost

15 Appendix III

Table 13: Conversion of alloy name in report to internal alloy name

Conversion of alloy names	
Name in report	Internal name
Fe**5Cr**Al2Si	alloy 32
Fe**10Cr**Al2Si	alloy 19
Fe**15Cr**Al2Si	alloy 16
Fe**20Cr**Al2Si	alloy 15
FeCrAl**0Si**	alloy 6
FeCrAl**1Si**	alloy 25
FeCrAl**2Si**	alloy 7(alloy 23)

Increased steam temperature in grate fired boilers - Steamboost

High temperature corrosion of superheater materials in waste fired boilers is a major challenge in utilization of the energy in domestic and industrial waste. This project investigates two pathways to reduce the corrosion of superheater materials in order to utilize higher steam data from these processes.

- A new position for superheaters over the grate where the heat flux is high.
- Investigate alumina-forming alloy such as the well-known FeCrAl alloys as superheater material.

The results show that both the use of a new position for the superheaters (Steamboost) and to utilize new materials (FeCrAl) that can cope with these aggressive environments are promising. It is possible to influence all aspects of the deposit formation at the furnace position, i.e. there is a potential to further optimize the deposit formation and reduce the corrosiveness. The investigation of pre-oxidized FeCrAl alloys showed that the alumina scale has a very large potential to protect the material in these environments if it is intact. The laboratory and field study of the FeCrAl model alloys without pre-oxidation in addition showed two different trends to increase the corrosion resistance, i.e. increasing the Cr content in the alloy and/or adding a small amount of Si to the alloy.

This new knowledge will contribute to:

- Higher steam parameters and thereby higher electrical efficiency.
- Development of novel solutions where steam is superheated in the furnace.
- Develop improved material solutions – including alumina forming alloys.